GRB10 AS A KEY REGULATOR CONTRIBUTING TO THE DEVELOPMENT OF CASTRATION-RESISTANT PROSTATE CANCER

by

Jun Hao

B.Eng., Shanghai Jiao Tong University, 2012

A THESIS SUBMITTED IN PARTIAL FULFILLMENT OF

THE REQUIREMENTS FOR THE DEGREE OF

DOCTOR OF PHILOSOPHY

in

THE FACULTY OF GRADUATE AND POSTDOCTORAL STUDIES

(Interdisciplinary Oncology)

THE UNIVERSITY OF BRITISH COLUMBIA

(Vancouver)

December 2019

Committee Page

The following individuals certify that they have read, and recommend to the Faculty of Graduate and Postdoctoral Studies for acceptance, the dissertation entitled:

GRB10 as a key regulator contributing to the development of castration-resistant prostate cancer

submitted by Jun Hao in partial fulfillment of the requirements

the degree of Doctor of Philosophy

in Interdisciplinary Oncology

Examining Committee:

Yuzhuo Wang, Department of Urologic Sciences
Supervisor

Christopher John Ong, Department of Urologic Sciences
Supervisory Committee Member

Marianne Sadar, Department of Pathology and Laboratory Medicine
University Examiner

Youwen Zhou, Department of Dermatology and Skin Science
University Examiner

Additional Supervisory Committee Members:

Colin Collins, Department of Urologic Sciences
Supervisory Committee Member

William Wei-Guo Jia, Division of Neurosurgery
Supervisory Committee Member

Abstract

Prostate cancer is the most commonly diagnosed cancer and the leading cause of cancer-related deaths in North American men. Androgen-deprivation therapy (ADT) is the standard treatment for patients with either locally-advanced or metastatic prostate cancer (PCa). While most PCa patients initially respond to androgen ablation, progression to recurrent castration-resistant prostate cancer (CRPC) commonly occur. Current therapies for CRPC, e.g. next-generation ADT including Enzalutamide and Abiraterone, can extend patients' lives but are not curative as resistance to their use eventually emerges. As such, there is an urgent need to identify hitherto unrecognized but critical molecular mechanisms driving CRPC, which may in turn lead to novel treatments that can be used in combination with ADT for more effective therapy.

In this doctoral dissertation, we examined the transcriptome profiling data of hormone-naïve prostate cancer (HNPC) patient-derived xenografts (PDXs) for gene expression changes at various time points after castration. Particular attention was given to expression changes that appeared early during CRPC development, indicative of genes acting as potential CRPC drivers. Eighty genes were found to be significantly upregulated at the CRPC stage, while 7 of them also showed elevated expression before CRPC development. Among the latter, Growth Factor Receptor Bound Protein 10 (GRB10), was the most significantly and consistently upregulated gene. Moreover, we found that GRB10 expression was elevated in clinical CRPC compared to HNPC in several clinical cohorts. Functionally, we found that GRB10 knockdown markedly reduced prostate cancer cell proliferation and AKT activity. Further investigation suggests that

GRB10 is transcriptionally regulated by androgen receptor through an androgen responsive element located in GRB10's intron. Mechanistically, through unbiased immunoprecipitation-mass spectrometry (IP-MS), we demonstrated that GRB10 could directly bind to and reduce the expression of protein phosphatase 2A (PP2A), a well-established tumor suppressor. These data suggest that GRB10 plays an important role in CRPC development and progression.

This research demonstrates the functional roles of GRB10 in CRPC development and defines its molecular mechanisms driving ADT resistance. This study improves our understanding of the mechanisms underlying prostate cancer progression, paving the road for developing therapeutic agents that would improve the efficacy of current CRPC treatments.

Lay Summary

Prostate cancer is the leading cause of cancer-related deaths in North American men. While most prostate cancer patients initially respond to androgen-deprivation therapy (ADT), the cancer commonly develops into an ADT-resistant cancer called castration-resistant prostate cancer (CRPC). By analyzing prostate cancer animal models, we found that GRB10 can promote CRPC development. Furthermore, CRPC patient samples tend to have more of this gene present. Decreasing the amount of this protein expression was sufficient to suppress CRPC growth and inhibit the activity of key regulators of CRPC development. We also demonstrated that the GRB10 protein can bind with and reduce the amount of a well-known tumor suppressor. Our findings strongly suggest that GRB10 is an important regulator contributing to CRPC development and progression. This study improves our understanding of the function of GRB10 and its associated machinery in regulating CRPC development. It potentially establishes a foundation for developing novel therapeutics for CRPC.

Preface

Prostate cancer specimens were obtained from patients following a protocol approved by the Clinical Research Ethics Board of the University of British Columbia, the Vancouver Coastal Health Research Institute, and the BC Cancer Agency (all patients signed a consent form approved by the Ethics Board). Animal care and experiments were performed in accordance with the guidelines of the Canadian Council and the Animal Care Committee of the University of British Columbia. The protocols for animal studies were approved by the Animal Care Committee of the University of British Columbia (A17-0165, A19-0032).

A version of Chapter 3 and Chapter 4 has been previously published in [Jun Hao], Xinpei Ci, Hui Xue, Rebecca Wu, Xin Dong, Stephen Yiu Chuen Choi, Haiqing He, Yu Wang, Fang Zhang, Sifeng Qu, Fan Zhang, Anne M. Haegert, Peter W. Gout, Amina Zoubeidi, Colin Collins, Martin E. Gleave, Dong Lin, and Yuzhuo Wang. *Patient-derived hormone-naive prostate cancer xenograft models reveal GRB10 as an AR-repressed gene driving the development of castration-resistant prostate cancer.* European Urology. 2018.(73):949-960. I was mainly involved in study concept and design, acquisition of data, analysis and interpretation of data, drafting of the manuscript, and performing statistical analysis. Hui Xue and Rebecca Wu were responsible for the animal work involved in the study. Anne M. Haegert and Colin Collins were in charge of the profiling and processing of the transcriptome data. Xin Dong and Lin Dong scored and analyzed the immunohistochemistry staining of the tumor samples. Stephen Yiu Chuen Choi and Peter

W. Gout gave critical reviews of the manuscripts. Dong Lin and Yuzhuo Wang supervised the study and were involved throughout the project.

A version of Chapter 5 is being prepared for publication. [Jun Hao], Xinpei Ci, Hui Xue, Stephen Yiu Chuen Choi, Anne M. Haegert, Colin Collins, Dong Lin, and Yuzhuo Wang. *GRB10 mediates increased glycolysis in CRPC through inhibition of PP2A.* I am mainly involved in study concept and design, acquisition of data, analysis and interpretation of data, drafting of the manuscript, and performing statistical analysis. Anne M. Haegert and Colin Collins are in charge of the profiling and processing of the transcriptome data. Stephen Yiu Chuen Choi is involved in reviewing the manuscripts. Dong Lin and Yuzhuo Wang supervised the study and were involved throughout the project.

Table of Contents

List of Tables

List of Figures

List of Abbreviations

&: and

°C: degrees Celsius

>: greater than

<: less than

µg: microgram

µm: micrometre

µM: micromolar

%: percent

±: plus or minus

×: times

18F-FDG: 2-deoxy-2-[fluorine-18] fluoro- D-glucose

ABI: Abiraterone

ABL: Tyrosine-protein kinase ABL1

ADT: Androgen-deprivation therapy

AKT: Protein kinase B

ALL: Acute lymphoblastic leukemia

AML: Acute myeloid leukemia

APA: Apalutamide

AR: Androgen receptor

ARE: Androgen responsive element

ARPI: AR pathway inhibitors

ATP: Adenosine triphosphate

BCA: Bicinchoninic acid

BCL-2: B-cell lymphoma 2-encoded protein

BCR: Breakpoint cluster region protein

BPH: Benign prostate hyperplasia

BPS: Between proline rich region and src homology 2 domain

BRN2: POU domain, class 3, transcription factor 2

CD44: Cluster of differentiation 44

CDH1: Cadherin-1

CDK: Cyclin-dependent kinase

cDNA: Complementary deoxyribonucleic acid

ChIP: Chromatin immunoprecipitation

CK5: Cytokeratin 5

CK8: Cytokeratin 8

CK14: Cytokeratin 14

CK18: Cytokeratin 18

CML: Chronic myeloid leukemia

CO_2: Carbon Dioxide

CRISPR: Clustered regularly interspaced short palindromic repeats

CRPC: Castration-resistant prostate cancer

CSS: Charcoal stripped serum

DAPI: 4',6-diamidino-2-phenylindole nuclear stain

DAR: Darolutamide

DRE: Digital rectal examination

DEPTOR: DEP domain-containing mTOR-interacting protein

EDTA: Ethylenediaminetetraacetic acid

EdU: 5-ethynyl-2-deoxyuridine

EGFR: Epidermal growth factor receptor

ENZ: Enzalutamide

ERBB2: Steroid hormone receptor ERR2

ERK: Extracellular signal–regulated kinases

FAK: Focal adhesion kinase

FBS: Fetal bovine serum

FDR: False discovery rate

FGFR: Fibroblast growth factor receptor

FKBP5: Peptidyl-prolyl cis-trans isomerase FKBP5

FLT3: Receptor-type tyrosine-protein kinase FLT3

FLU: Flutamide

FOXA1: Forkhead box A1

GAPDH: Glyceraldehyde-3-phosphate dehydrogenase

GATA2: GATA binding protein 2

GEO: Gene expression omnibus

GEMM: Genetically engineered mouse models

GM: Grb and Mig

GRB7: Growth factor receptor-bound protein 7

GRB10: Growth factor receptor-bound protein 10

GRB14: Growth factor receptor-bound protein 14

GSEA: Gene set enrichment analysis

H&E: Haematoxylin and eosin

HEAT: Huntington-Elongation-A subunit-TOR

HNPC: Hormone-naïve prostate cancer (HNPC)

JNK: Mitogen-activated protein kinase

Ki-67: Marker of proliferation Ki-67

KIT: Mast/stem cell growth factor receptor Kit

KLK3: Kallikrein peptidase 3

IF: Immunofluorescence

IGFR: Insulin-like growth factor receptor

IgG: Immunoglobulin G

IP: Immunoprecipitation

IPA: Ingenuity pathway analysis

IR: Insulin receptor

IRS1: Insulin receptor substrate 1

LC: Liquid chromatography

LHRH: Luteinizing hormone-releasing hormone

M: Metastasis

MEK1: Mitogen-activated protein kinase kinase 1

MET: Hepatocyte growth factor receptor

mL: millilitre

mM: millimolar

mm: millimetre

mm^3: cubic millimetre

MRI: Magnetic resonance imaging

mRNA: Messenger ribonucleic acid

MS: Mass spectrometry

MSigDB: Molecular Signatures Database

MSKCC: Memorial Sloan Kettering Cancer Center

mTOR: Mechanistic target of rapamycin kinase

MTS: 3-(4,5-dimethylthiazol-2-yl)-5-(3-carboxymethoxyphenyl)-2-(4-sulfophenyl)-2H-tetrazolium

MYC: Myc proto-oncogene protein

N: Node

NE: Neuroendocrine

NEDD4: E3 ubiquitin-protein ligase NEDD4

NEPC: Neuroendocrine prostate cancer

NES: Normalized enrichment score

NKX3.1: NK3 homeobox 1

NIL: Nilutamide

nM: nanomolar

nm: nanometre

NOD/SCID: Nonobese diabetic/severe combined immunodeficiency

OXPHOS: Oxidative phosphorylation

p53: Tumor protein p53

p63: Tumor protein p63

PAGE: Polyacrylamide gel electrophoresis

PB: Probasin protein

PCa: Prostate cancer

PCR: Polymerase chain reaction

PDGF: Platelet-derived growth factor

PDGFR: Platelet-derived growth factor receptor

PDX: Patient-derived xenograft

PEG10: Retrotransposon-derived protein PEG10

PET/CT: Positron emission tomography/ computed tomography

PFA: Paraformaldehyde

pH: potential of hydrogen

PH: Plechstrin homology

PHLPP: PH domain leucine-rich repeat-containing protein phosphatase

PI: Propidium iodide

PI3K: Phosphatidylinositol 3-kinase

PIN: Prostatic intraepithelial neoplasia

PLA: Proximity ligation assay

PP2A: Serine/threonine-protein phosphatase 2A

PR: Proline Rich

PSA: Prostate-specific antigen

PTEN: Phosphatase and tensin homolog

qPCR: Quantitative polymerase chain reaction

RA: Ras-associating

RAF1: RAF proto-oncogene serine/threonine-protein kinase

RAS: GTPase Ras protein

RB: Retinoblastoma transcriptional corepressor 1

RNA: Ribonucleic acid

RPTOR: Regulatory-associated protein of mTOR

RTK: Receptor tyrosine kinase

SC: Subcutaneous

SDS: Sodium dodecyl sulfate

SEM: Standard error of the mean

SH2: Src homology 2

SHC: SHC-transforming protein

SMAD4: Mothers against decapentaplegic homolog 4

SRC: Subrenal capsule

STAT5: Signal transducer and activator of transcription 5

SV40: Simian Virus 40

T: Tumor

TCA: Tricarboxylic acid cycle

TCGA: The Cancer Genome Atlas Program

TEC: Tyrosine-protein kinase Tec

TNM: Tumor, node, metastasis

TRAMP: Transgenic adenocarcinoma of the mouse prostate

TSC2: Tuberous Sclerosis Complex 2

TSS: Transcription start site

UGM: Urogenital mesenchyme

UGS: Urogenital sinus

VEGFR2: Vascular endothelial growth factor receptor 2

Acknowledgements

A journey towards a PhD degree is never easy and can never be completed without the kind help from all the fantastic people around me.

First, I would like to take this chance to express my heartfelt gratitude to my mentor, Dr. Yuzhuo Wang. YZ took me in during my darkest time. I was confused and frustrated about what to do after finishing my undergraduate degree. He enlightened me and helped me discover what I really wanted to pursue in my future life. Over the years, YZ showed me how to think, how to question, and how to act like a research scientist. More importantly, the trust and the confidence he gave me encouraged me to be a more independent researcher. The freedom he granted me enabled me to explore various projects I was interested in. Despite the mistakes I made as a rookie during these years, I learned from these lessons, and they became precious gifts for my life. I am also grateful to YZ for getting me involved in the grant application process. This experience provided me opportunities to practice my scientific writing skills and pushed me to reshape my project with the help of critical reviewer comments. All of these contributed to my publications and my thesis and will continue to be essential to my future career. I would also like to extend my sincere gratitude to my supervisory committee, Dr. Christopher Ong, Dr. William Jia, and Dr. Colin Collins. Thank you so much for your kind comments and suggestions, and also for your time and constructive reviews of this thesis.

I would also like to thank all past and current lab mates. Thanks to Dr. Peter Gout for his tremendous help in improving my English writing. Without your help, I could not get this far. Many thanks to Hui, Rebecca, Yuwei, and Hongwei for their countless efforts in developing the PDX models. They were foundational for my studies. Thanks to Fang and Dong for your scientific advice for my project. I still remember the days when Dong, Xindy and I were working together, screening potential targets. Thank you so much. You helped me determine the target and guided me throughout the project. Thanks to Ting for her guidance through all the basic lab techniques. Your help led to my first publication. Thank you, Stephen, you are the real hero behind all my proposals and papers. I am so happy to witness your happiness and to have you in mine. Special thanks to my dear Xinpei, you are more like a supervisor than a colleague to me. It is your generous support and guidance that helped me move forward. Do you remember that Christmas night we resubmitted the revised manuscript? My research can never go smoothly without you. I am also thankful for all the previous academic sisters and brothers who have worked with me: Iris, Sifeng, Pier-Luc, Abhijit, Xinya, Sarah. The list goes on. I would also like to extend my appreciation to the financial support from Mitacs and the BC Cancer Foundation, as well as the Chinese Government Award for Outstanding Self-Financed Students Abroad.

Last but not least, I would particularly like to express my profound thanks to my parents and auntie, whose constant support, both mentally and physically, are the keys to all my achievements. I am and will always be grateful for all the love and support you give me.

To my parents

&

In memory of my grandpa

Chapter 1 Introduction

1.1 Prostate Cancer

1.1.1The Prostate

The prostate is the largest reproductive exocrine gland in males. The primary function of the prostate gland is to produce and secrete prostatic fluid, which is slightly alkaline and accounts for 30% of the seminal fluid, which protects sperm and increases its mobility [1, 2]. In adult males, the prostate is the size of a walnut, surrounds the urethra, and is located directly under the bladder [3].

Anatomically, the human prostate can be divided into 4 zones: the Peripheral Zone, the Central Zone, the Transition Zone, and the Anterior Fibro-muscular Stroma [4] (Fig 1.1). The Peripheral Zone accounts for about 70% of the total of the prostate, and 70%-80% of prostate cancers develop in this area [5-7]. The Central Zone represents about 25% of the prostate gland. While prostate carcinoma developing in the Central Zone is rare (about 2.5%), they are proven to be more aggressive [8]. The Transition Zone is one of the smallest regions of the prostate. Since both the glandular epithelial and stromal cells in this area constantly proliferate, benign prostate hyperplasia (BPH) mainly arises from this zone [9]. The Anterior Fibro-muscular Stroma region accounts for only 5% of the total prostate and is mainly composed of smooth muscle cells, fibrous stroma, and fewer glandular epithelial cells [8, 10].

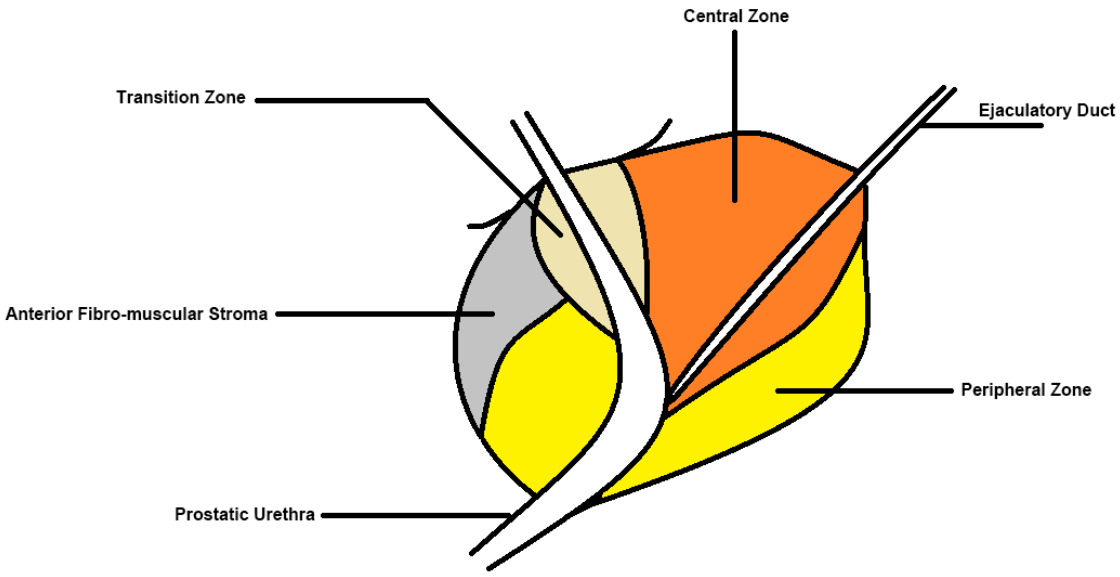

Figure 1.1. The anatomy of the human prostate

The human prostate is located under the bladder with the prostatic urethra and the ejaculatory duct passing through. The human prostate is divided into four anatomical zones: the Peripheral Zone, the Central Zone, the Transition Zone, and the Anterior Fibro-muscular Stroma.

The prostate contains tubuloalveolar glands, with pseudostratified columnar epithelium embedded in the fibromuscular stroma [7]. The secretory function of the prostate comes from the epithelium, which is composed of tall columnar luminal secretory cells, low-cuboidal basal cells, and very few neuroendocrine (NE) cells [11]. The luminal secretory cells are responsible for the secretion of prostatic fluids. These cells are highly responsive to androgen stimulation and express cytokeratin 8 and 18 (CK8 and CK18), prostate-specific antigen (PSA), and androgen receptor (AR) [12]. Basal cells form a

single-cell layer surrounding the luminal cells and express basal cell markers such as cytokeratin 5 and 14 (CK5 and CK14), p63 and CD44 [12]. NE cells are rare and scattered among the basal cells. NE cells have no AR expression and thus do not respond to androgens. These cells express chromogranin A, serotonin and various neuropeptides [11, 13]. Emerging evidence suggests that there is another cell type in the prostate epithelium, known as the intermediate or transit-amplifying cells [12, 14, 15]. These cells were reported to be prostate progenitor/ stem cells, which share molecular features with embryonic urogenital sinus epithelial cells expressing both luminal and basal cell markers such as CK5 and CK18 [14].

The human prostate develops from the endoderm of the urogenital sinus (UGS) during the 10th-week of gestation and fully matures after puberty [3]. The development of the human prostate is dependent mainly on the androgen secreted by the Leydig cells in the fetal testes [16]. AR in the urogenital mesenchyme (UGM) is stimulated by androgens, which activates paracrine growth factors, cytokines, and hormones to induce epithelial budding, proliferation, and differentiation of the urogenital epithelium. The UGM differentiates into interfascicular fibroblasts and smooth muscles [3]. AR in the UGM but not the UGE is required for prostate differentiation, as evidenced by early studies using tissue recombination techniques. The androgen sensitivity of the UGM determined the fate of prostatic glandular formation, regardless of the origin of the epithelium component [17-20].

1.1.2 Prostate Cancer

Prostate carcinoma (PCa) is the most commonly diagnosed non-skin cancer in North American men [21] and the second-most commonly diagnosed cancer in men worldwide [22]. According to the latest Global Burden of Disease Study, about 1.5 million new PCa cases were diagnosed, with more than 336,000 PCa-related deaths were reported in 2015 worldwide [23]. In the United States, approximately 174,000 men will be diagnosed with PCa in 2019, and 31,620 men are estimated to die from it [21]. By January 1, 2019, the total number of patients who are alive with a history of PCa is projected to be more than 3.6 million in the US alone, and by the year 2030, this number will increase to more than 5 million [24]. In Canada, PCa is still the most commonly diagnosed cancer in men with an estimated 21,300 new cases in 2017 (Canadian Cancer Statistics 2017: http://www.cancer.ca/Canadian-Cancer-Statistics-2017-EN). The overall five-year survival of PCa is among the highest of all cancers. It is greater than 95% in Canada and closer to 97% in the United States [24, 25]. However, the five-year survival rate drops dramatically to 30% when cancer is diagnosed at a later stage (distant metastasis) [24, 25].

Most PCa is adenocarcinoma, which arises from prostatic epithelial cells [26-28]. Rare histological variants can include NE carcinoma [29]. In the clinic, PCa is a multi-focal and heterogeneous disease. Varying degrees of prostatic intraepithelial neoplasia (PIN) and multiple isolated foci of prostatic carcinoma with distinct genetic alterations can be found in a single prostate [30-32]. The vast majority of PCa, particularly treatment-naïve PCa, express AR and rely on androgen signalling for growth and survival. Therefore,

androgen-deprivation therapy (ADT) is the most effective treatment for early-stage PCas [33]. However, PCa will inevitably progress into castration-resistant prostate cancer (CRPC), which is currently incurable [34].

1.1.3 Screening, Diagnosis and Grading of Prostate Cancer

Recent studies of PCa screening oppose population-wide screening for PCa based on the fact that potential harms of over-treatment outweigh the potential benefits of early diagnosis [35]. Symptoms of early-stage PCa include frequent or difficulty with urination and presence of blood in urine or seminal fluid. Late-stage PCa with bone metastasis result in bone pain, weight loss, and fatigue [36]. For many asymptomatic patients, the rise of serum PSA levels and the detection of abnormal prostatic growth via prostate digital rectal examinations (DRE) during routine physical examinations suggest the possibility of PCa [37, 38]. PSA is a kallikrein-associated serine protease, which is known as kallikrein peptidase 3. In humans, it is encoded by the *KLK3* gene and its expression is regulated by androgen and AR [39]. PSA is secreted by the healthy prostate, but is released into the bloodstream when the cancerous lesions destroy the prostatic structure [40]. However, since the elevation of serum PSA and abnormal DRE results could come from BPH and prostatitis, the gold standard of PCa diagnosis is still the histopathologic evaluation of prostate needle biopsies [37]. Usually, a prostate biopsy will contain 8-12 core samples depending on the area and the transrectal ultrasound result. Pathologists will then examine the fixed and haematoxylin and eosin (H&E) stained core samples [41]. The cancerous area will be graded based on the Gleason grading system developed by Dr. Donald F. Gleason in the 1970s [42]. The Gleason grading system scores the

histopathological feature of the tumor based on the glandular pattern from 1 being the most differentiated to 5 being the most undifferentiated glandular structure [43]. Typically, the most common score and the next-most common score will be combined to get a final Gleason score of a particular biopsy sample [44, 45]. The Tumor, Node, Metastasis (TNM) stage is a cancer staging system used for patient stratification [44, 46]. Tumor (T) describes the size of the tumor and whether the tumor has invaded nearby tissues. T1 is a primary tumor that not visible by imaging. T2 is a tumor confined within prostate. T3 is a tumor extends through the prostatic capsule. T4 is a tumor invaded into adjacent tissues other than seminal vesicles [44, 46]. Node (N) is determined by whether the PCa has spread to the regional lymph node. N0 stands for no regional lymph node metastasis, and N1 refers to cancer metastasis to lymph nodes [44, 46]. Metastasis (M) is used to describe the distant metastatic status of the tumor. M0 means no sign of distant metastasis. M1a shows metastasis to nonregional lymph nodes. M1b shows metastasis to bone(s). M1c shows metastasis to other organs [44, 46].

1.1.4 Clinical Management of Prostate Cancer

The clinical management of PCa depends on the potential risk that a particular tumor presents to the patient. Since the staging of PCa, the treatment options, and the treatment outcomes vary, a proper risk stratification system is needed for the better management of PCa. The risk stratification systems are different worldwide, but the vast majority of them are based on a combination of Gleason score, TNM stage, and the serum PSA level at diagnosis. D' Amico risk classification, which is adopted by both American Urological Association and the European Association of Urology, is one of the most widely

used risk stratification systems to evaluate the potential risk of PCa recurrence following radical prostatectomy and external-beam radiotherapy, two routine therapies used against localized PCas [47-49]. The D' Amico system groups patients into three risk groups, low-risk, intermediate-risk, and high-risk, based on all three grading systems mentioned above. Low-risk PCas are cancers with T1/T2a, PSA $\leqslant$10 ng/ ml, and Gleason score $\leqslant$6. High-risk cancers are cancers having any one of the following: T2c or higher, PSA >20 ng/mL, or Gleason 8–10. Any cancers in between are grouped as intermediate-risk cancers [47].

Different treatment options are then recommended based on the risk groups. Active surveillance is recommended to low-risk, localized PCa patients [50, 51]. Active surveillance refers to no immediate treatment since the prostate tumor is unlikely to harm the patient. This approach can reduce the side effects caused by any invasive treatment [52]. However, a strict follow-up, including PSA blood tests and DREs, is required to monitor the disease progression. Treatment may be needed if the tumor progresses rapidly. For high-risk PCa patients, immediate intervention is required, which includes surgery (radical prostatectomy) and radiation therapy (prostate brachytherapy and external beam radiotherapy) [53, 54]. These two therapies are considered curative since the 5-year survival rate at this stage is more than 99% [24, 25].

Since Dr. Huggins revealed that PCas are largely dependent on androgens for growth and survival [55], ADT has become the standard treatment for locally advanced

or metastatic PCas [55, 56]. Surgical castration and luteinizing hormone-releasing hormone (LHRH) agonists and antagonists, which inhibit testicular androgen production, are traditional approaches to diminish androgen level systemically [57]. Recent randomized controlled trials support several new strategies to be used for metastatic, castration-sensitive PCas, including the use of chemotherapy docetaxel [58, 59], Abiraterone (ABI) plus Prednisone [60, 61], Enzalutamide (ENZ) [62], and Apalutamide (APA) [63].

1.1.5 Castration-Resistant Prostate Cancer

ADT is the most effective therapy for advanced PCa. However, treatment resistant PCa, termed CRPC, inevitably develops within two years of treatment [64]. CRPC is an extremely lethal disease, with an approximate median overall survival of two years [34, 65, 66].

The exact molecular mechanism underlying CRPC development remains unclear, while several known factors contribute to this event. AR is one of the most critical factors mediating the development of CRPC. According to recent large-scale clinical PCa genomic screening, the occurrence of AR genetic alterations, including AR mutation and AR amplification, is dramatically higher in CRPC (nearly 60%) compared to hormone-naïve prostate cancer (HNPC) (less than 2%) [67-73]. Mechanistically, AR gain-of-function mutations, AR splicing variants such as AR-V7, and activation of AR co-factors were reported and demonstrated to help PCa regain AR signaling, contributing to the

androgen-independent progression of CRPC [74-82]. Besides hyper-activated AR, increased intratumoral dihydrotestosterone (DHT) levels also contribute to the development of CRPC. It is reported that the intratumoral DHT concentration can reach as high as 1nM, which is sufficient to activate AR [83-85]. Emerging evidence suggests that intratumoral DHT is produced *de novo* through a 'backdoor' pathway using precursors secreted by the adrenal gland [86-88]. Mechanistically, in CRPC patient tumors, a key enzyme catalyzing the rate-limiting step in such 'backdoor' DHT synthesis, 3β-hydroxysteroid dehydrogenase type 1 (3βHSD1), was reported to harbour a gain-of-function mutation [89]. Several other mechanisms were proposed to promote the development of CRPC, including the overexpression of Bcl-2 [90, 91], the activation of the PI3K/AKT pathway [92, 93], the overexpression of glucocorticoid receptor [94-96], and the transdifferentiation to neuroendocrine prostate cancer (NEPC) [97, 98].

Docetaxel was the only effective drug for CRPC treatment [99] until 2011, when a randomized phase III clinical trial showed that ABI increased survival in mCRPC patients [100]. Since then, several new AR pathway inhibitors (ARPIs) have been developed and approved for the treatment of both non-metastatic and metastatic CRPC such as ENZ [101-103], and Darolutamide (DAR) [104]. Other than ARPIs, Cabazitaxel was approved as a second-line chemotherapy for Docetaxel-resistant PCa. Compared to Docetaxel, Cabazitaxel has a lower binding affinity to the adenosine triphosphate-dependent drug efflux pump P glycoprotein 1, which exports Docetaxel and causes treatment resistance [105, 106]. Despite the success in developing new therapeutic agents for the management of CRPC, none of the treatment options is curative and treatment resistance

invariably occurs [107]. Therefore, there is still an urgent need to better understand the disease and develop more effective therapies.

1.2 Models of Prostate Cancer

1.2.1 Prostate cancer cell lines

Cell lines are immortalized cultured cells that can proliferate indefinitely. Cancer cell lines are the most feasible and easy-to-manipulated models to study the development and progression of cancers. Commonly used PCa cell lines include both PCa cells derived from patient samples and from PCa xenografts. The LNCaP cell line was initially isolated from a needle aspiration biopsy of a left supraclavicular lymph node from a 50-year-old Caucasian metastatic PCa patient [108]. LNCaP cells are responsive to androgen treatment and show significant growth inhibition in the androgen-ablation culture system. At the molecular level, LNCaP expresses AR and PSA. The AR in LNCaP contains a T877A mutation, which leads to an altered binding specificity to different steroids and anti-androgens [109]. PTEN in LNCaP is also deleted in one allele and mutated in the other, resulting in no PTEN protein expression [110]. A number of LNCaP sublines have been developed over the years, with C4-2 being of the most popular. The C4 line was isolated from a xenograft tumor 4 weeks following host castration. The xenograft was developed by co-inoculating LNCaP with the MS human osteosarcoma fibroblast cell line into an intact athymic male nude mouse. Later, the C4-2 line was derived from the C4+MS xenograft established in a castrated host. C4-2 cells were able to form tumors in castrated mice without MS co-injection [111, 112]. Thus, C4-2 was considered an androgen-independent CRPC subline of LNCaP. Another subline of

LNCaP used in the study is MR49F. It was isolated from a third-generation LNCaP xenograft tumor under long-term ENZ treatment (10 mg/kg/day). The xenograft was harvested and single cell suspensions grown under continuous ENZ pressure (10 μM). MR49F cells express both AR and PSA protein [113],[114].

22Rv1 and VCaP are two AR^+ PCa cell lines commonly used in PCa studies. 22Rv1 was derived from an androgen-dependent patient-derived xenograft (PDX) model, CWR22, after undergoing multiple rounds of host castration-induced regression and relapse [115, 116]. Compared to LNCaP, 22Rv1 expresses wild-type PTEN but contains a Q331R p53 mutation. AR in 22Rv1 contains a H874Y mutation and an in-frame duplication of its exon 3, both contributing to its androgen independent growth [117-119]. It also expresses a high level of AR-V7, which is an AR splicing variant thought to be the critical regulator driving its androgen-independent growth [115, 119, 120]. VCaP was established from a bone metastasis lesion from a 59-year-old CRPC patient [121]. VCaP has wild-type but amplified AR. VCaP cell line also represents a good model for studying *TMPRSS2-ERG* gene fusion, which was presented in 40% to 50% of clinical prostate cancers [73, 122]. It also harbours an A248W p53 mutation [119, 121]. Both 22Rv1 and VCaP were able to form tumors in castrated mice, suggesting they are capable of androgen-independent growth.

PC-3 and DU 145 are two of the oldest PCa cell lines, being established in 1979 and 1978 respectively [123, 124]. PC-3 was isolated and established from a bone metastasis from a 62-year-old patient [123], and DU 145 cells were derived from a brain

metastasis [124]. Interestingly, neither cell line expresses AR. Evidence suggests that the DNA hypermethylation located at the AR promoters in PC-3 and DU 145 cells silenced their expression [117]. Therefore, these two cell lines do not respond to either androgen stimulation or androgen-ablation treatment and should be used to study AR^- PCas.

1.2.2 Genetically engineered prostate cancer mouse models

Genetically engineered mouse models (GEMMs), or transgenic mouse models, are another type of model commonly used to study the malignant progression of PCa. Compared to PCa cell lines, GEMMs can recapitulate PCa development in living tissues and can represent various stages of PCa including its establishment, progression, and metastasis. Up to now, there are more than a dozen GEMMs that have been developed by either prostate-specific induction of oncogenes or deletion of tumor suppressors [125, 126]. Transgenic adenocarcinoma of the mouse prostate (TRAMP) is one of the first reported GEMM of PCa [127]. In this model, a small fragment prostate-specific rat probasin (*Pb*) gene promoter (-426 to +28, sPB) was used to drive the expression of Simian Virus 40 (SV40), which is a polyomavirus gene coding oncogenic large T and small t antigen. The androgen dependence of the model is variable, while the relapsed tumors after host castration are 100% synaptophysin positive [128] and later found to be a small cell NE carcinoma [129]. A similar model, LADY, was then established using a large fragment of the *Pb* gene promoter (12kb in size, LPB) to express the SV40 large T antigen [130]. Consistent with the finding using the TRAMP model, all metastatic LADY models were found to be NE tumors [131]. Recent evidence in genomic NEPC studies and in mouse NEPC development studies revealed that the loss of p53 and Rb tumor

suppressors could lead to the development of NEPC [132-134]. Since SV40 large T antigen was known to bind to and inhibit p53 and Rb, this suggests that these two models recapitulate the development of AR^- NEPCs.

Along with p53 and Rb, phosphatase and tensin homolog deleted on chromosome 10 (PTEN) is one of the most critical tumor suppressors and one of the most frequently mutated/deleted genes in human PCas [135]. The establishment of a prostate-specific deletion of *Pten* PCa GEMM was reported in 2003 [136]. The model was established by crossing $Pten^{loxp/loxp}$ mice with ARR_2PB-Cre4 transgenic mice where Cre expression was driven by a modified, higher-sensitivity PB promoter containing an extra copy of androgen responsive region [136, 137]. The prostate-specific homozygous *Pten* deletion led to the development of invasive PCa (100% of cases), and these tumors responded to castration treatment as indicated by increased apoptosis [136]. The establishment of conditional *Pten* knockout mice supported a number of studies that generally focused on the involvement of particular genes in the development and progression of PCa, e.g., crosses with *Tp53* deletion [138], *Smad4* deletion [139], and *Nkx3.1* deletion [140].

Myc overexpression and amplification is another recurrent feature observed in PCa [141-143]. Transduction of *Myc* was able to give rise to cancers in various mouse tissues [144-146] including PCa [147]. Prostate-specific *Myc* transduction (Hi-Myc) was achieved by using the ARR_2/probasin-*Myc* plasmid in a similar approach to the PB-Cre4 transgenic line. Hi-Myc resulted in prostate intraepithelial neoplasia that later developed into invasive prostate adenocarcinomas (19/20 of cases). The Hi-Myc transgenic line also responds to

castration, as indicated by a low proliferation index (low Ki67 staining) and low AR expression [147].

1.2.3 Patient-derived xenograft models

Despite the advantages of PCa cell lines and GEMMs, there are still limitations. For examples, while cell lines are easy to use at a low cost, they lack tumor heterogeneity and cancer-stromal interactions. GEMMs are *in vivo* models representing tumor development in living tissues. However, they are murine PCas and are more focused on a particular type of genetic alteration as introduced to develop the model. More importantly, none of these models recapitulate the development of CRPC from HNPC. PCa cell lines are derived from mCRPC patients, and the response of GEMMs to castration cannot fully reflect the shrinkage-to-relapse progression. Therefore, better models are needed to study this process.

PDX models are promising tools to fulfill this demand. PDX models are established by grafting patients' tumor tissue specimens into immune-compromised mice. In this way, PDX models can retain the genetic and gene expression features of the original tumors [148, 149], preserve the stromal components [150], and more importantly, mimic the response to treatments [151]. However, the development of PCa PDX models has long been a challenge due to the low take rates and long latency times [152, 153]. Groups from around the world established several strategies to improve the take rate of PCa PDXs, including coating patient's tumors with Matrigel [154-156], or using mouse seminal

vesicle mesenchyme [157]. While they were improvements, these methods still involve the introduction of artificial or mouse-origin stroma, which may affect tumor biology. Additionally, the site of implantation is another aspect worth considering. Subcutaneous (SC), orthotopic, and subrenal capsule (SRC) are popular sites to establish PDX models. Compared to SC and orthotopic xenografts, grafting tumor tissues under mice kidney capsule is more successful, which could be due to the high vascularization of the kidney, allowing the xenografts to get enough nutrients, growth factors and hormones [158-161]. In fact, several independent groups have reported that, grafting patients' tumors at SRC sites gave the highest take rate compared to grafting at SC or orthotopic sites [152, 162, 163]. The SRC PDX models were derived from either primary or metastatic tumors at various stages ranging from HNPC to mCRPC [151, 152]. Evidence suggests that these high fidelity SRC PDX models are able to retain the histopathological and molecular features of the original tumors [98, 151]. More importantly, these models recapitulate the tumor progression. In particular, the development of CRPC from HNPC was observed in a number of these SRC HNPC PDX lines, which spontaneously gave rise to recurrent CRPC tumors after host castration [151, 164].

1.3 Growth Factor Receptor-Bound Protein 10 (GRB10)

1.3.1 Growth Factor Receptor-Bound Protein Family

In this doctoral dissertation, we identified growth factor receptor-bound protein 10 (GRB10) is a potential driver for the development of CRPC. GRB10 belongs to the Grb (Growth factor receptor-bound) protein family, which consists of three family members, GRB7, GRB10, and GRB14 based on their conserved protein structure. All of the three

proteins contains an N-terminal Proline Rich (PR) region, a central GM (Grb and Mig) region that contains a Ras-Associating (RA) domain, a Pleckstrin Homology (PH) domain, and a Between PH and SH2 (BPS) domain, and a C-terminal Src Homology 2 (SH2) domain [165]. The multidomain structure of Grb proteins enables them to interact with a variety of proteins at the same time and allows them to function as scaffold adaptor proteins. The Grb proteins were all originally identified as EGFR binding proteins by yeast two-hybrid screening of a bacterial expression library using autophosphorylated EGFR as a bait [166]. Back in 1992, GRB7 was the first protein in the family to be discovered. It contains an SH2 domain responsible for its interaction with EGFR [166]. In 1995, another Grb protein, GRB10, was identified by the same research group using a NIH/3T3 cDNA library [167]. GRB10 was found to be highly-related to GRB7 and highly-similar to the previously reported C. elegans gene mig-10 and mouse gene meg1 (meiosis expressed gene 1), suggesting an involvement in meiosis [167-169]. Later in 1996, GRB14 was identified and cloned using a human breast epithelial cell cDNA library [170]. The identification, characterization, and isolation of Grb proteins revealed that these three family members shared a similar but unique protein structure, allowing them to regulated diverse downstream signaling pathways.

Since GRB7 was isolated using EGFR, a known oncogene, as bait, the study of GRB7 function was focused on cancer since the beginning. The human *GRB7* is located on chromosome 17q12 and is in close proximity to *ERBB2*, a driver and therapeutic target for many human cancers including breast cancer, ovarian cancer, colorectal cancer, and non-small-cell lung cancer [171-174]. Thus, *GRB7* is within the *ERBB2* amplicon and is

usually coamplified and coexpressed with *ERBB2* in human cancers [175, 176]. Upon interaction with ERBB family proteins, GRB7 activates its downstream signal cascades such as Shc, Ras, ERK1/2, JNK, and FAK, to promote tumor cell proliferation, resistance to apoptosis, cell migration, and tissue invasion [177-180].

GRB14, on the other hand, was reported to be more associated with endocrine signaling and has a higher affinity to IR and FGFR but not EGFR [181]. It is shown that the interaction between GRB14 and IR or FGFR inhibits their function, possibly through competition for its downstream effector binding sites [181-183]. Several studies have reported that GRB14 is associated with cancer, but the role of GRB14 is still inconclusive. GRB14 has been reported to be overexpressed in some clinical cancer specimens and cancer cell lines [184-186]. However, another report suggested a higher expression of GRB14 was a favorable prognostic marker [187]. Thus, the function of GRB14 can vary depending on the type of cancer and the proteins it interacts with.

1.3.2 Molecular Function of GRB10

The GRB10 protein was identified in 1995 by the same group that identified GRB7. They used the same protocol, probing a bacterial expression library derived from mouse NIH/3T3 cells with tyrosine autophosphorylated carboxyterminus of EGFR [167]. Later that year, human GRB10 was identified by using the cytoplasmic domain of human insulin receptor (IR) as bait to screen human liver and Hela cDNA libraries [188]. Northern blot analysis suggested that the gene was highly expressed in human skeletal muscles and

adipose tissues [188]. Since then, the study of GRB10 function has largely focused on its role in IR and IGFR (insulin-like growth factor I receptor) signaling. However, the role of GRB10 in insulin or IGF-I induced signaling remains inconclusive and is dependent on the particular cellular context and experimental approach. On the one hand, both microinjecting and using cell membrane-penetrating GRB10 SH2+BPS domain peptides inhibited insulin and IGF-I mediated mitogenesis in NIH/3T3 and baby hamster kidney fibroblasts [189-191]. It was suggested that GRB10 function was impaired via competition between introduced peptides and endogenous GRB10. These effects were proven to be specific since introducing of these peptides could not affect PDGF-mediated cell proliferation [189]. Moreover, overexpression of GRB10 in human Rat-1 fibroblasts, rat L6 myoblasts, and rat PC12 pheochromocytoma cells increased insulin-mediated PI3K catalytic activity and the subsequent metabolic response including glycogen synthesis, glucose and amino acid uptake, and lipogenesis [192]. On the other hand, GRB10 was also reported to be a negative regulator of IR and/or IGFR signaling. The interaction of GRB10 and IR in Chinese hamster ovary (CHO) cells, mouse embryonic fibroblast cell line 3T3-L1, and primary rat hepatocytes physically blocked the binding between IRS and IR and/or IGFR, which in turn led to decreased phosphorylation of IRS1 and its downstream signaling pathways including PI3K and AKT [188, 193-195].

In addition to EGFR, IR and IGFR, GRB10 has been reported to interact with a number of other cell surface receptors, many of which are receptor tyrosine kinases (RTK). The interaction of GRB10 with ligand-activated platelet-derived growth factor receptor (PDGFR) through its SH2 domain mediates the function of PDGFR and is critical for

PDGF-induced mitogenesis [189, 196]. Vascular endothelial growth factor receptor-2 (VEGFR2) is another well-studied RTK that has been reported to bind to GRB10 [197, 198]. Evidence suggests that GRB10 protects VEGFR2 from NEDD4-induced degradation by constitutively interacting with NEDD4, leading to enhanced VEFG-mediated MAPK activation [197, 198]. Some other RTKs were also reported to bind to GRB10, but the function of these interactions have not been elucidated. They include proto-oncogene tyrosine-protein kinase receptor Ret, EPH receptor B1, fibroblast growth factor receptor 1, and hepatocyte growth factor receptor Met [189, 199, 200].

Other than RTKs, GRB10 interacts with several other cell-signaling transduction kinases as well. Tyrosine-protein kinase Tec, which regulates T cell development, function and differentiation [201], was reported to be negatively regulated by its interaction with GRB10 [202]. Several proteins involved in Mitogen-activated protein kinases (MAPK) pathway, including NRAS, RAF1, and MEK1, were reported to directly bind to GRB10 [203-205]. The MAPK pathway is responsible for the regulation of gene expression, cell proliferation and apoptosis [206]. The interaction of GRB10 with these signaling cascades indicates GRB10's role as a key regulator in such cellular processes. The PI3K/ AKT pathway is another major signaling pathway regulating cell division and programmed cell death [207]. The interaction of GRB10 with PI3K and AKT is long-established [192, 208-210]. However, the role of these interactions is still elusive and could be cell context-dependent. GRB10 has been shown to positively regulate AKT signaling by directing AKT to the cell surface when AKT is activated [208, 209]. Two phospho-proteomics studies

suggested that GRB10 was a substrate of mTORC1, with its upregulation leading to decreased AKT activity in $TSC2^{-/-}$ mouse embryonic fibroblasts [211, 212].

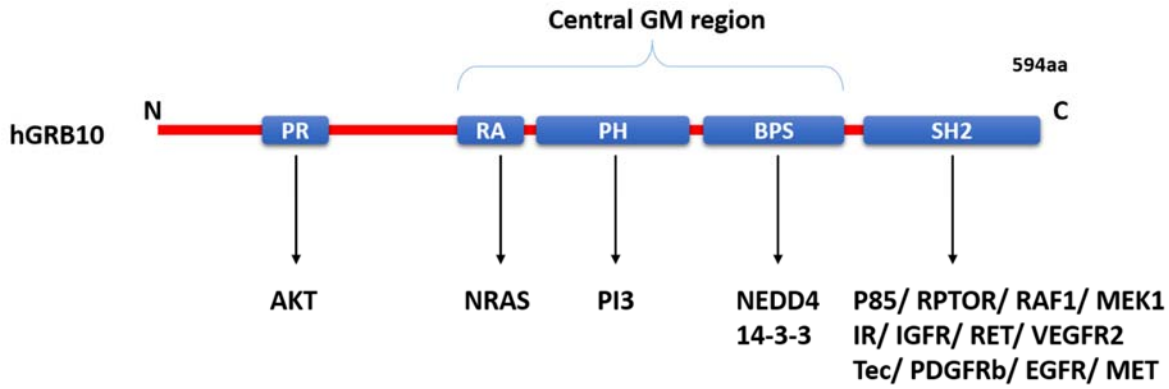

Figure 1.2. The structure of the human GRB10 protein and its reported interacting proteins.

The human GRB10 protein contains an N-terminal Proline Rich (PR) region, a central GM (Grb and Mig) region consisting of a Ras-Associating domain (RA), a Pleckstrin Homology (PH) domain, and a Between PH and SH2 (BPS) domain, and a C-terminal Src Homology 2 (SH2) domain. Through its functional domains, GRB10 can interact with multiple pathways and proteins and plays a critical role in cell signaling transduction. N: the amino-terminus; C: the carboxyl-terminus; aa: amino acids.

1.3.3 Role of GRB10 in Human Cancers

In human cancers, GRB10 is mostly studied in leukemia. GRB10 expression was reported to be significantly upregulated in acute myeloid leukemia (AML), and its elevated expression is correlated with cancer relapse and poor prognosis [210, 213]. Moreover, higher expression of GRB10 was also observed in the arsenic trioxide-resistant Jurkat acute T cell leukemia cell line, suggesting that its elevated expression could drive treatment resistance [214]. Mechanistically, GRB10 was found to directly bind to an

oncogenic tyrosine kinase fusion protein, BCR-ABL, which is found in all chronic myeloid leukemia (CML) as well as a subset of AML and acute lymphoblastic leukemia (ALL) [215, 216]. The interaction supports the function of BCR-ABL, while abrogation of GRB10 could reduce cancer cell proliferation and induce apoptosis both *in vitro* and *in vivo* [215, 216]. FLT3, a growth factor receptor involved in hematopoiesis and a commonly mutated gene contributing to AML development [217], was also reported to interact with GRB10 [210]. It has been shown that the interaction between FLT3 and GRB10 promote AKT phosphorylation and STAT5 activation, which increased AML cell proliferation, survival, and colony formation [210].

The role of GRB10 in solid cancers is under-studied. In several large-scale microarray studies of clinical samples, we, along with other groups, found that GRB10 was upregulated in colorectal cancer [218, 219] and CRPC [164, 220] but downregulated in thyroid cancer [221], hepatocellular carcinoma [222], and adrenocortical tumors [223]. However, the precise functions and the molecular mechanisms of GRB10 in these tumors remain unclear. In this dissertation, we are the first to report the involvement of GRB10 in PCa, the regulation of its expression, and the mechanism of GRB10-mediated CRPC development.

1.4 Thesis Theme and Rationale

CRPC poses a significant challenge in the clinical management of advanced PCa. Although increasingly-powerful ARPIs such as ENZ and ABI have shown promising

results in the clinic, the cancers commonly return in a lethal, resistant form. As a result, there is an urgent need for a deeper understanding of the molecular mechanisms driving CRPC development such that more highly effective therapeutics can be developed.

To study the mechanisms of CRPC and to develop new therapeutics, reliable, clinically-relevant cancer models are of paramount importance. We have established over 45 high-fidelity PCa PDX models derived from clinical specimens [151]. Importantly, we overcame the significant obstacles in developing PDX models from clinical HNPC tissues and have successfully developed 11 HNPC PDXs (http://www.livingtumorlab.com/index.html). These clinically-relevant models not only retain the histopathological and molecular characteristics of the parental patient tumors, they also recapitulate the clinical disease progression from HNPC to CRPC after host castration [151, 164]. Therefore, these “next-generation” models provide unique tools for studying mechanisms underlying CRPC development and discovering novel drivers for the disease.

By comparing the gene expression data between the paired HNPC and CRPC PDX models, we have identified GRB10 as a potential driver of CRPC development. Next, we validated our finding that upregulation of GRB10 in CRPC was clinically relevant. We further investigated the pro-proliferation function of GRB10 in PCa cell lines. We were also the first to confirm that GRB10 is transcriptionally regulated by the androgen receptor. Finally, we explored the function of GRB10 in PCa by studying the transcriptomic changes

induced by GRB10-knockdown, describing the GRB10 interactome, and clarifying the function of these interactions in the development of CRPC.

The overall objective of this study is to discover the role of GRB10 in the development of CRPC and to elucidate the associated molecular mechanisms involved in driving the deadly disease.

1.5 Hypotheses and Specific Aims

The **hypotheses** of what constitutes a CRPC driving gene are as follows: (1) CRPC driving genes are commonly expressed in CRPC, (2) CRPC driving genes are upregulated following castration as an early and continuous event, and (3) CRPC driving genes remain upregulated after CRPC development. (Fig 1.3)

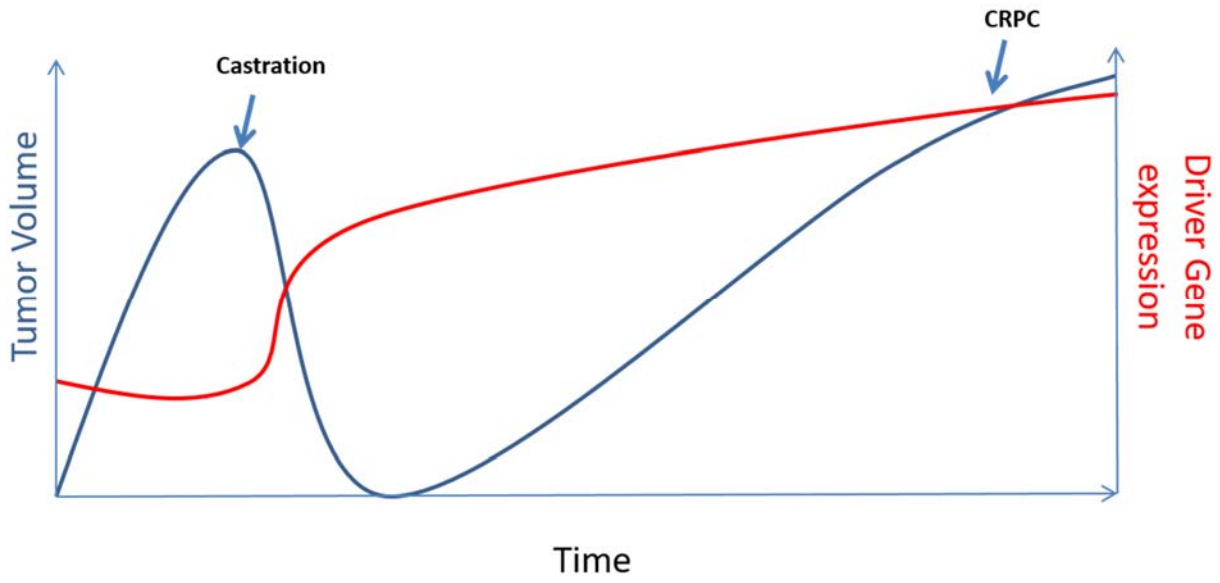

Figure 1.3. Hypothetical characteristics of a CRPC driving gene

The expression of CRPC driving genes should be upregulated after castration treatment as an early and continuous event.

Accordingly, we propose the following Specific Aims:

Specific Aim 1: To identify potential CRPC driving genes using high-fidelity HNPC-to-CRPC PDX models;

Specific Aim 2: To investigate the functional role of the identified driving gene;

Specific Aim 3: To explore the mechanisms associated with the identified driving gene by analyzing its direct upstream/ downstream pathways and its role in biological processes in PCa.

Chapter 2 Materials and Methods

2.1 SRC grafting and development of transplantable HNPC lines

All 10 PDX PCa tissue lines used in this study were established and maintained in non-obese diabetic (NOD)/SCID mice (NOD.CB17-Prkdcscid/J). PCa specimens were obtained from patients following a protocol approved by the Clinical Research Ethics Board of the University of British Columbia and the BC Cancer Agency (all patients signed a consent form approved by the Ethics Board). Patient HNPC tissues were cut into pieces ($1 \times 3 \times 3$ mm^3) and grafted into the SRC site of male NOD/SCID mice supplemented with testosterone. After 3 to 6 months (or earlier if reaching humane endpoint is reached), the host mice were sacrificed in a CO_2 chamber. Tumors were then harvested and regrafted into another set of NOD/SCID mice at the SRC site. At each passage, a sample of the xenografts were also harvested, measured, and fixed for histopathologic analysis.

2.2 Histopathology and Immunohistochemistry

Tumor specimens were fixed in 10% neutral-buffered formalin and embedded in paraffin. Blocks were cut into 5 μm-thick sections and mounted on glass slides. For histopathology analyses, the slides were de-waxed in Histoclear (National Diagnostic) and hydrated in graded alcohol and water for hematoxylin and eosin staining. IHC staining was carried out using anti-AR (Abcam, ab108341, 1:100), anti-PSA (Santa Cruz, sc-7638, 1:100) and anti-Ki67 (Thermo Fisher, RM-9106, 1:100). Biotinylated secondary antibody (Vector Laboratories) peroxidase-linked avidin/biotin complex reagents (Vector Laboratories) and diaminobenzidine (DAB, Sigma-Aldrich) were used for staining.

The staining intensities of Ki67, AR and PSA were evaluated independently by two pathologists, Dr. Dong Lin and Dr. Xin Dong. Ki67 was scored by averaging the percentage of positively stained tumor cells in 10 random high-power fields. The final expression index of AR and PSA was calculated by multiplying the intensity of staining (0 = no staining, 1 = low, 2 = moderate, and 3 = high) with the percentage of positively stained tumor cells.

2.3 Gene Set Enrichment Analysis (GSEA)

Gene Set Enrichment Analysis (GSEA) (http://www.broad.mit.edu/gsea/) was used to determine whether AR signaling was significantly and concordantly different between PDX tumors before and after host castration [224]. Microarry normalization was performed by Dr. Anne M. Haegert. Normalized transcriptomic data were used for GSEA analysis. The gene sets used in ths study were downloaded from the Molecular Signature Database (MSigDB) provided by GSEA.

GSEA was also used to determine whether a defined set of genes show significant, concordant differences between two treatment groups (e.g. shC vs. shGRB10). All GSEA analyses in those studies used whole transcriptomic data without expression level cut-offs as the expression datasets. Normalized values were used to generate pre-ranked gene lists based on p-value from lowest to highest. Unbiased analysis was performed using the latest MSigDB database for each collection. Gene set permutation was applied.

False discovery rate (FDR) q values were calculated using 1000 permutations, and a geneset was considered significantly enriched if its normalized enrichment score (NES) has an FDR q below 0.05.

2.4 Cell lines and Stable *GRB10*-knockdown/overexpression cell line construction using viral-based approaches

LNCaP, C4-2, and 293T cell lines were obtained from the American Type Culture Collection (ATCC). LNCaP and C4-2 cells were maintained in RPMI-1640 medium (Hyclone) supplemented with FBS (10%) (Gibco). 293T cells were maintained in DMEM medium (Hyclone) containing 5% FBS (Gibco). ENZ-resistant MR49F PCa cells were maintained in RPMI-1640 medium with 5% FBS, supplemented with 10 μM ENZ [3].

Two shRNAs targeting GRB10 were obtained from Dharmacon (TRCN0000063683 and TRCN0000063686). Lentiviruses containing GRB10-targeting shRNA were produced by transient transfection of 293T cells using the Lipofectamine 3000 following the manufacturer's protocol (Thermo Fisher). Culture media of 293T cells were collected 72 hours after transfection and then filtered and applied to LNCaP and C4-2 cultures for transduction. GRB10-knockdown cells were selected and maintained using 1 μg/ml puromycin (Gibco).

The GRB10 coding sequence was cloned from the plasmid "pRK5 Flag Grb10 wt long", a gift from Dr. David Sabatini (Addgene plasmid # 37481) [211], using primers listed in Appendix A. It was then inserted into the pLNCX retroviral vector (Clontech).

Retroviruses expressing GRB10 were produced by transient transfection of 293T cells. Culture media of 293T cells were collected 72 hours after transfection and then filtered and applied to LNCaP for transduction. GRB10-overexpressed cells were selected and maintained using 150 ug/ml Hygromycin B (Thermo Fisher).

2.5 Transient GRB10 knockdown using siRNA

SMARTpool ON-TARGETplus GRB10 siRNA (Dharmacon) was used to transiently knock down GRB10 in MR49F cells. Lipofectamine RNAiMAX was used following the manufacturer's protocol. Cell proliferation assays were performed one day following transfection.

2.6 Total RNA Isolation, Reverse Transcription and Quantitative Real Time-PCR (qRT-PCR)

Total RNA was extracted from cultured cells or PDX tissues using the RNeasy Mini Kit (Qiagen) following the manufacturer's protocol. One µg of total RNA was used to synthesize cDNA using the QuantiTect Reverse Transcription Kit (Qiagen). qRT-PCR was performed using the ABI ViiA 7 Real-Time PCR system (Applied Biosystems) with KAPA SYBR Fast Universal Master Mix (Kapa Biosystems). Primers used in the study are listed in Appendix A. Relative gene expression was calculated using the 2-ΔΔct method with GAPDH as an internal reference gene.

2.7 Western Blotting

Total protein from cultured cells or PDX tissues was isolated using RIPA lysis buffer (50 mM Tris-HCl pH 7.4, 150 mM NaCl, 1% IGEPAL, 0.5% Na-deoxycholate, 0.1% SDS) supplemented with complete protease inhibitor cocktail (Roche) and PhosSTOP phosphatase inhibitor (Roche). Protein concentration was determined using the BCA protein assay (Thermo Fisher Scientific). Total protein samples were run on an 8% SDS polyacrylamide gel, transferred to a PVDF membrane with 0.45 μm pores (Millipore), and then incubated with primary antibodies overnight at 4℃ for Western blotting. The following antibodies were used: anti-GRB10 (Cell Signaling Technology, #3702, 1:1000), anti-AKT (Cell Signaling Technology, #2920, 1:1000), anti-phosphoSer473-AKT (Cell Signaling Technology, #4060, 1:2000), anti-Actin (Sigma, #A2066, 1:2000), anti-Vinculin (Sigma, V4505, 1:1000), anti-PP2Aa (Cell Signaling Technology, #2041, 1:1000), antiPP2Ab (Cell Signaling Technology, #2209, 1:1000), and antiPP2Ac (Cell Signaling Technology, #2259, 1:700).

2.8 MTS cell proliferation and EdU assay

Viable cell numbers were determined using the MTS CellTitre 96 Aqueous One Solution Cell Proliferation Assay (Promega) and Click-iT EdU Alexa Fluor 488 Imaging Kit (Thermo Fisher) following the manufacturer's protocols. For the MTS assay, cells were seeded into a 96-well culture plate (3000 cells/ well) either with regular medium or 10 μM ENZ-containing medium. The absorbance of reduced MTS was measured once every two days at O.D. 490 nm. The relative absorbance was calculated based on Day 0 readings. For the EdU assay, cells were seeded into a Nunc 8-well chamber slide

(Thermo Fisher) (10000 cells/ well) with either regular medium or 10 μM ENZ-containing medium. Two days later, the cells were fixed and stained with EdU following the manufacturer's protocol and imaged with an AxioObserver Z1 microscope (Zeiss) (10x magnification; 10 fields). EdU-positive cells (green), and Hoechst-stained cells (blue) were counted using ImageJ software (NIH, USA, http://rsbweb.nih.gov/ij/).

2.9 Cell cycle analysis

LNCaP, C4-2, and MR49F cells with GRB10 or control knockdown were seeded in six-well plates either with complete medium or with medium containing 10 μM ENZ. The cells were collected 72 hours later, washed twice with ice-cold PBS, fixed with ice-cold 70% ethanol overnight, and incubated with 25 μg/ml RNase (Sigma) and 50 μg/ml propidium iodide (PI, Invitrogen) at room temperature for 30 min. The DNA content was measured using FACSCanto II (BD) flow cytometry and analyzed with the FlowJo software (Tree Star).

2.10 Colony formation assay

Cells were seeded into a 12-well culture plate (100 cells/ well) for a 4-week incubation. They were then fixed with 4% paraformaldehyde (PFA) (Sigma) and stained with 0.5% crystal violet (Sigma). Stained cells were imaged with a digital camera and the number of colonies were counted manually.

2.11 Immunoprecipitation assay

An immunoprecipitation (IP) assay was performed using LNCaP cells transfected with Flag-GRB10 and AKT. The plasmids used for the transfections were plasmid “pRK5 Flag Grb10 wt long”, a gift from Dr. David Sabatini (Addgene plasmid # 37481) [211], and plasmid “pcDNA3.1-HA AKT1”, kindly provided by Jaewhan Song (Addgene plasmid # 78778) [225]. Both transfections were carried out using Lipofectamine 3000 (Thermo Fisher) following the manufacturer’s protocols. For the IP assay, GRB10/AKT and Flag/AKT transfected LNCaP cells were washed and lysed with NETN buffer (100 mM NaCl, 20 mM Tris-HCl pH8.0, 0.5 nM EDTA, 0.5 % v/v IGEPAL [Sigma]). Protein concentrations were then determined using the BCA protein assay (Thermo Fisher Scientific) and 5% of the input was collected. Then, 1 mg of protein from each sample was incubated with FLAG M2 magnetic beads (Sigma) at 4℃ overnight. The next day, magnetic beads were collected using a magnetic stand and washed 5 times with ice-cold NETN buffer. The beads were then boiled with SDS-PAGE sample-loading buffer for 3 min and analyzed via Western Blotting.

For endogenous IP, monoclonal mouse anti-GRB10 (C-11, Santa Cruz) was used. To block the interference of IgG heavy/ light chain on Western Blotting detection of target protein, VeriBlot for IP Detection Reagent (ab131366, Abcam) was used as secondary antibody.

2.12 Immunofluorescence (IF) and proximity ligation assay (PLA)

For IF assays, cells were counted and seeded into a Nunc 8-well chamber slide (Thermo Fisher) (5000 cells/ well) and incubated for 2 days with either regular medium or 10 μM ENZ-containing medium. Cells were then fixed, permeabilized and stained with both anti-GRB10 (1:50, Cell Signaling Technology, #3702), and anti-AKT (1:100, Cell Signaling Technology, #2920) antibodies; Secondary antibodies with Alexa Fluor 488 (1:1000) were obtained from Thermo Fisher. Slides were mounted using DAPI mounting solution (Vector Laboratories).

PLA assays were performed using the Duolink In Situ Red Starter Kit Mouse/Rabbit (Sigma) following the manufacturer's protocol. In brief, cells were treated, fixed, permeabilized, and incubated with primary antibody following the same protocol as used for the IF assay. The next day, secondary probe incubation, ligation, amplification reactions, and mounting were carried out following the manufacturer's suggestions. Both IF and PLA slides were imaged using an LSM 780 Confocal Microscope (Carl Zeiss).

2.13 Clinical Relevance Analysis

Clinical cohorts used in this study included Grasso et al. 2012 [67], TCGA 2015 [73], Varambally et al. 2015 [226], Ross-Adams et al. 2015 [227], and Robinson et al. 2015 [68]. Gene expression, protein expression, DNA copy number and clinical information of the TCGA cohort was obtained through cBioPortal [228, 229]. Gene expression and its correlation to progression free survival from the Cambridge [227], Stockholm [227], and MSKCC [230] cohort was obtained and visualized by camcAPP

[231]. For other cohorts, gene expression data were accessed from the Gene Expression Omnibus (GEO) database.

2.14 Chromatin Immunoprecipitation (ChIP)

ChIP assays were performed using the ChIP-IT High Sensitivity Kit (Active Motif) following the manufacturer's protocol. LNCaP cells were treated with either ethanol (vehicle control) or 10 nM R1881 for 16 hours before the assay. Cells were cross-linked with 1% formaldehyde (Sigma) for 10 min at room temperature. Chromatin was sonicated with a Microtip sonicator (Model 120, Fisher) to an average length of 400~800 bp. Sheared chromatin was then incubated with Pierce Protein A/G Agarose (Thermo Fisher) for 30 min at 4°C to remove nonspecific binding. 10% Input was collected. One µg Anti-AR antibody (Millipore, 17-10489) or normal rabbit IgG (Santa Cruz, sc2027) was used to immunoprecipitate cleared chromatin at 4°C overnight. The next day, precipitated chromatin samples were incubated for 3 hours with 20 µl Pierce protein A/G magnetic beads (Thermo Fisher) at 4°C followed by washing with washing buffer (5 times). Reverse cross-linking and DNA purification was performed using the ChIP-IT High Sensitivity Kit (Active Motif) following the manufacturer's protocol. The ChIP-PCR primers used are listed in Appendix A.

2.15 Luciferase reporter plasmid construction and dual luciferase reporter assay

The pGL3-Basic plasmid (Promega) was used as a backbone for luciferase reporter construction. The reported PSA enhancer and promoter region (-5752 to +10) was cloned and inserted using HindIII restriction enzyme into the pGL3-Basic (Fig. 2.1)

[232]. Briefly, potential AR binding sites in GRB10 intron regions, ARE1 (chr7: 50677642-50678150), ARE2 (chr7: 50657378-50657948), and ARE3 (chr7: 50653818-50654513), were cloned from 293T genomic DNA by PCR with primers listed in Appendix A. A PSA luciferase reporter plasmid containing the PSA promoter region PSAluc-ARE1, PSAluc-ARE2 and PSAluc-ARE3 were constructed by inserting amplified and purified ARE1, ARE2 and ARE3 PCR products into the multiple cloning sites of the PSA luciferase reporter plasmid at the 5' end of the PSA promoter insert. The restriction enzymes combinations of Nhe1/Mlu1, Mlu1/Sac1, and Xho1/Nhe1 (Thermo Fisher) were used. PSAluc-ARE2 plasmids with point mutations and deletions were amplified using PCR with primers listed in Appendix A.

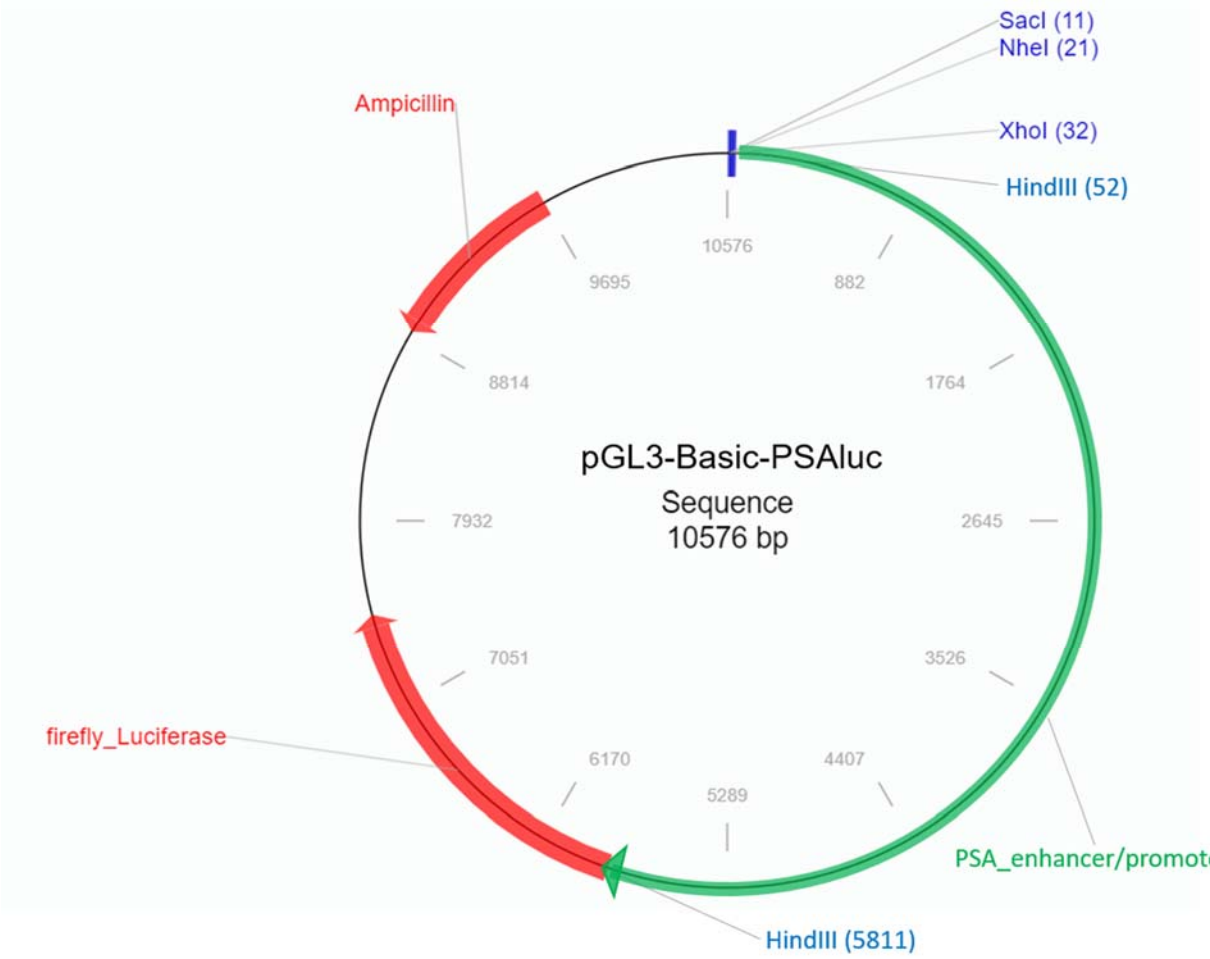

Figure 2.1 Illustration of structure of the pGL3-Basic-PSAluc plasmid

As illustrated, the pGL3-Basic-PSAluc luciferase reporter plasmid was constructed based on pGL3-Basic plasmid (Promega). The reported PSA enhancer and promoter region (-5752 to +10) was cloned and inserted using HindIII restriction enzyme into the multiple cloning site of the pGL3-Basic plasmid.

For dual luciferases reporter assays, 293T cells were seeded into 24-well culture plates (50000 cells /well) in triplicates for each experimental condition. 0.2 µg of luciferase reporter, 0.4 µg of pSG5-AR and 5 ng of pGL4.70 Renilla reporter (Promega) were

transfected together using Lipofectamine 3000 (Thermo Fisher). Cells were incubated with either EtOH or 10 nM R1881 overnight. Dual luciferase reporter assay was performed using Dual-Luciferase Reporter Assay System (Promega) following the manufacturer's instructions. Luciferase activity was measured using the Infinite 200Pro Microplate Reader (Tecan). Transfection efficiency was normalized to Renilla luciferase activity.

2.16 Transient AR knockdown using siRNA

SMARTpool ON-TARGETplus AR siRNA (Dharmacon) was used to transiently knock down AR in LNCaP cells. Lipofectamine RNAiMAX was used to perform the transfection following the manufacturer's protocol. RNA samples were collected two days after transfection.

2.17 Gene expression data profiling

Total RNA was extracted from stable GRB10-knockdown and control LNCaP cells using the RNeasy Mini Kit (Qiagen) following the manufacturer's protocol. The quality of the RNA samples was checked with the Agilent 2100 Bioanalyzer. Only samples with RNA Integrity Number (RIN) ≥8.0 were used for one-color labelling using Agilent's One-Colour Microarray-Based Gene Expression Analysis Low Input Quick Amp Labelling v6.0 (Agilent Technologies). Total RNA (100 ng) was used to generate cyanine-3-labelled cRNA. Two replicates from each sample group (shGRB10- or shControl-treated cells) were hybridized on Agilent SurePrint G3 Human GE 8x60K Microarray v2 (Design ID 039494). Arrays were scanned with an Agilent DNA Microarray Scanner at a 3 μm scan

resolution and data were processed with Agilent Feature Extraction 11.0.1.1. Processed signals were quantile normalized with Agilent GeneSpring 12.0. RNA quality control and microarray analysis were performed by the Laboratory for Advanced Genome Analysis at the Vancouver Prostate Centre, Vancouver, Canada.

2.18 Ingenuity Pathway Analysis (IPA)

The gene expression microarray dataset of GRB10-knockdown and control LNCaP cells were analyzed to identify upstream regulatory genes and significantly enriched Diseases and Bio Functions using the Ingenuity Pathway Analysis tool (IPA, Qiagen) following the developer's manual. Differentially expressed genes were selected based on the criteria that their student's t-test p-value between groups (i.e. shC vs. shGRB10) were below 0.05.

2.19 Liquid chromatography–mass spectrometry (LC-MS)

The LC-MS/MS assays were conducted at the Proteomics Core Facility at the University of British Columbia. Briefly, the immunoprecipitated samples on FLAG magnetic beads were boiled in SDS-PAGE loading buffer and ran in a 10% PAGE gel. Gel lanes were excised and destained overnight. Proteins in these gel pieces were in-gel digested [233] and cleaned up on STAGE tips [234]. After digestion, peptides from different samples were reductively dimethylated with differing isotopolouges of formaldehyde as described [235]. Triplex protein quantification based on stable isotope labeling by peptide demethylation was applied to cell and tissue lysates [235]. This

imparts a light (flag only samples) or heavy (flag-GRB10 samples) mass tag on the lysines and N-termini of peptides, which then can be mixed in equal ratios and analyzed concurrently in the mass spectrometer. Two ug of resuspended samples were loaded onto a nanoflow-LC-MS/MS system (Bruker Impact II Q-Tof, with Proxeon EasyLC system, featuring in-house packed 400mm x 50um integrated emitter columns) and run with 90-minute H_2O/ACN gradients. The mass spectrometer was operated in data-dependant MS/MS mode, with up to 15 MS/MS scans triggered from every MS scan. Data files were searched against the Uniprot human database and quantified using MaxQuant software v1.6.0.13 [236] with tryptic digestion specificity, default values for Bruker QToF data (including 1% FDR), and the duplex demethylation quantitation mode.

2.20 Statistical analysis

Statistical analysis was performed using the GraphPad Prism software. The statistical difference between two groups was analyzed using the Student's t-test (2-tailed, unpaired). A linear correlation between two groups was assessed using the Pearson correlation (95% confidence interval). Graphs for clinical data were presented in vertical scatter plots or box-and-whisker plots. In the vertical scatter plots, the middle line and error bars represent the mean and standard error of the mean (SEM) respectively. In the box-and-whisker plots, the middle line represents the median, the box represents the 5%-95% percentile values, and the whiskers show the highest and lowest values in the group. The Kaplan-Meier method was used for estimating progression-free survival curves. The Log-rank test was used to compare the curves between two groups of patients stratified on the basis of *GRB10* mRNA expression. Gene correlation analysis was also graphed

and calculated via Graphpad. Results with p-values lower than 0.05 are considered statistically significant. The level of significance is indicated by * for $p<0.05$, ** for $p<0.01$, *** for $p<0.001$, and **** for $p<0.0001$.

Chapter 3 Identification of GRB10 as a potential driver for the development of CRPC

3.1 Introduction

As AR signaling is the major contributor to the progression of HNPC, ADT is the most commonly used treatment for advanced PCa [55, 56]. However, in most cases, the tumor recurs in an androgen-independent manner within two years. These androgen-independent recurrent tumors were termed hormone-refractory PCas or, more recently, CRPCs. CRPC patients are treated with increasingly powerful ARPIs such as ENZ, DAR, and ABI. Unfortunately, these new therapies are only marginally effective [237]; as a result, there is an urgent need for a better understanding of molecular mechanisms driving the development of CRPC and for developing more effective therapeutics.

To better understand the mechanism of CRPC development, we aimed to identify potential CRPC driving-genes. In particular, the elevated expression of these genes will be evident initially and sustained into CRPC. Such genes would have a more critical function in CRPC development by inducing bypass pathways to circumvent the AR pathway, as opposed to genes whose elevated expression is solely involved in CRPC aggressive growth. Therefore, we proposed that CRPC driver genes should: (1) be upregulated in CRPC, (2) show elevated expression before and during the progression from HNPC to CRPC; and (3) be functionally essential for CRPC development.

To study this complex and challenging problem, a highly clinically-relevant model system is required to recapitulate the entire process of CRPC development and allow for the identification of early drivers of castration resistance. PDX models of HNPC that could develop into CRPC following ADT are powerful tools to identify such drivers [151, 157]. In our laboratory, using the SRC grafting technique, we have established over 45 transplantable PCa PDX lines modelling HNPC, CRPC, and NEPC tumors (www.livingtumorlab.com) [151]. In this study, we applied host castration to 10 of our HNPC PDX lines (Table 3.1). Following castration, seven of these lines developed recurrent CRPC tumors spontaneously. By longitudinally analyzing the gene expression profiles of these PDX lines before castration, at 12-weeks following castration, and after CRPC development, we obtained evidence that the *GRB10* gene fulfills the above criteria as a CRPC driver.

The *GRB10* gene encodes an adaptor protein, GRB10 (growth factor receptor-bound protein 10), that modulates the coupling of specific signaling pathways to cell surface receptor kinases [238]. Here, we provided evidence that GRB10 could be a driver of CRPC development and hence a potential therapeutic target for the disease.

	Original patient tumor information			Transplantable tumor line information					
PDX ID	Diagnosis	AR	PSA	Doubling time (days)	Androgen sensitivity	AR	PSA	PTEN	Development of CRPC after host castration
LTL310	AC	+	+	20-32	Yes	+	+	-/-	+
LTL311	AC	+	+	~10	Yes	+	+	-/-	+
LTLT313B	AC	+	+	11-20	Yes	+	+	-/-	+
LTLT313H	AC	+	+	11-13	Yes	+	+	-/-	+
LTL418	AC	+	+	17-19	Yes	+	+	+/+	+
LTL467	AC	+	+	14-25	Yes	+	+	-/-	+
LTL471	AC	+	+	6-11	Yes	+	+	+/+	ND
LTL484	AC	+	+	8-10	Yes	+	+	-/-	+
LTL508	AC	+	+	9-13	Yes	+	+	+/+	ND
LTL556	AC	+	+	11-15	Yes	+	+	-/-	ND

Table 3.1 Summary table of the PDX lines used in the study. AC: Adenocarcinoma; ND: Not detected.

3.2 Results

3.2.1 Early elevated expression of GRB10 in Prostate Cancer PDX models

To elucidate the molecular mechanisms underlying CRPC development, we applied castration to 10 HNPC PDX models established in our laboratory (Table. 3.1, Fig. 3.1A). Castration of tumor-bearing mice leads to a marked reduction in tumor volume within the first week accompanied by a substantial drop in host serum PSA levels (Fig. 3.1B). This mirrors the clinical response of PCas to ADT. Within a few months after castration, 7 of these tumor lines, such as the LTL-313B line, gave rise to castration-resistant tumors with increased host serum PSA levels (Fig. 3.1B). On the histopathological level, we checked the expression of AR, PSA, and Ki67 in LTL-313B samples collected before host castration, at various time points after host castration, and in recurrent tumors. After the first week of host castration, AR had diffused to the cytoplasm, and PSA and Ki67 expression had markedly decreased, indicative of reductions in AR transcriptional activity and cell proliferation (Fig. 3.1C, Table 3.2). After tumor recurrence (approximately four months later), the scores of these markers had returned beyond pre-castration levels, showing even higher expression of AR and PSA (Fig. 3.1C, Table 3.2).

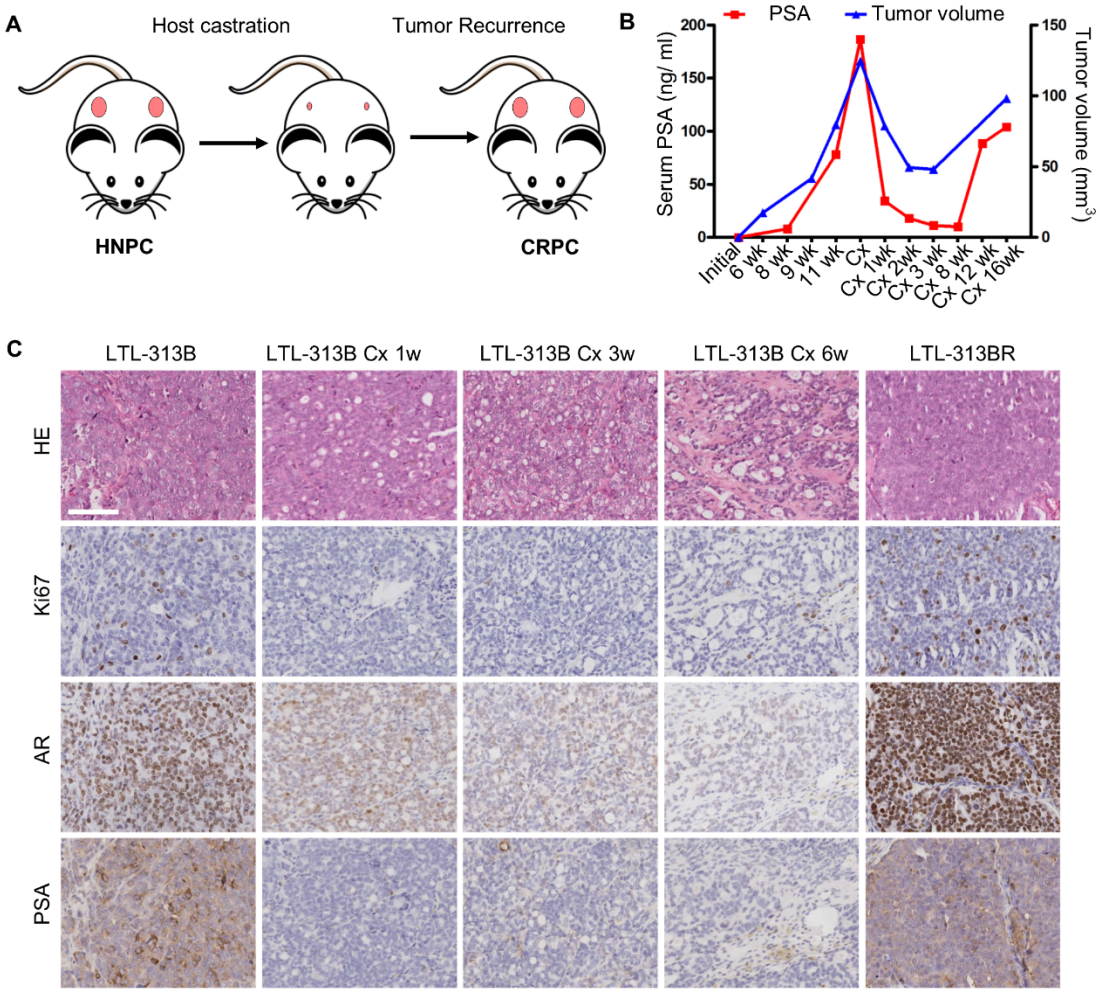

Figure 3.1 Use of hormone-naïve prostate cancer PDX models to identify potential CRPC driving genes

(**A**) As illustrated, surgical castration of a mouse bearing SRC PDXs (pink) of a patient's HNPC led to an initial reduction in tumor volume. A few months later, the tumor recurs, i.e. CRPC development. (**B**) Volumes of HNPC LTL-313B xenografts and mouse serum PSA levels at various time points before, during, and after castration-induced CRPC development. (**C**) Hematoxylin and eosin staining of LTL-313B tumor sections, as well as the levels of Ki67, AR and PSA in tumor sections (determined via

immunohistochemistry) at various time points before host castration and after host castration, and in recurrent tumors. Scale bar indicates 100 μm.

	Pre	Cx 1w	Cx 3w	Cx 6w	Relapse
Ki67 (%)	5.62±0.46	0.14±0.07	0.20±0.06	2.21±0.42	5.80±0.36
AR (score)	2.7	1.1	1.2	2.1	2.85
PSA (score)	2.3	0.1	0.1	0.2	2.9

Table 3.2 The summary of IHC scores in LTL-313B PDX models at various time points after host castration. The percentage of Ki67 positive cells and the IHC scores of AR and PSA in each tumor sample, with representative images shown in Fig. 3.1. Ki67 positive percentage was calculated by the ratio of the number of positively stained cells to the total cell number, shown with mean ± SEM. The IHC score of AR and PSA was calculated by multiplying the intensity of staining (0 = no staining, 1 = low, 2 = moderate, and 3 = high) with the percentage of positively-stained tumor cells. Ten random high-power fields were used.

Among the 10 HNPC PDX lines we used in the study, 7 of them developed into CRPC after host castration (Table 3.1). To identify potential driver genes of CRPC development, we first analyzed gene expression differences between the 7 pairs of CRPC tumor lines and their parental HNPC lines. Consistently upregulated genes in all seven pairs were then ranked based on their statistical significances between pooled HNPC

lines and CRPC lines. Eighty genes were identified to be significantly upregulated in CRPC ($p<0.05$; Fig. 3.2A, Appendix B). Next, we checked the expression of these 80 genes in all 10 HNPC PDX lines at 12 weeks after castration. At this time point, the tumors have not fully relapsed to CRPC, as indicated by the sustained inhibition of AR signaling suggested by GSEA (Fig. 3.2C-F). Of these 80 genes, *GRB10* was the top-ranked gene based on the statistical significances between HNPCs and 12-week castrated samples (Fig. 3.2B, Appendix B). Therefore, this datum demonstrates that GRB10 is not only upregulated in CRPC tumors but is also increased before CRPC fully develops, suggesting that it is a potential early driver of CRPC development (Fig. 3.2D).

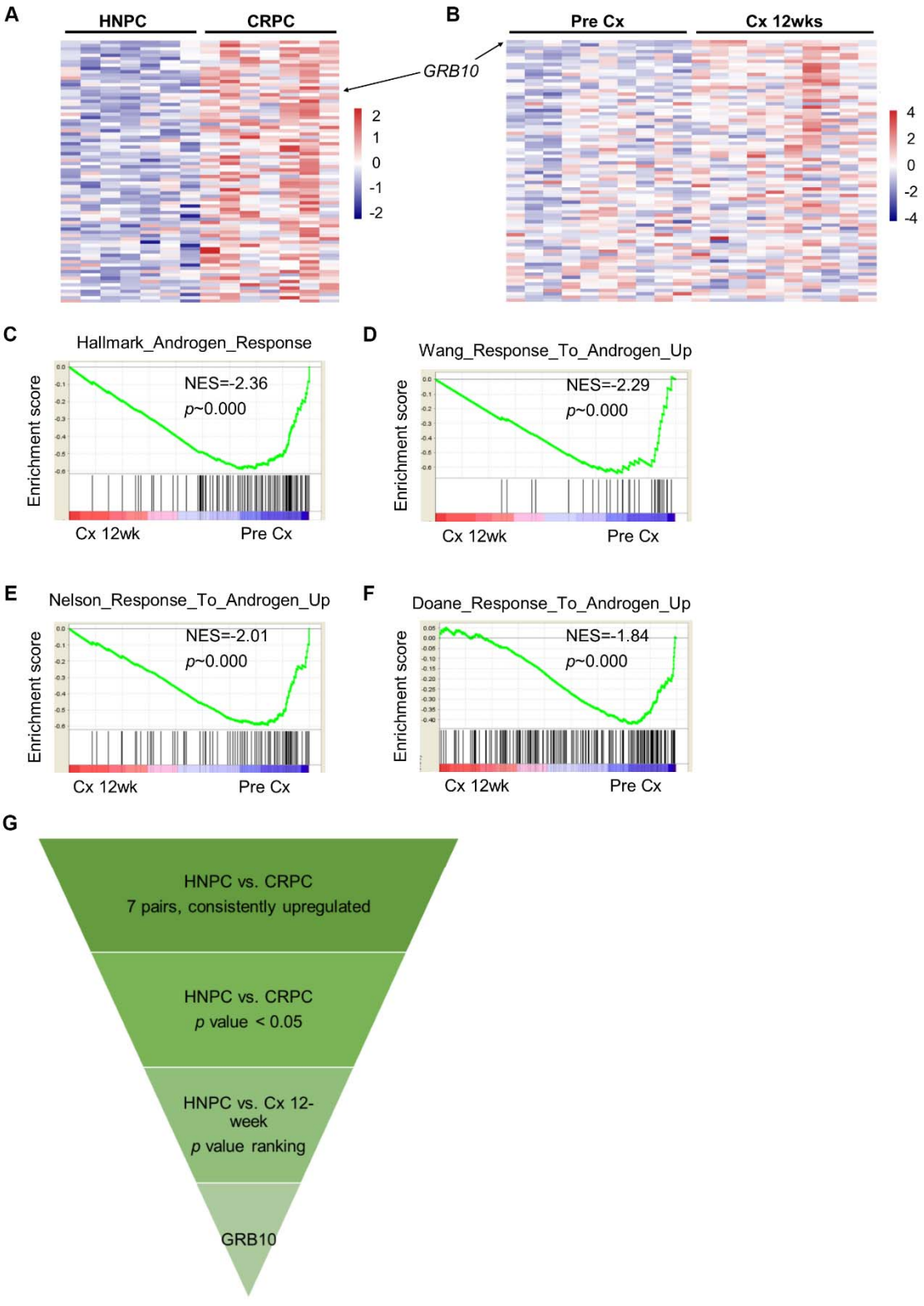
A
HNPC
CRPC
GRB10
2
1
0
-1
-2
B
Pre Cx
Cx 12wks
4
2
0
-2
-4
C
Hallmark_Androgen_Response
NES=-2.36
p~0.000
Enrichment score
Cx 12wk
Pre Cx
D
Wang_Response_To_Androgen_Up
NES=-2.29
p~0.000
Enrichment score
Cx 12wk
Pre Cx
E
Nelson_Response_To_Androgen_Up
NES=-2.01
p~0.000
Enrichment score
Cx 12wk
Pre Cx
F
Doane_Response_To_Androgen_Up
NES=-1.84
p~0.000
Enrichment score
Cx 12wk
Pre Cx
G
HNPC vs. CRPC
7 pairs, consistently upregulated
HNPC vs. CRPC
p value < 0.05
HNPC vs. Cx 12-week
p value ranking
GRB10

Figure 3.2 Identification of GRB10 as a potential driver of CRPC development

(**A**) A heat map showing that 80 genes were significantly upregulated in in 7 CRPC PDX lines compared to their parental HNPCs. (**B**) A heat map showing *GRB10* as the most consistently upregulated gene following host castration of the 80 identified genes. Genes ranked according to p-value (Student's t-test). A detailed list of genes and gene expression changes used in Figures 3.2A and 3.2B is shown in Appendix B. (**C-F**) Sustained inhibition of AR signalling in PDX tumors at 12 weeks post host-castration as shown by GSEA. AR–related gene sets were analyzed using transcriptomic data of 10 pooled HNPC PDX lines at pre-castration and 12 weeks following castration. (**G**) A flow chart summarizing the strategy used to identify the potential early driver of CRPC development. Briefly, genes which are consistently upregulated in the CRPC tumour compared to their own parental HNPC tumour in the 7 pairs of PDX models were selected. The p-value of each gene comparing pooled CRPC to HNPC PDX lines was calculated. Eighty genes were found to be consistently and significantly upregulated in CRPC. Next, the p-values of these 80 genes when comparing HNPC PDX tumors at 12 weeks following castration to their parental lines were determined. Finally, among these 80 genes, GRB10 was identified to be the most significantly upregulated gene (lowest p-value) at 12 weeks following castration. Cx: host castration treatment; NES: normalized enrichment score; p: nominal p-value.

Next, we validated our findings from high-throughput microarray data using RT-PCR and Western Blot. *GRB10* mRNA expression was significantly elevated in post-castration PDX samples (Fig. 3.3A). Furthermore, we checked *GRB10* mRNA expression

in the LTL-313B tumor line during the development of CRPC. As shown in Figure 3.3B, the *GRB10* mRNA expression was markedly elevated following castration and remained at a high level during CRPC development and at the CRPC stage (i.e. in LTL-313BR tumor tissue). Similarly, GRB10 protein levels were significantly higher in CRPC samples than in the parental samples (Fig. 3.3C, D).

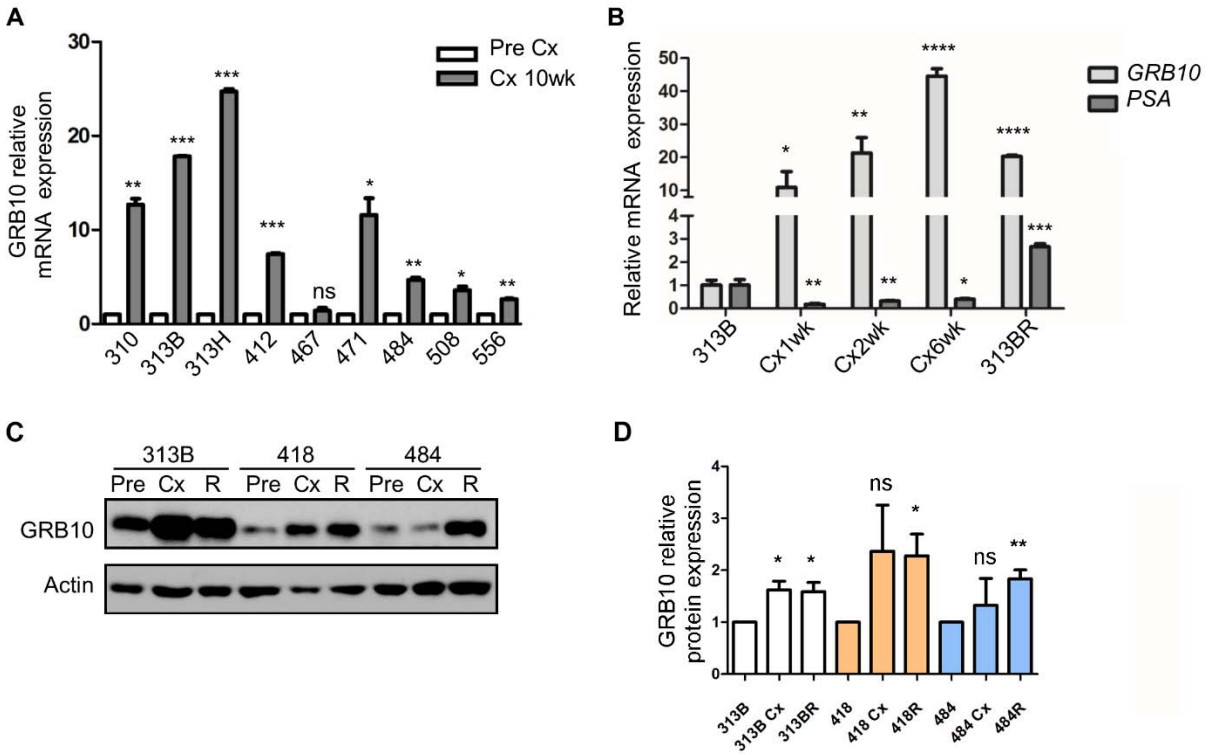

Figure 3.3 Elevated expression of GRB10 in prostate cancer PDX

(**A**) Effects of host castration on the expression of *GRB10* in multiple PDX HNPC lines as determined by qRT-PCR; *p*-values for each tumor line were determined relative to its parental tumor. The results are presented as means ± SEM. (**B**) *GRB10* and *PSA* mRNA expression in the LTL-313B tumor line were determined by qRT-PCR at various time points after host castration; *p*-values for each sample were determined relative to parental tumors. Results are presented as means ± SEM. (**C**) GRB10 protein expression in LTL-313B, LTL-418, and LTL-484 tumor tissues before castration, 10 weeks after castration and after CRPC development were assessed by Western Blotting. (**D**) Relative band density of Western Blotting results shown in Fig. 3.3C were quantified using ImageJ (NIH, USA, https://imagej.nih.gov). GRB10 protein expression was normalized by Actin as

internal control. Bar graphs show mean ± SEM. The p-values were calculated by unpaired two-tail Student's t-tests comparing tumor samples collected 12 weeks following castration and recurrent CRPC tumors with parental untreated tumors based on three replicated experiments. Pre: pre-castration; Cx: castration; wk: weeks after castration; R: CRPC.

3.2.2 Elevated expression of GRB10 in clinical CRPC tissues

To further validate whether our discovery that GRB10 is elevated in CRPC was clinically relevant, we checked the expression of GRB10 in publically available clinical gene expression data [9]. In reported clinical PCa cohorts, we found that the expression of *GRB10* in clinical CRPC samples was significantly elevated compared to HNPC and benign prostate samples [67, 226, 227] (Fig. 3.4A-C). Additionally, patients exhibiting elevated *GRB10* expression show a shorter progression-free survival time, which suggests that the expression of *GRB10* could be a potential prognostic biomarker (Fig. 3.4D).

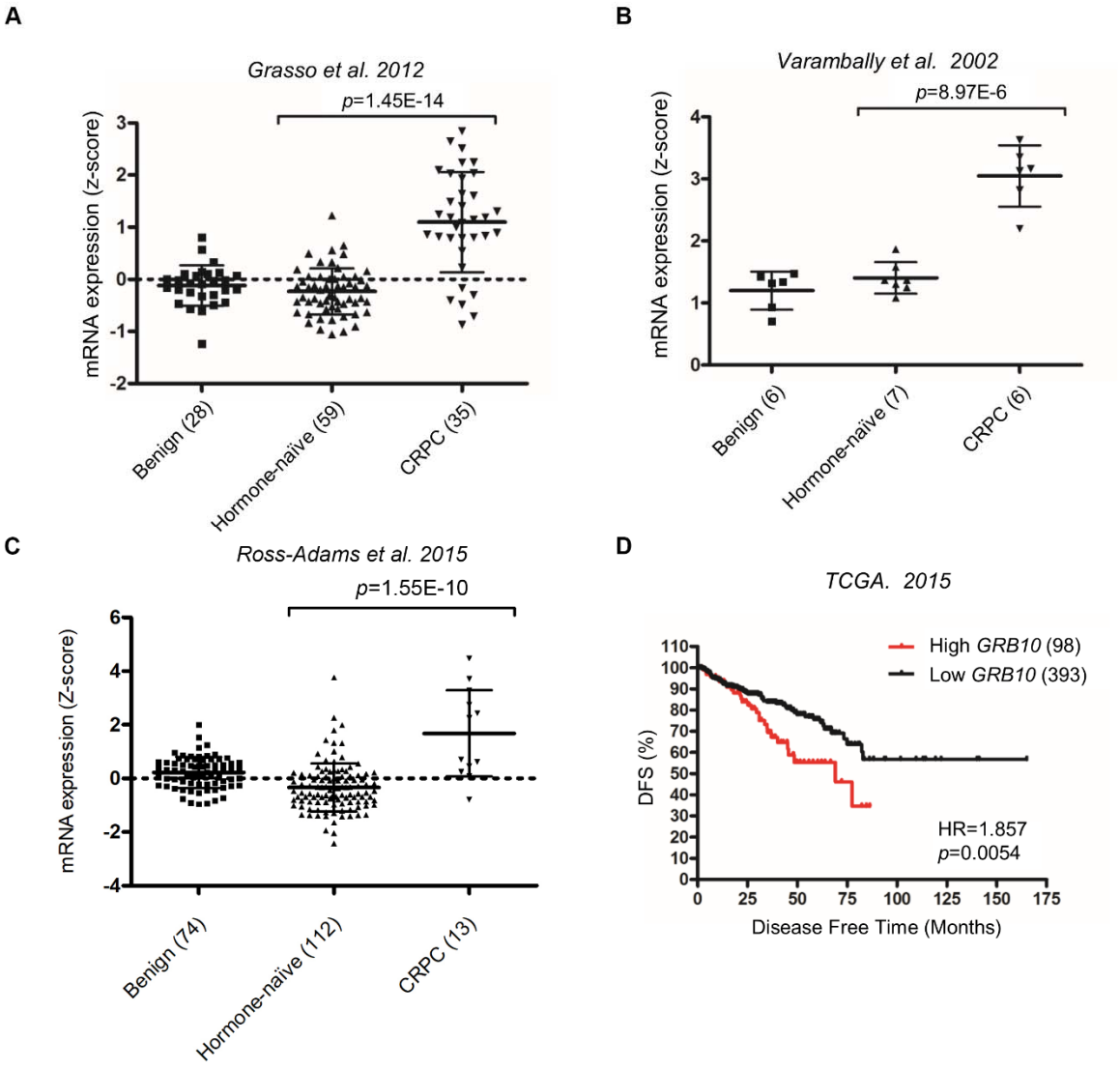

Figure 3.4. Elevated expression of GRB10 in clinical CRPC tissues

(**A**-**C**) *GRB10* mRNA expression of benign prostate tissues, HNPC tissues, and CRPC tissues were derived from *Grasso et al. 2012* (**A**), *Varambally et al. 2002* (**B**), and *Ross-Adams et al. 2015* (**C**) clinical PCa cohorts. The vertical scatter plots show means ± SEM. (**D**) Kaplan-Meier plots indicate disease-free survival times of PCa patients grouped according to *GRB10* expression. Significance between the groups was analyzed by the log-rank test.; DFS: disease-free survival; HR: hazard ratio; ns: not significant.

3.2.3 GRB10 gene silencing reduces in vitro cell proliferation of prostate cancer cells

To study the function of GRB10 in PCa, we performed *GRB10*-knockdown using two independent GRB10-targeting shRNAs which target the *GRB10* extron and 3'UTR. First, we checked the expression of GRB10 in seven commonly used benign prostate and PCa cell lines. We found that *GRB10* was expressed at the highest level in AR+ LNCaP and C4-2 cells (Fig. 3.5A). As such, we subsequently utilized these two cell lines to investigate GRB10's cellular functions. We constructed GRB10 stable knockdown LNCaP and C4-2 cells using two independent shRNAs and validated the knockdown efficiency at both the mRNA and protein levels (Fig. 3.5B-D).

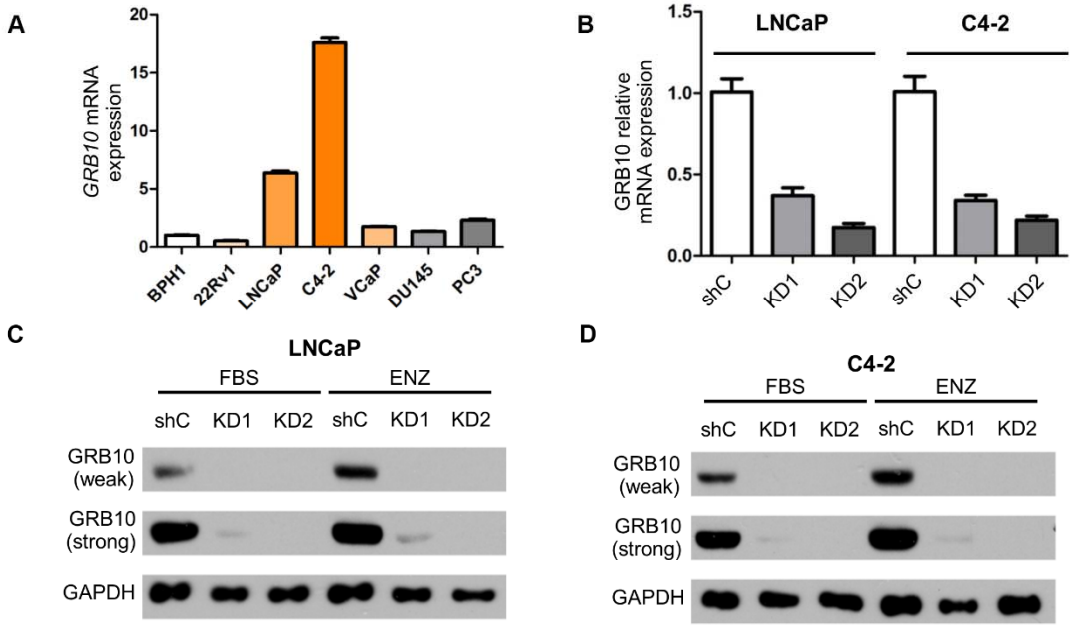

Figure 3.5. Construction of GRB10 stable knockdown LNCaP and C4-2 cells

(**A**) Endogenous GRB10 mRNA expression in multiple PCa cell lines was determined using qPCR and normalized relative to BPH1. Cells were supplemented with 10% FBS. Bar graph shows mean ± SEM. (**B-D**) Effects of GRB10 knockdown on the expression of GRB10 at both the mRNA and protein level in LNCaP and C4-2 cells.

Then, we examined the function of *GRB10* in LNCaP and C4-2 cells. Knockdown of *GRB10* led to inhibition of LNCaP and C4-2 cell proliferation (Fig. 3.6A, B). Combining *GRB10* knockdown and treatment with ENZ led to increased inhibition of cell proliferation (Fig. 3.6A, B). Moreover, knockdown of *GRB10* restricted the ability of these PCa cells to form colonies, especially when combined with ENZ treatment. (Fig. 3.6C, D).

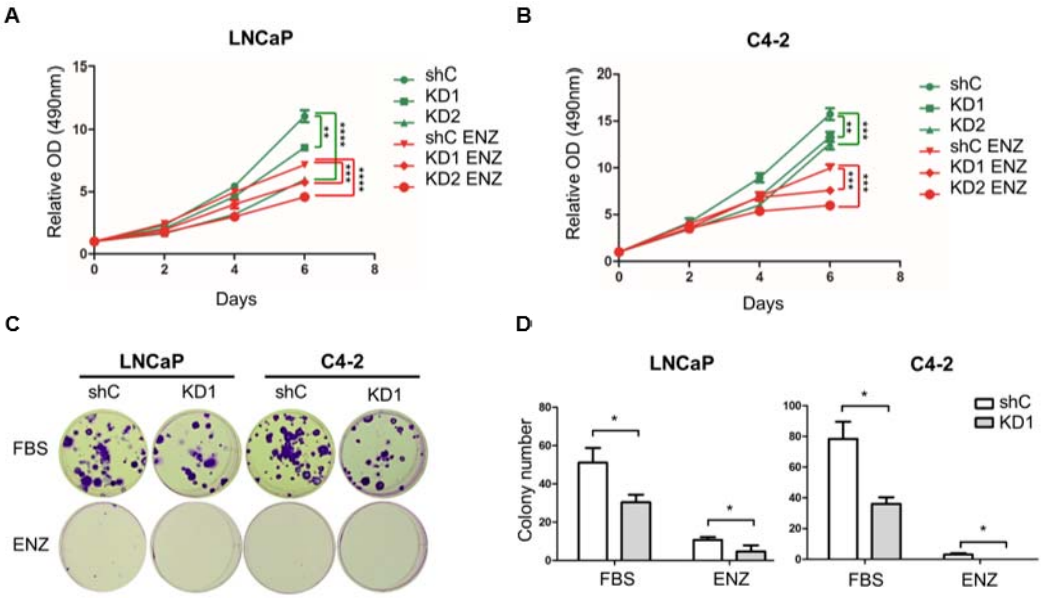

Figure 3.6. *GRB10* knockdown inhibited the proliferation and colony formation abilities of LNCaP and C4-2 cells

(**A, B**) The potential function of GRB10 in the proliferation of LNCaP and C4-2 cell lines was assessed using stable *GRB10* knockdown (KD1, KD2) and control (shC) cells by means of the MTS cell proliferation assay. The effect of ENZ (10 μM) treatment (in red) was also determined. O.D. values at 490 nm were normalized based on Day 0 readings. Results are presented as means ± SEM. (**C, D**) Effects of *GRB10* knockdown on colony formation ability were determined; cells were seeded into 6-well plates (100 cells/well) and incubated for 4 weeks. Colonies were then stained with crystal violet and imaged; representative images are shown. Bars (colony number of each sample) show means ± SEM. shC: control shRNA stable transfected cells; KD1: *GRB10* stable knockdown cell line 1; KD2: *GRB10* stable knockdown cell line 2; ENZ: Enzalutamide.

We further investigated the role of GRB10 in cell proliferation and found that GRB10 was critical for cell cycle progression. Knockdown of *GRB10,* regardless of ENZ treatment, led to decreased DNA synthesis as indicated by decreased number of cells undergoing DNA replication (Fig. 3.7A, B). Consistantly, *GRB10* knockdown induced G0/G1 cell cycle arrest as measured by increased population of cells in G0/G1 phase by flow cytometry (Fig. 3.7C-F). These data indicated that the decrease in proliferation of *GRB10*-knockdown cells could be caused by delayed cell cycle progression.

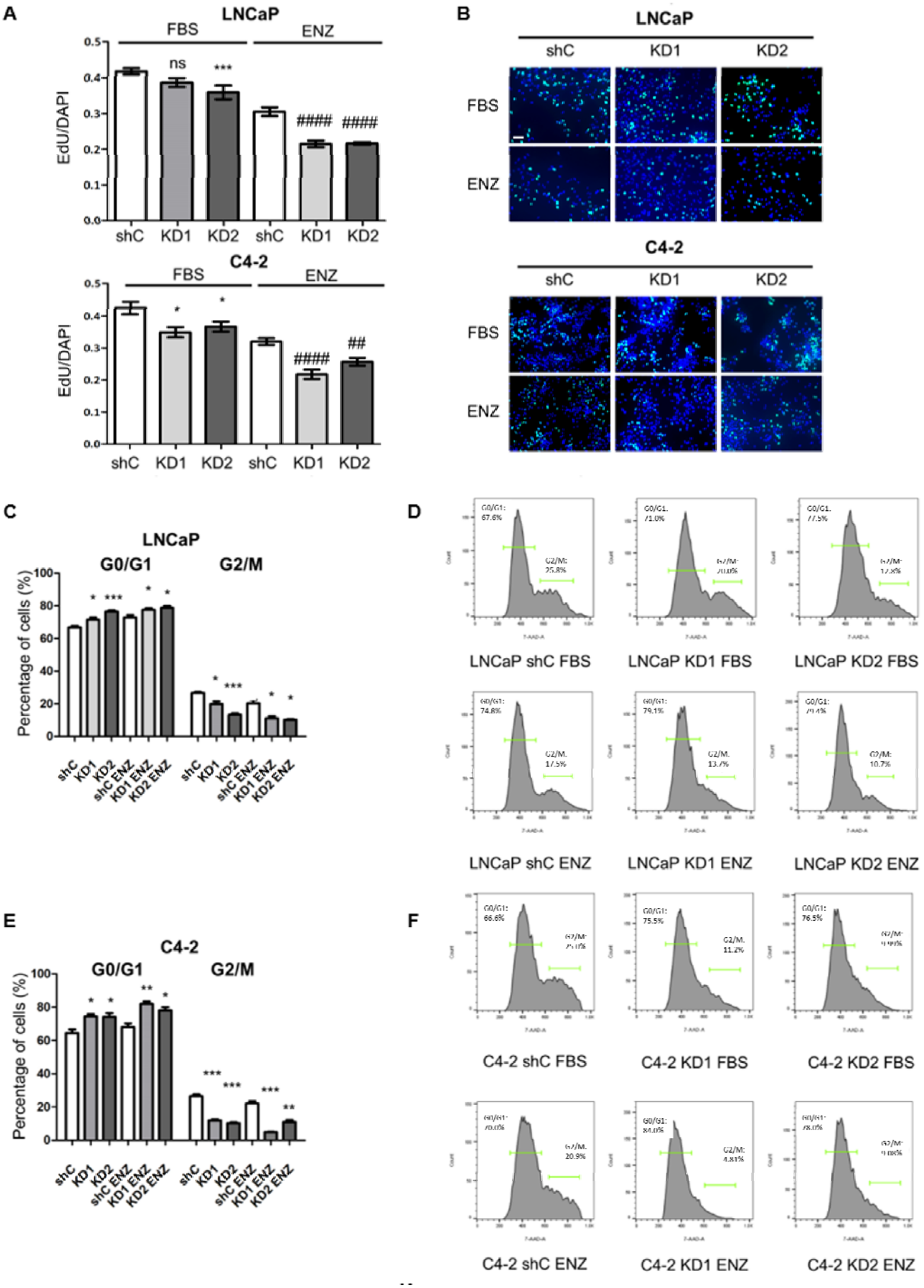
A
LNCaP
FBS
ENZ
EdU/DAPI
ns
***
####
####
shC
KD1
KD2
shC
KD1
KD2
C4-2
FBS
ENZ
EdU/DAPI
*
*
####
##
shC
KD1
KD2
shC
KD1
KD2
B
LNCaP
shC
KD1
KD2
FBS
ENZ
C4-2
shC
KD1
KD2
FBS
ENZ
C
LNCaP
G0/G1
G2/M
Percentage of cells (%)
shC
KD1
KD2
shC ENZ
KD1 ENZ
KD2 ENZ
D
LNCaP shC FBS
LNCaP KD1 FBS
LNCaP KD2 FBS
LNCaP shC ENZ
LNCaP KD1 ENZ
LNCaP KD2 ENZ
E
C4-2
G0/G1
G2/M
Percentage of cells (%)
F
C4-2 shC FBS
C4-2 KD1 FBS
C4-2 KD2 FBS
C4-2 shC ENZ
C4-2 KD1 ENZ
C4-2 KD2 ENZ

Figure 3.7. *GRB10* knockdown inhibits DNA synthesis and cell cycle progression of prostate cancer cells

(**A, B**) Effects of *GRB10* knockdown on DNA synthesis were determined using an EdU assay; cells were incubated for 4 hours with 10 μM EdU. EdU-labeled cells (green) and total cell numbers counterstained with DAPI (blue) were counted with 10 images taken at 10-fold magnification. Bars (EdU positive/total cells) show means ± SEM. Representative images are shown with a 100-μm scale bar. (**C, E**) Effects of GRB10 knockdown on cell cycle progression in LNCaP (**C**) and C4-2 (**E**) cells were measured using propidium iodide staining and flow cytometry. Data are presented as mean ± SEM. (**D, F**) Cell cycle distributions were analyzed and visualized using the FlowJo software. Percentages of cells in G0/G1 phase and G2/M phase are labeled. shC: control shRNA stable transfected cells; KD1: *GRB10* stable knockdown cell line 1; KD2: *GRB10* stable knockdown cell line 2; ENZ: Enzalutamide; EdU: Ethynyl Deoxyuridine; DAPI: 4',6-Diamidino-2-Phenylindole.

Since ARPI resistance commonly develops, we then focused on studying whether GRB10 plays a role in ARPI resistance. MR49F is an ENZ-resisant PCa cell line isolated from a LNCaP xenograft after multiple rounds of ENZ treatment [113]. Transient depletion of *GRB10* led to significant inhibition of cell proliferation, DNA synthesis, and cell cycle progression similar to what we observed in LNCaP and C4-2 cells (Fig. 3.8A-E).

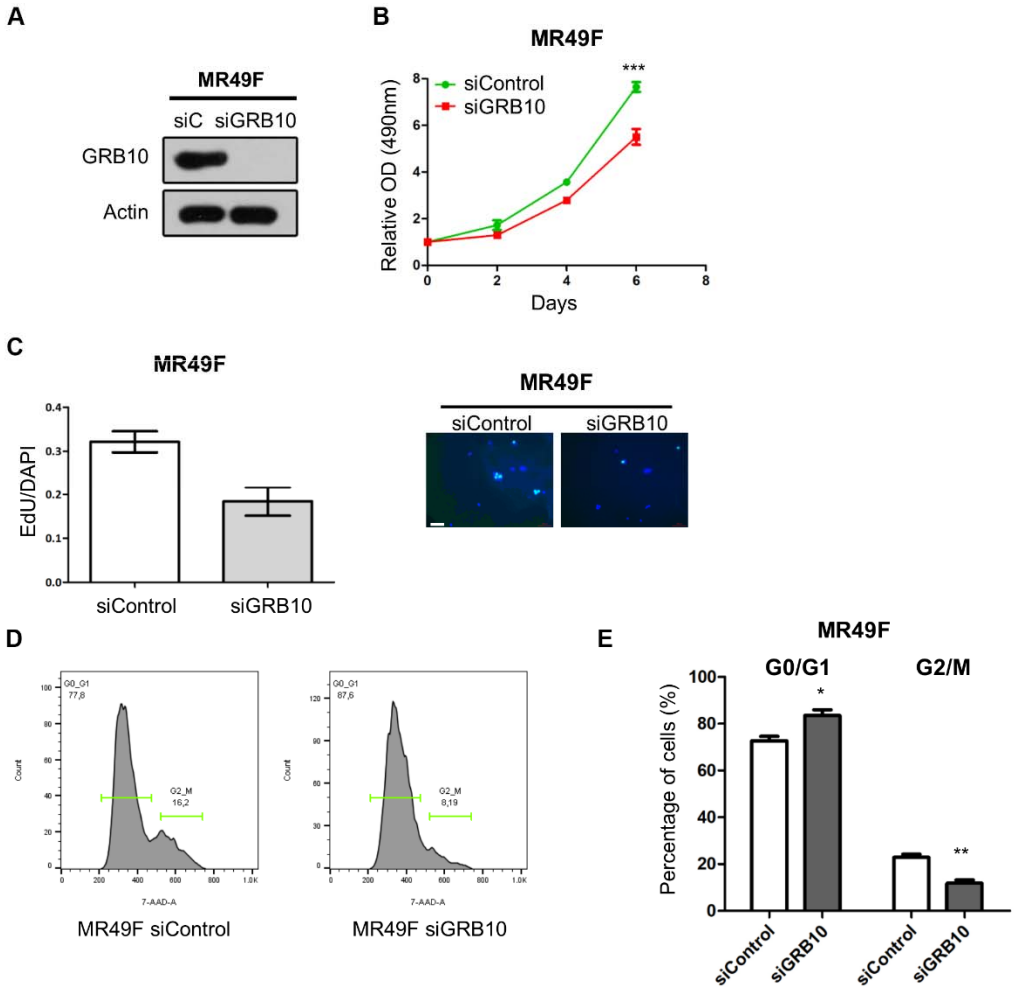

Figure 3.8. *GRB10* knockdown markedly inhibits the proliferation, DNA synthesis and colony formation of ENZ-resistant MR49F prostate cancer cells

(**A**) Effects of *GRB10* knockdown on GRB10 protein expression in ENZ-resistant MR49F cells as determined by Western Blotting (**B**) The potential function of GRB10 in the proliferation of the MR49F cell line was determined using transient *GRB10* knockdown (siGRB10) and control (shC) cells. Transient *GRB10* knockdown (siGRB10) and control (siControl) cells were kept in complete media containing 10 μM ENZ. O.D. values at 490 nm were normalized based on Day 0 readings. Results are presented as means ± SEM.

(**C,D**) MR49F cells were incubated for 4 hours with 10 μM EdU. EdU-labeled cells (green) and total cell numbers counterstained with DAPI (blue) were counted in 10 images taken at 10-fold magnification. Bars (EdU positive/total cells) show means ± SEM. Representative images are shown with a 100-μm scale bar. (**E**) Effects of *GRB10* knockdown on cell cycle progression in MR49F cells were measured using propidium iodide (PI) staining and flow cytometry. Data are presented as mean ± SEM. EdU: Ethynyl Deoxyuridine; DAPI: 4',6-Diamidino-2-Phenylindole.

3.2.4 Overexpression of GRB10 promotes PCa proliferation and resistance to ARPI treatment *in vitro*

To determine the function of GRB10 in driving ARPI resistance, we ectopically expressed GRB10 in LNCaP, an androgen-sensitive PCa cell line with a low endogenous GRB10 level, and treated them with ENZ. Notably, *GRB10* overexpression partially led to ENZ resistance as indicated by an MTS cell proliferation assay (Fig. 3.9A, B). Together, these results suggest that *GRB10* is a driver of CRPC development. *GRB10*-targeting therapy could thus enhance the anti-tumor activity of ARPIs and suppress the development of CRPC.

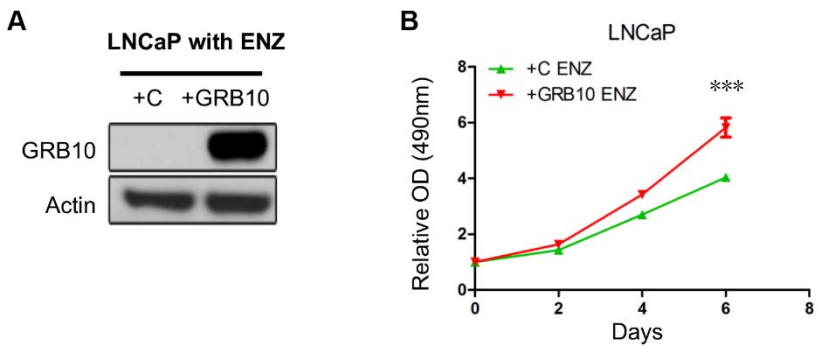

Figure 3.9. Functional study of GRB10 in promoting ARPI resistance

(**A, B**) The effects of *GRB10* overexpression on driving ENZ resistance was assessed in LNCaP cells stably overexpressing *GRB10* (+GRB10, in red) or control (+C, in green) as confirmed by Western Blotting. Cell proliferation was determined using the MTS assay.

3.2.5 A Role of GRB10 in regulating AKT signaling

AKT is a well-established driver of CRPC [239]. As reported in other systems, manipulating the expression of GRB10 can lead to either enhanced or reduced AKT activity [7]. Here, we observed that the knockdown of *GRB10* in LNCaP, C4-2, and ENZ-resistant MR49F cells consistently led to a decrease in S473 phosphorylation levels of AKT. Similar results were also observed following ENZ treatment (Fig. 3.10A, B). These data suggest that increased expression of GRB10 promotes AKT activation.

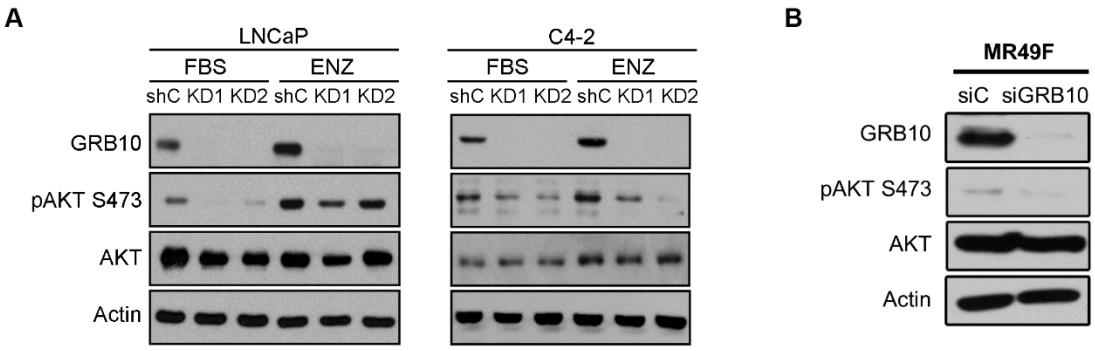

Figure 3.10. GRB10 knockdown reduced AKT activity in prostate cancer cells

(**A**) The effects of GRB10 knockdown on phosphorylated AKT levels in LNCaP and C4-2 were determined by Western Blotting using stable GRB10 knockdown (KD1, KD2) and control (shC) cell lines. Total protein was isolated from cells treated with or without 10 μM ENZ for 3 days. (**B**) The effects of GRB10 knockdown on phosphorylated AKT levels in ENZ-resistant MR49F cells were determined by Western Blotting using transient GRB10 knockdown (siGRB10) and control (siC) cells. Cells were maintained in regular medium with 10 μM ENZ. ENZ: Enzalutamide.

Since GRB10 is an adaptor protein, we tried to determine whether GRB10 can bind to AKT in PCa cells using a co-immunoprecipitation (Co-IP) assay. GRB10 was able to precipitate AKT, indicating binding of GRB10 to AKT (Fig. 3.11A). An immunofluorescence (IF) assay further indicated that endogenous GRB10 (green) and AKT (red) were co-localized in the cytosol and on the plasma membrane. Furthermore, ENZ treatment led to increased cell membrane co-localizations (Fig. 3.11B). This suggests that, upon ENZ treatment, the AKT and GRB10 complex moved towards the

plasma membrane where AKT would be activated. *In situ* interaction between GRB10 and AKT was also confirmed by proximity ligation assay (PLA) (Fig. 3.11B). Consistent with IF results, more PLA signals were found on the plasma membrane when cells were treated with ENZ. The data suggest that GRB10 can bind to AKT and lead to its activation.

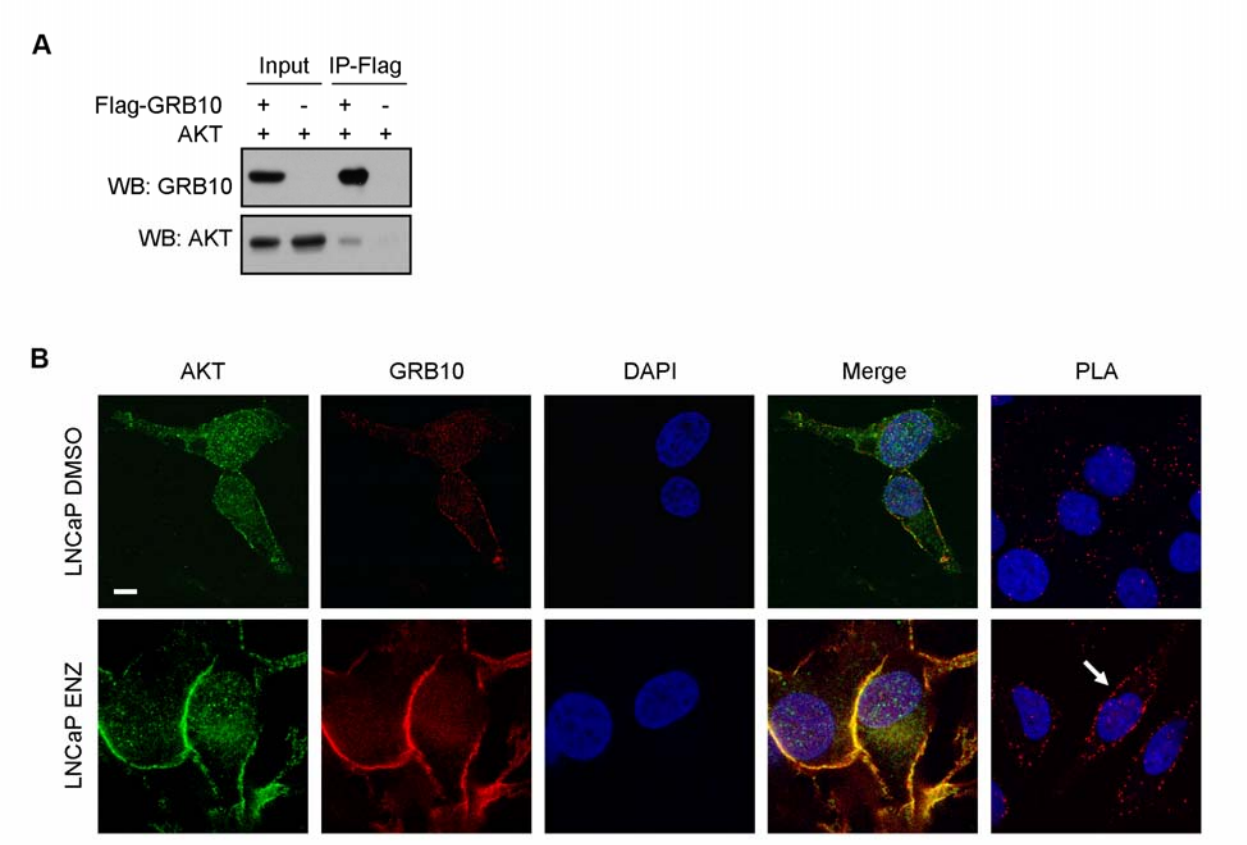

Figure 3.11. GRB10 directly interacted with AKT in prostate cancer cells

(**A**) The binding of GRB10 to AKT was confirmed by Co-IP. LNCaP cells expressing Flag-GRB10/AKT or Flag/AKT were collected and lysed with NETN buffer. Five percent of input was collected for each sample. One mg of each protein sample was incubated with FLAG magnetic beads. Then GRB10 and AKT were detected via Western Blotting. (**B**) AKT (green) and GRB10 (red) localizations in LNCaP cells treated with DMSO (vehicle control) or 10 μM ENZ were determined using immunofluorescence staining. Representative images are shown with a 10 μm scale bar. Interaction between AKT and GRB10 was also validated using a proximity ligation assay. Specific protein-protein interaction signals are shown in red. ENZ: Enzalutamide; IP: immunoprecipitation; WB: Western Blotting.

We then further elucidated the association of GRB10 expression and AKT activation in multiple PCa clinical cohorts. In the TCGA and Grasso cohorts [67, 73], *GRB10* upregulation was significantly correlated with *PTEN* deletion, a well-documented genetic alteration initiating AKT activation in clinical CRPCs (Fig 3.12A, B). Furthermore, *GRB10* expression was found to be significantly upregulated in the *PTEN*-deleted samples following treatment with ABI or ENZ [68] (Fig. 3.12C), which is consistent with our previous findings. The data support the hypothesis that upregulated expression of *GRB10*, together with *PTEN* deficiency, promotes AKT activation and leads to CRPC development. As such, *GRB10* may be considered a critical driver of CRPC.

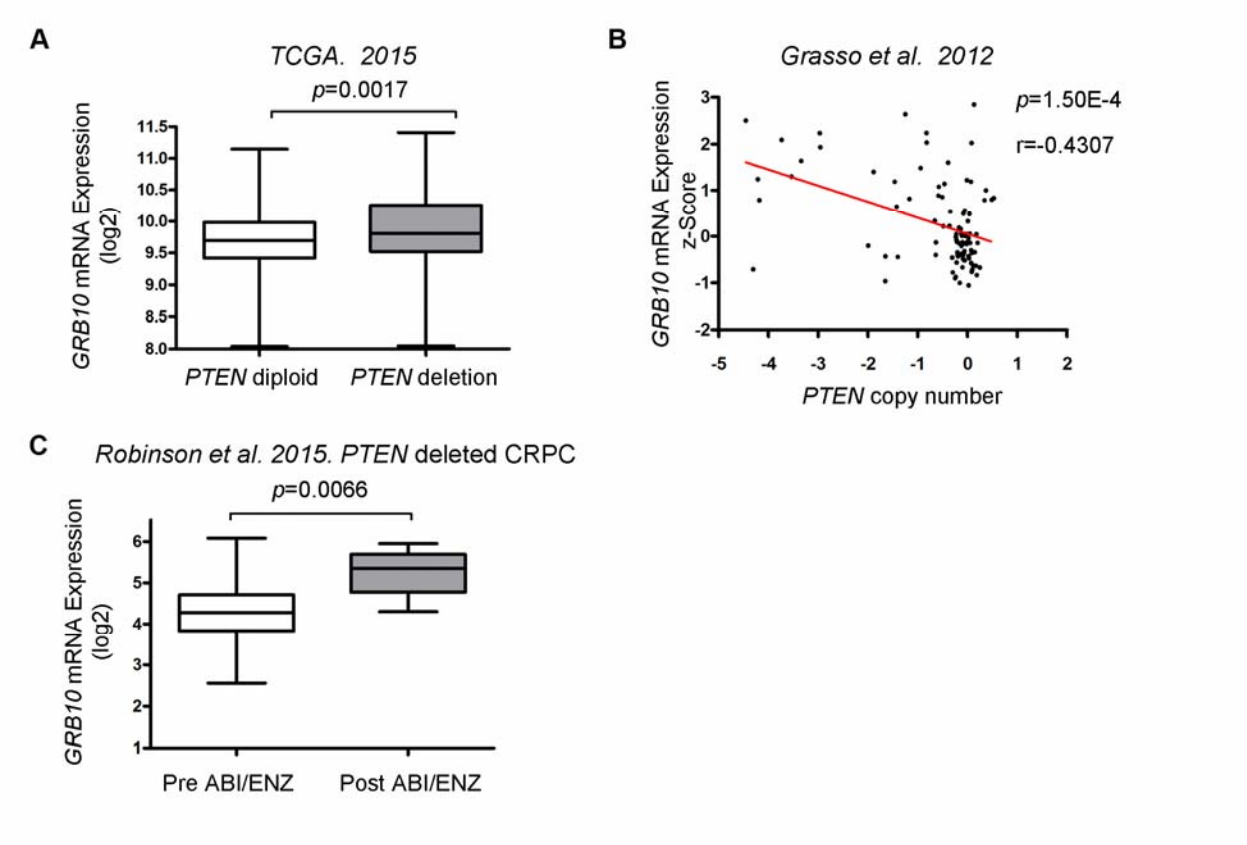

Figure 3.12. *GRB10* expression was negatively correlated with PTEN copy number in clinical prostate cancers

(**A**) A difference in *GRB10* mRNA expression between *PTEN* diploid and *PTEN*-deleted clinical samples as indicated by box-and-whisker plots. Gene expression data were collected from the *TCGA 2015* patient cohort. (**B**) A Pearson correlation between *GRB10* mRNA expression and *PTEN* copy number was established. Data were extracted from the *Grasso et al. 2012* patient cohort; the trend line is shown in red. Copy number 0 indicates *PTEN* diploid status. Negative copy number indicated *PTEN* deletion. (**C**) A difference in *GRB10* mRNA expression between *PTEN*-deleted CRPC patients treated with or without ABI/ENZ as indicated using box-and-whisker plots. Gene expression data were collected from the *Robinson et al. 2015* patient cohort.

3.3 Discussion

Development of treatment resistance to first-line hormonal therapy, e.g., orchiectomy, LHRH agonists or antagonists, and more recently, ABI, is currently a major challenge in the management of advanced PCa. This is further exacerbated by the fact that next-generation ARPIs such as ENZ and APA only have marginal efficacy [237]. In efforts to develop more effective therapies, it is critical to improve the understanding of the molecular mechanisms underlying the development of CRPC. A major hurdle of PCa research has been the lack of clinically relevant cancer models and, in particular, models representing clinical HNPCs. Unlike other research groups using methods that recombine patient-derived tissues with mouse seminal vesicle mesenchyme [157], our laboratory has established over 45 transplantable PCa PDX lines including HNPC, NEPC, and castration-resistant prostate adenocarcinoma by directly grafting patient tumors under the mouse renal capsule. Importantly, this technique allows the xenografts to retain key features of the original patients' tumors, including tumor heterogeneity, the tumor microenvironment, tissue architecture, and cancer-stromal interactions. These PDX models also mimic patients' treatment responses, as evident by spontaneous CRPC development with minimal artificial manipulation [151]. While organoid culturing provides an opportunity to study advanced patient-derived PCa cells *in vitro* [240], it does not allow the development of HNPC models at present,. Additionally, recent studies presented at the 2019 AACR Annual Meeting (Potentials and pitfalls of organoid technology to study PCa by Dr. Yu Chen and Patient-derived organoid models of bladder cancer by Dr. Michael M Shen) suggests that the treatment response of these patient-derived organoids

is significantly altered by the abundant growth factors and hormones added to the culture system, limiting their usage in studying treatment response and resistance. GEMMs of PCa are powerful tools for studying mechanisms underlying CRPC development [136, 147]. These models have an advantage over PDX models which are developed in mice lacking a functional immune system. This makes GEMMs more suitable to study cancer-immune interaction. However, GEMMs do not reflect the intertumoral genomic heterogeneity of the disease [67, 68, 73]. In this study, we were able to identify common molecular events occurring in CRPC development regardless of specific genetic background by using seven pairs of hormone-naive PDX models and their related castration-induced CRPC models.

Our study shows that GRB10 is critical for AR^+ PCa cell proliferation, which is consistent with another independent publication suggesting that GRB10 is a pro-proliferative protein in PCa [220]. In AR^- PCa cell lines such as PC-3 and DU145, where AR expression is diminished due to other mechanisms [241], the expression of GRB10 is much lower (Fig. 3.5A). This suggests that other mechanisms such as FGFR [242] or polycomb repressor complex 1 [243] might be involved in treatment resistance in such scenarios. Thus, *GRB10* can be considered a universal ARPI resistance-driving gene in AR^+ PCa.

GRB10 has been shown to regulate AKT activation but with contradictory observations in different contexts [238]. For example, GRB10 has been reported to disrupt the interaction between insulin receptor (IR) and insulin receptor substrate 1 (IRS1)

in mouse embryonic fibroblasts, eventually leading to inhibition of insulin-induced AKT activation [212]. However, in human leukemic cell lines Mo7e and K562, GRB10 has been reported to enhance AKT activation independent of PI3-K activity [208, 209]. Our findings in the present study clarify that increased expression of GRB10 promotes AKT activation in PCa. Interestingly, we also found that elevated expression of *GRB10* co-occurs with *PTEN* deletion. Consistently, higher endogenous expression of GRB10 was found in *PTEN* deleted AR^+ PCa cell lines (Fig. 3.5A). This evidence suggests that *PTEN* deletion could initiate the baseline expression of *GRB10*.

AKT pathways have been reported to be critical for CRPC development and progression [239]. When ARPI is applied, the dramatic upregulation of GRB10 further enhances the activation of AKT, providing proliferative and survival advantages to the residual tumor cells. This provides the cells with enough time to accumulate the genomic alterations we observed clinically in terminal CRPC, which includes AR mutation, AR amplification and TP53 mutation, which ultimately results in the development of ARPI resistance. This mechanism could potentially explain the enrichment of *PTEN*-deletion in CRPC patients [67, 227, 230]. However, treatment of CRPC based on targeting only the AKT pathway has had limited effect [244, 245]. As such, targeting GRB10, a potential upstream mediator of AKT, could improve the current treatment of CRPC. Consistent with our findings, a recent publication reported the pro-proliferative function of GRB10 in PCa. In their study, AKT activity was also found to be increased by ectopic expression of GRB10, which could promote the tumor growth *in vivo* [220].

Other than GRB10, there are some other genes shown upregulation at post-castration time points among the 80 genes we identified to be significantly upregulated in 7 pairs of HNPC/CRPC PDX tumor lines (Appendix B). For example, FGFR2 expression was elevated at both post-castration and CRPC time points compared to parental HNPC PDX lines.

Chapter 4: Discovery of GRB10 as an AR transcriptionally repressed gene

4.1 Introduction

AR is critical for PCa development and progression [246], and ADT is the most effective treatment in the management of PCa. However, treatment resistance invariably develops. The alterations of AR including AR amplification, gain-of-function mutations, and constitutively active AR splicing variants have been observed in more than half of clinical CRPCs [67, 68]. These AR alterations suggest that AR is still one of the major drivers of prostate cancer lethality. The newly-developed next generation ARPIs such as ABI, ENZ, and DAR, are only marginally effective. Interestingly, the success of sequential usage of the anti-androgen drugs mentioned above suggests that ARPI resistance is dependent on AR as well.

The AR is a nuclear receptor as well as a transcription factor. Upon binding to its ligand, usually dihydrotestosterone, in the human prostate, AR translocates into the nucleus where it forms a homo-dimer [247] and binds to androgen responsive elements. This either induces or suppresses downstream gene transcription, depending on the co-factors it binds with [248]. For years, AR was well-studied for its role in transcriptional initiation. To induce transcription of AR target genes, pioneer transcription factors such as FOXA1 and GATA2 are first recruited to open the condensed chromatin. Then, AR binds to androgen responsive elements (ARE) located around the promoter, which leads to the recruitment of RNA polymerase II to the transcription start site (TSS). Other

transcription factors such as CBP and SRC-1 are AR co-factors that form a complex with AR to induce the transcription of its target genes. AR-induced genes are reported to be involved in a variety of functions such as normal prostate development, lipid metabolism, cell proliferation, differentiation and apoptosis [246]. For example, PSA (*KLK3*), one of the best-known AR-induced genes, is considered not only as a marker of AR activity, but also as a commonly-used biomarker indicating PCa diagnosis, progression, and recurrence [249].

Besides inducing gene transcription, AR can also act as a transcriptional repressor. By combining transcriptome analysis of androgen-inhibited genes with chromatin immunoprecipitation-sequencing (ChIP-seq)-based whole genome ARE location analysis, a wide range of genes were discovered to be directly transcriptionally repressed by AR. AR has been reported to repress of both cancer-promoting and tumor-suppressing genes, e.g., DEPTOR [250], CDH1 [251], MET [252], BRN2 [253], PEG10 [98], and AR itself [254]. Since ADT is the most-commonly used treatment for advanced PCa, it is of great importance to study whether a particular gene is directly regulated by AR.

In the previous chapter, we demonstrated that GRB10 expression was significantly upregulated after host castration in HNPC PDX models (Fig 3.3). In clinical CRPC, ENZ and ABI treatment would further increase the expression of GRB10 (Fig 3.4). Taken together, the consistent and marked response of GRB10 to AR signaling inhibition suggested that GRB10 expression was regulated by AR. In this section, we discover and

validate that GRB10 is transcriptionally repressed by AR through an androgen responsive element located in GRB10's intron.

4.2 Results

4.2.1 GRB10 is an AR-repressed gene in AR+ PCa cells

To address AR regulation of *GRB10*, we used the AR^+ lineage-related human PCa cell lines LNCaP and C4-2 and subjected them to androgen deprivation and AR blockade. In androgen-dependent LNCaP cells, ablation of androgen led to increases in both GRB10 mRNA and protein expression; the upregulated expression could be reduced by addition of the synthetic androgen R1881 (Fig. 4.1A-C). These results are consistent with previous studies of androgen regulation using high-throughput technology [255, 256] (Fig. 4.1D, E). In androgen-independent but AR-signaling active CRPC C4-2 cells, treatment with the AR antagonist ENZ also led to the upregulation of GRB10 expression (Fig. 4.1F-H). We also found that transient depletion of *AR* by siRNA can upregulate GRB10 expression (Fig 4.1I, J). All of these data indicate that AR itself is a direct repressor of GRB10 expression.

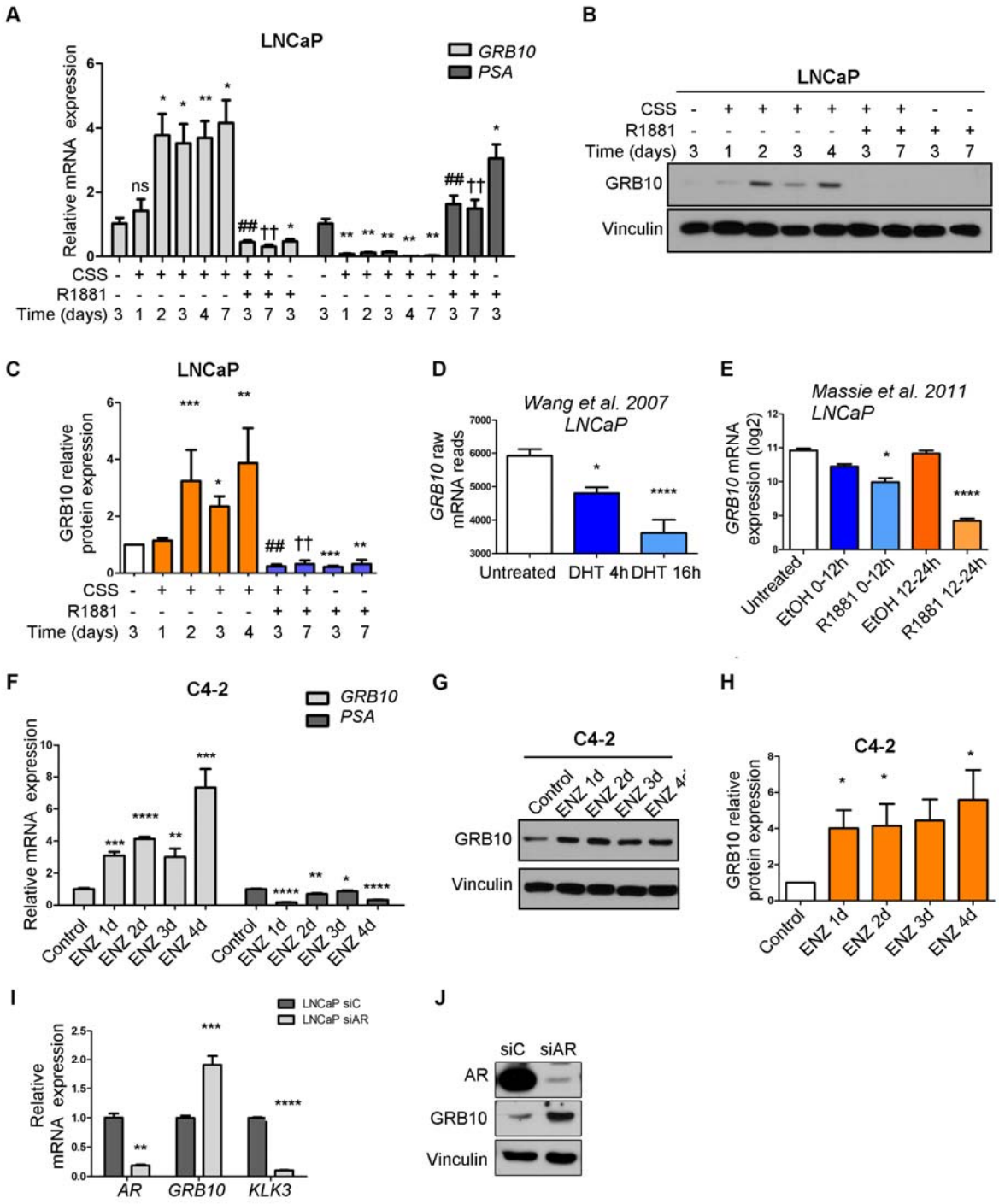

Figure 4.1. *GRB10* is an AR-repressed gene in AR$^+$ prostate cancer cells

(**A-B**) Effects of androgen deprivation on GRB10 expression in LNCaP cells (by culturing in CSS medium) were determined by qRT-PCR and Western Blotting. To some cultures, 10 nM of AR ligand R1881 was added. P-values for each sample were determined based

on untreated controls (*), cells cultured in CSS medium for 3 days (#), and cells cultured in CSS medium for 7 days (†). Bar graphs show means ± SEM. (**C**) Relative band densities of Western Blotting results shown in Fig. 4.1B were quantified using ImageJ (NIH, USA, https://imagej.nih.gov). GRB10 protein expression was normalized to Vinculin as internal control. Bar graphs show mean ± SEM. The p-values for each sample were determined based on untreated controls (*), cells cultured in CSS medium for 3 days (#), and cells cultured in CSS medium for 7 days (†) and calculated by unpaired two-tail Student's t-tests based on three replicate experiments. (**D, E**) *GRB10* mRNA expression upon AR stimulation in LNCaP cells was analyzed with two publically available microarray datasets [255, 256]. Bar graphs show means ± SEM. (**F, G**) Relative GRB10 mRNA and protein expression in C4-2 cells were determined after treatment with 10 μM ENZ. Bars show means ± SEM. (**H**) Relative band densities of Western Blotting results shown in Fig. 4.1G were quantified using ImageJ (NIH, USA, https://imagej.nih.gov). GRB10 protein expression was normalized to Vinculin as internal control. Bar graphs show mean ± SEM. (**I, J**) Effects of *AR* knockdown on GRB10 expression in LNCaP cells were determined by qPCR and Western Blotting. Bars show means ± SEM.

4.2.2 Expression of GRB10 was upregulated by anti-androgen treatment in PCa mouse model and clinical PCa samples

Next, we checked the expression of *Grb10* in the *Pb-Cre4;*$^{Ptenflox/flox}$*;R26*$^{ERG/ERG}$ murine PCa model with available gene expression data [257]. *Grb10* was significantly elevated in mice subjected to castration (Fig. 4.2A). Furthermore, in multiple PCa clinical cohorts [67, 73, 226, 227, 230], the expression of *GRB10* in PCa samples tends to be

negatively correlated with *PSA* expression (Fig. 4.2B, C). In addition, we found that GRB10 expression was significantly upregulated in patients' samples collected after neoadjuvant ADT compared with clinical HNPCs (Fig. 4.2D) [258]. This upregulation of GRB10 expression is in agreement with our findings in PDX models. All of these results suggest that AR directly regulates the expression of GRB10.

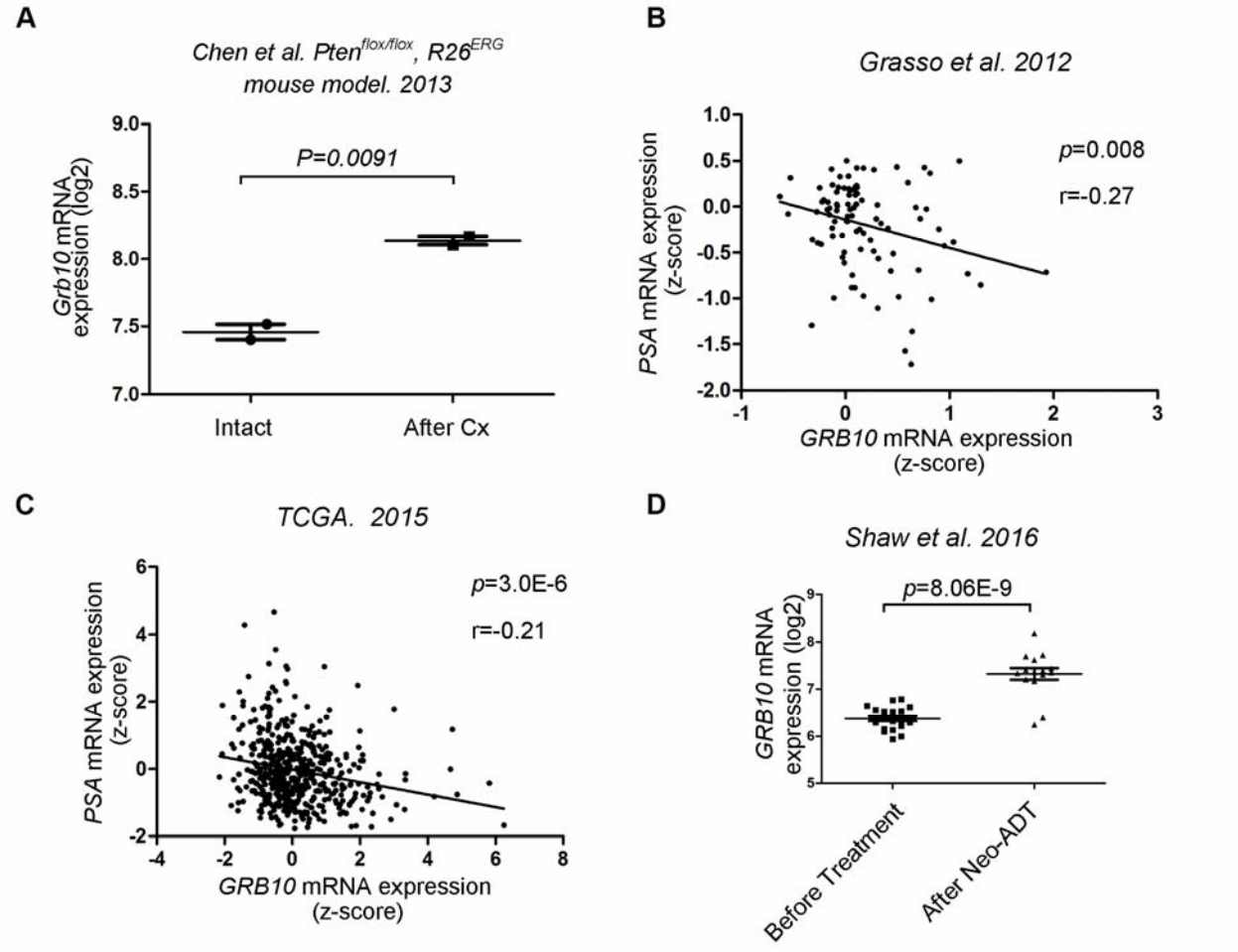

Figure 4.2. *GRB10* is an AR-repressed, ADT-inducible-gene in AR$^+$ prostate cancers

(**A**) *Grb10* mRNA expression in intact and castrated *Pten*$^{flox/flox}$, *R26*^{ERG} transgenic mouse models constructed by *Chen et al, 2013* [257]. The vertical scatter plots show means ± SEM. (**B, C**) Pearson correlation between *GRB10* and *PSA* mRNA expression was determined using transcriptomic data of *Grasso et al. 2012* and *TCGA 2015* clinical PCa cohorts. (**D**) *GRB10* mRNA expression in clinical PCa samples before and after 7-day neoadjuvant ADT was analyzed using the *Shaw et al. 2016* patient cohort [258]. The scatter plots show means ± SEM. ENZ: Enzalutamide; ns: not significant.

4.2.3 AR represses expression of GRB10 by binding to an androgen responsive element located in its intron

AR is a transcription factor which directly binds to DNA to initiate or repress downstream gene transcription. To examine whether *GRB10* is transcriptionally regulated by AR, we analyzed a reported AR chromatin immunoprecipitation-DNA sequencing (ChIP-seq) dataset [259]. Three potential AR-binding sites were identified to be located in the *GRB10*'s intron region (intron 2 and intron 3), i.e. ARE1, ARE2 and ARE3 (Fig. 4.3A). To confirm the occupancy of AR on these predicted AREs, we performed ChIP-PCR assays on LNCaP cells treated with 10 nM R1881 or ethanol (control). The treatment with R1881 resulted in significant AR enrichment at all three AREs (Fig. 4.3B). Consistently, similar AR enrichment on the *GRB10* gene was also observed in other AR ChIP-seq datasets [255, 260]. Clinically, the occupancy of AR on the *GRB10* gene was enriched in untreated PCa patients' samples and decreased in ADT-responsive patients' samples (Fig. 4.3C) [260].

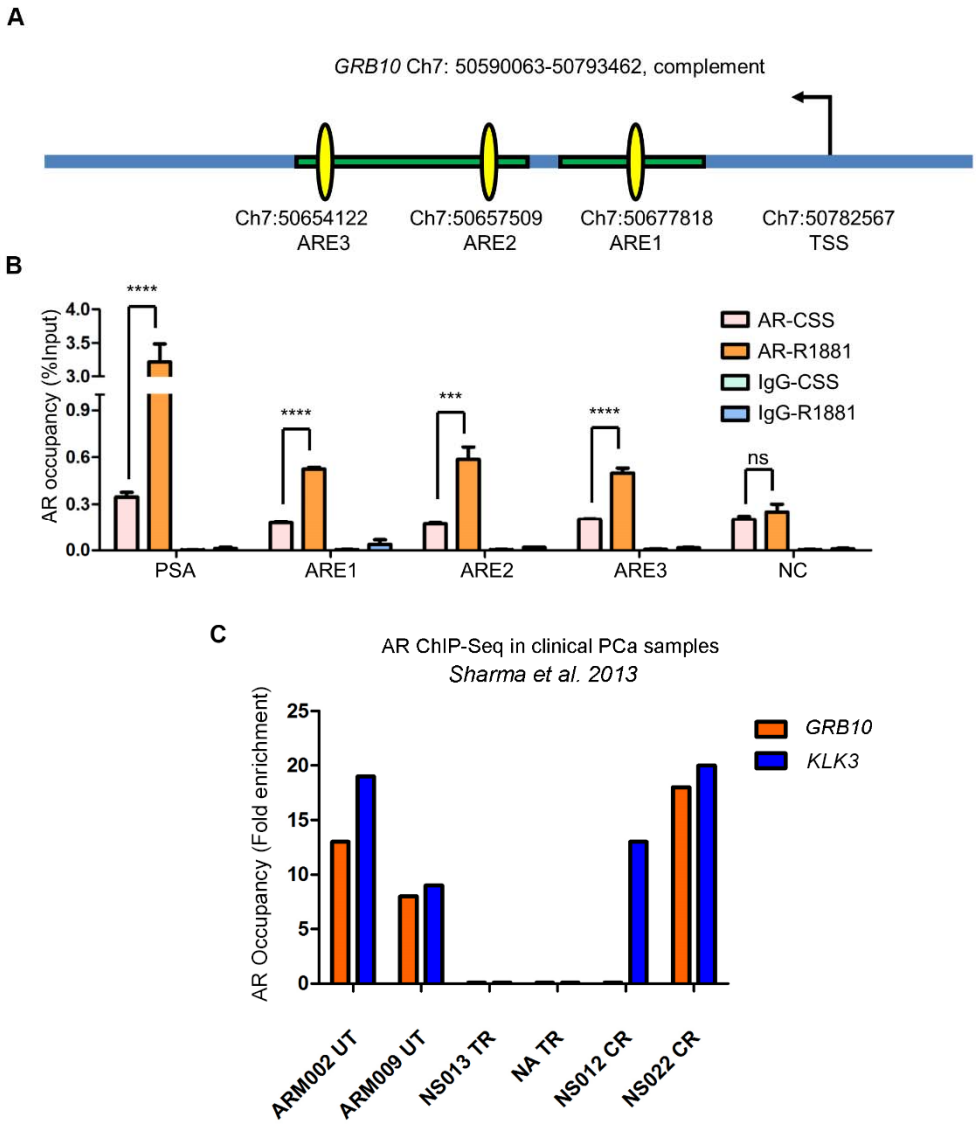

Figure 4.3. AR represses expression of *GRB10* by binding to an ARE located in its Intron

(**A**) Potential androgen responsive elements (AREs, yellow) and their locations in the *GRB10* introns (green) were identified by analyzing reported ChIP-seq data [259]. Based on the reported consensus sequences of AREs and useing a computational analysis tool (http://consite.genereg.net/cgi-bin/consite), a potential ARE appears to be located within

each of the 3 potential AR-binding sites. Three potential AREs are labeled based on their distances to the transcription start site (TSS; black arrow). Genomic location was aligned based on GRCh38 assembly. (**B**) AR occupancies at several DNA locations were measured using ChIP-PCR. The *PSA* enhancer region (*PSA*) was used as a positive control whereas an AR non-binding site was used as a negative control (NC). Bars show means ± SEM. (**C**) AR enrichment at identified androgen responsive elements on the *GRB10* gene and on the *PSA* gene enhancer was analyzed using publically available ChIP-seq data of clinical samples [260]. Ch7: chromosome 7; ARE: androgen responsive element; NC: negative control; UT: untreated; TR: treatment responsive; CR: castration-resistant.

4.2.4 ARE2 located in GRB10's intron is a silencer regulated by AR

To further confirm the biological function of AR binding at these potential AREs, we performed a dual luciferase reporter assay. Here, we constructed luciferase reporters by inserting the three potential AREs as cis-regulatory elements into separate PSA luciferase reporters whose expression was regulated by the PSA promoter. The relative luciferase signals from the reporter plasmid into which ARE2 had been inserted (PSAluc-ARE2) was significantly reduced by treatment with R1881; this was not observed for the reporter plasmids containing ARE1 or ARE3 (Fig. 4.4A). We then constructed two modified PSAluc-ARE2 reporter plasmids in which the potential ARE sequence was either mutated or deleted. These modifications led to the rescue of the luciferase signal (Fig. 4.4B). Taken together, the data demonstrate that AR can act as a transcriptional

repressor of *GRB10* by binding to an ARE located in the *GRB10* intron region (chr7: 50657497-50657511).

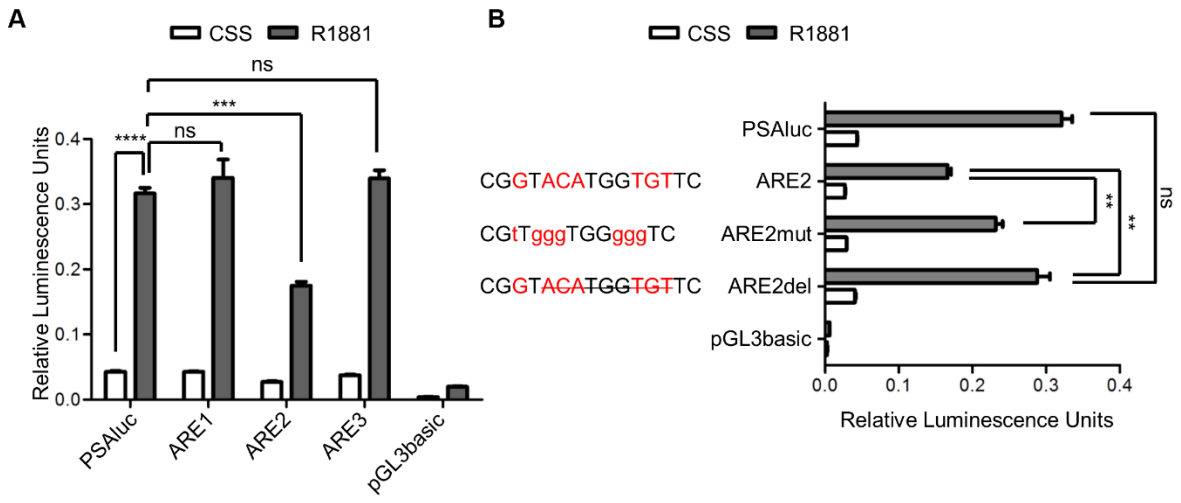

Figure 4.4. AR represses expression of *GRB10* by binding to an ARE located in its Intron

(**A**) The transcriptional inhibitory functions of potential AREs are indicated by reduced luciferase reporter activity. Luminescence units were normalized using *Renilla* luciferase signal. Bars show means ± SEM. (**B**) Transcriptional activation abilities of ARE mutants (sequences are shown) were assessed by dual luciferase reporter assay. Nucleotides in red are sequences of consensus ARE, mutated ARE, and deleted ARE respectively. Bars show means ± SEM. ns: not significant.

4.3 Discussion

It is well-accepted that AR is responsible for most CRPC progression. Multiple potent ARPIs have been shown to extend the survival of CRPC patients [261]. However, treatment resistance invariably develops, and in most cases AR is still promoting cancer progression [246]. Here, we provided evidence that *GRB10* is transcriptionally repressed

by AR. This finding is echoed by a recent study in adrenocortical tumors where they found GRB10 to be upregulated by cetrorelix acetate, a gonadotropin-releasing hormone receptor antagonist [223]. Thus, ARPIs, including androgen ablation and AR blockade, would increase the expression of *GRB10*, which in turn eventually mediates the development of treatment resistance.

With regards to crosstalk between AR and AKT, it has been shown that ADT can lead to increased AKT activity in PCa cells [239]. In this connection, *FKBP5*, an AR-responsive gene, has been reported to promote dephosphorylation of AKT in PCa through recruiting PHLPP phosphatase [262], which in turn leads to increased AKT activation during ADT. Many studies have shown that AR is highly expressed and transcriptionally active in CRPC (summarized in [246]), suggesting that decreased AKT activity in CRPC can be expected as a result of recurrent *FKBP5* expression. However, following the development of CRPC, AKT is still highly active [239]. Therefore, a better understanding of this crosstalk is required to explain the discrepancy. In the present study, the findings that *GRB10* is transcriptionally repressed by AR and mediates the activation of AKT can fill this gap between AR and AKT. Following castration, the expression of GRB10 is elevated, resulting in the activation of AKT. When CRPC has developed, the effect of AR on enhancer elements is stimulated by low, castrate-levels of androgen. However, its effect on suppressor elements remains inhibited [254], leading to consistent upregulation of GRB10 and promotion of AKT activation. This notion is supported by our observations that treatments with ENZ and ABI will further increase GRB10 expression in CRPC. As a

result, our findings provide a molecular bridge between AKT and AR, suggestive of a critical role for GRB10 in the development of CRPC.

As a key regulator of the IGFR pathway, GRB10 expression has also been linked to Type II diabetes [263]. In transgenic mouse models, overexpression of GRB10 has also been shown to lead to insulin resistance [264, 265]. Interestingly, when PCa patients are treated with ADT, higher incidences of type 2 diabetes and obesity are observed [266-269]. This effect can be partially explained by our finding that GRB10 is an AR repressed gene. Therefore, GRB10-targeting therapy may benefit patients not only by controlling PCa progression, but also by improving the patients' quality of life.

Chapter 5: Elucidation of GRB10 function in the development of CRPC

5.1 Introduction

Despite the successes of controlling tumor growth by first-line hormonal therapy such as surgical or chemical castration, in most cases, CRPC will develop [237]. Interestingly, androgen signaling is reactivated in CRPC, as evident by the biochemical recurrence of PSA, an AR regulated gene. This phenomenon suggests that further androgen blockade will benefit patients. This led to the development of next-generation ARPIs, including ENZ, ABI, APA, and DAR [270]. However, these drugs are only marginally effective [237], and the mechanism underlying the development of castration/ ARPI resistance remains unclear.

In the previous chapters, we have provided evidence that *GRB10* is a potential driver gene for the development of CRPC. *GRB10* encodes Growth Factor Receptor Bound Protein 10 (GRB10), which is an adaptor protein interacting with various specific signaling cascades. It plays different biological and pathological functions in a context-dependent manner. GRB10 was reported to directly interact with key components in signal transduction pathways including receptor tyrosine kinases (IR, IGFR, EGFR, FDGFR, KIT, VEGFR2), non-receptor tyrosine kinases (BCR-Abl fusion), serine/threonine kinases (PI3K, Raf1), ubiquitin ligase (NEDD4), and growth hormone receptors [238, 271]. Moreover, it was also reported that GRB10 can regulate AKT, a well-accepted driver of CRPC development [239, 262]. Biologically, GRB10 knockdown in cervical squamous cell cancer and BCR-ABL-positive leukemia cell lines significantly

inhibited cell growth [216], while GRB10-knockout mice were reported to have markedly elevated muscle mass [272]. Therefore, it is our interest to study the function of elevated GRB10 expression as observed in our PDX models during CRPC development. In this chapter, we performed a multi-omics study of GRB10 by analyzing the transcriptomic change after GRB10 knockdown and the interactome of GRB10 in PCa cells in order to reveal the molecular mechanisms underlying GRB10-promoted CRPC development.

Protein phosphatase 2 (PP2A) is of particular interest among the various GRB10-interacting proteins we discovered using high-throughput LC-MS/MS. PP2A is a ubiquitously-expressed serine/threonine phosphatase heterotrimeric protein complex. It consists of a structural “A” subunit, a regulatory “B” subunit, and a catalytic “C” subunit [273]. The A subunit is the scaffold of the protein complex and consists of 15 Huntington-Elongation-A subunit-TOR (HEAT) repeats. It provides the docking sites for the B and C subunits. The C subunit is the catalytic subunit of PP2A responsible for the serine/threonine phosphatase activity. The A and C subunits are highly conserved throughout eukaryotes and contain two isoforms each, encoded by different genes with the alpha isoform being the most predominantly expressed. The B subunit, on the other hand, consists of 4 distinct families of isoforms, i.e., B55 family (B), B56 family (B’), PR72 family (B’’), and PR93/PR110 family (B’’’). To date, there are 13 isoforms of B subunits described, all of which are responsible for the regulation of PP2A to target specific substrates and subcellular localizations [273, 274]. Thus, the diversity of B subunits allow PP2A to control multiple cellular processes at the same time.

PP2A has been reported to be a tumor suppressor that dephosphorylates and regulates multiple pro-survival and proliferation signaling cascades. These include, but are not limited to, AKT, SRC, ERK, and AR [275-279]. PP2A expression is downregulated in multiple human malignancies including breast cancer, lung cancer, colorectal cancer, hepatocellular cancer, ovarian cancer, cervical cancer, endometrial cancer, bladder cancer, PCa, and leukemia [280-287]. Here, we investigate the interaction between GRB10 and PP2A and the role of GRB10 in regulating PP2A in PCa.

5.2 Results

5.2.1 Knockdown of GRB10 led to a significant change in the transcriptomic landscape of prostate cancer cells

To study the function of GRB10 in PCa cells, we first performed an RNA microarray analysis using a control (shCntl) and two independent *GRB10-knockdown* (shGRB10) LNCaP cells. As a positive control, GRB10 expression was shown to decrease more than 7-fold in the shGRB10 group compared to the shCntl group. Overall, there are a similar number of genes significantly upregulated (n=1370) or downregulated (n=1460) at a threshold of $p<0.05$. To investigate which pathways were regulated by GRB10, we utilized the GSEA and unbiasedly analyzed the transcriptome upon GRB10 knockdown unbiasedly. First, in hallmark gene sets, ten cancer-related hallmarks including androgen response, mTORC1 signaling, and glycolysis were significantly downregulated by GRB10-knockdown. However, none of the hallmark gene sets were found to be upregulated by GRB10-knockdown at a threshold of FDR<0.05 (Fig 5.1A). As for Gene Ontology (GO) gene sets, many more molecular functions and biological process-related

pathways were inhibited by GRB10-knockdown rather than being promoted (Appendix C). The top-ranked GO pathways inhibited by GRB10-knockdown included sterol biosynthesis, antigen processing and presentation, and small molecule biosynthetic process.

Next, we used Ingenuity Pathway Analysis (IPA) to further analyze the connection between the most significantly altered-genes after GRB10-knockdown ($p<0.05$). Based on the fold changes of these genes, IPA predicted that the Diseases and Bio Functions including cell death of tumor cells (p=1.74E-3) and cell death of cancer cells (p=3.54E-3), were significantly increased by GRB10 knockdown, while genes related to pelvic tumor (p=6.44E-12), lung tumor (p=1.30E-3), and respiratory tumor (p=5.32E-3) were significantly decreased. Consistent with GSEA, RPTOR (the major component of mTORC1) was predicted to be inhibited by GRB10 knockdown (activation z score =-2.887, Fig 5.1B). Overall, these analyses suggest that GRB10 is a key regulator in promoting multiple cancer progression-related pathways in PCa.

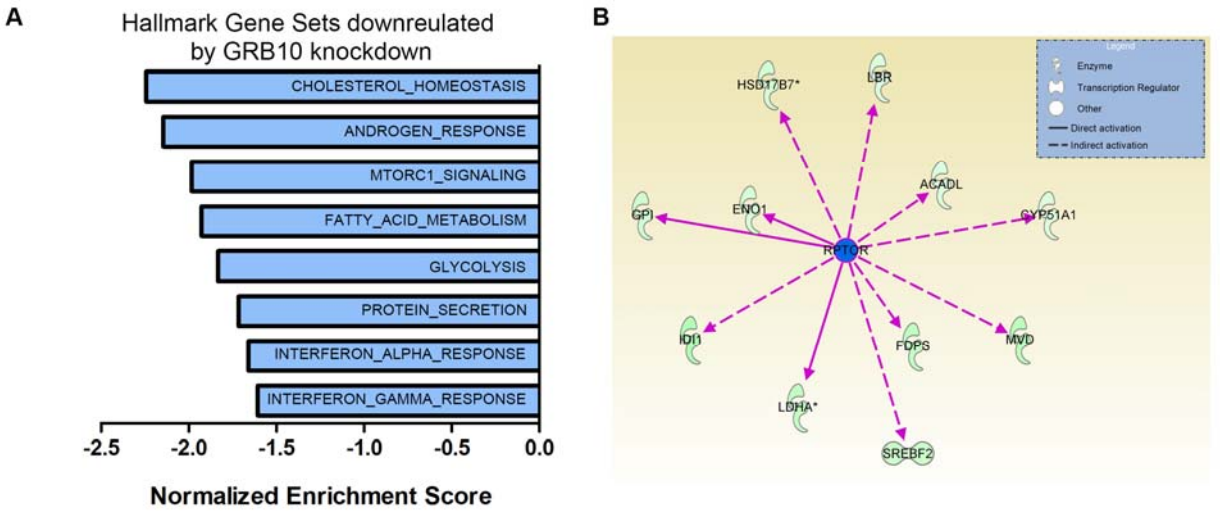

Figure 5.1. Transcriptome analysis of GRB10-regulated pathways

(**A**) Genes were ranked based on the significance p-value significance between control LNCaP and GRB10-knockdown LNCaP cells. Gene ranking was then uploaded on GSEA (http://software.broadinstitute.org/gsea/index.jsp) to identify GRB10-knockdown enriched gene sets. Bar chart showed Hallmark Gene Sets which were significantly downregulated by GRB10 knockdown (FDR<0.05). (**B**) Genes that were significantly affected by GRB10 knockdown ($p<0.05$) were uploaded to Ingenuity Pathway Analysis (https://www.qiagenbioinformatics.com/products/ingenuity-pathway-analysis/) for discovery of potential upstream regulators regulated by GRB10. Several genes significantly downregulated by GRB10 knockdown were downstream of RPTOR, suggesting that RPTOR was inhibited by GRB10 knockdown.

5.2.2 Discovery of GRB10 interactome in prostate cancer

Given the fact that GRB10 is an adaptor protein, it is known to interact with various specific signaling cascades and has different context-dependent biological and pathological functions in a context-dependent manner. To understand the interactome of GRB10 in CRPC, we performed an unbiased, semi-quantitative, isotope dimethylated, liquid chromatography-mass spectrometry (LC-MS) analysis of GRB10-associated immunoprecipitated complexes derived from LNCaP and C4-2 cells. We precipitated Flag-GRB10 and discovered high-confidence, potential GRB10-binding partners. In the precipitated samples from both LNCaP and C4-2, GRB10 is among the top-ranked proteins detected based on the ratio between Flag-GRB10 samples and Flag control samples. Another protein, 14-3-3, which was previously reported to interact with GRB10, was also detected (Table 5.1). These positive controls suggest that our findings are reliable. Among all the common proteins identified by IP-MS, some were chaperone proteins such as heat shock protein 70 family protein 8 (*HSPA8*), heat shock protein 70 family protein 5 (*HSPA5*), and heat shock protein 70 family protein 1A (*HSPA1A*) (Table 5.1). The other group of proteins detected include cell skeleton-related proteins such as tubulin and actin. Interestingly, several metabolism-related proteins, e.g., glyceraldehyde-3-phosphate dehydrogenase, pyruvate kinase, ADP/ATP translocase 2, ATP synthase, and D-3-phosphoglycerate dehydrogenase, were also identified to be potential GRB10-bound proteins (Table 5.1). This suggests that GRB10 is closely involved in cell metabolism pathways and regulating cell proliferation and survival.

Protein names	Gene names	Ratio H/L normalized
GRB10	GRB10	43.638
PP2AB	PPP2R2A	29.346
HS71A	HSPA1A	20.699
HSP7C	HSPA8	17.752
PP2AA	PPP2R1A	17.539
GAPDH	GAPDH	13.103
BiP	HSPA5	11.529
1433G	YWHAG	9.9941
1433Z	YWHAZ	7.5171
ADT2	SLC25A5	5.8242
ATPA	ATP5A1	4.9334
PKM	PKM	4.8438
PP2AC	PPP2CA	4.3147
PHGDH	PHGDH	3.4016
1433E	YWHAE	2.4893
ATPB	ATP5B	1.943

Table 5.1. Proteins which potentially interacted with GRB10 as detected by LC/ MS. Proteins were ranked based on the ratio of signal detected in Flag-GRB10 and Flag-control cells. H: heavy (Flag-GRB10); L: light (Flag-control).

5.2.3 GRB10 binds to and inhibits PP2A activity in prostate cancer

Among all the proteins that potentially interact with GRB10 in PCa cells, we found that all three subunits of PP2A, i.e., Serine/threonine-protein phosphatase 2A 65 kDa regulatory subunit A alpha isoform (gene name *PPP2R1A*), Serine/threonine-protein phosphatase 2A 55 kDa regulatory subunit B alpha isoform (gene name *PPP2R2A*), and Serine/threonine-protein phosphatase 2A catalytic subunit alpha isoform (gene name *PPP2CA*), were detected at a high confidence level. Further, PP2AB is the highest ranking protein besides GRB10 itself (Table 5.1). By Co-IP of ectopically-expressed

GRB10, we validated that GRB10 interacts with PP2A in C4-2 cells (Fig 5.2A); this association has never been reported before. Furthermore, in C4-2 cells, we also confirmed endogenous binding between GRB10 and PP2A (Fig. 5.2B).

Since PP2A is a well-established tumor suppressor [280], we explored whether GRB10-PP2A binding affects the status of PP2A in CRPC. We examined the PP2A protein level in GRB10 knockdown and their matched control cells. We observed that both transient and stable GRB10 knockdown increased the protein expression of PP2Ac, the subunit responsible for its phosphatase activity (Fig. 5.2C). Consistently, overexpression of GRB10 dramatically decreased the protein expression of PP2Ac in LNCaP cells (Fig. 5.2D). Interestingly, we did not see GRB10 knockdown affecting the mRNA levesl of the two isoforms (PPP2CA and PPP2CB) encoding PP2Ac when comparing GRB10 knockdown cells with control cells (Fig. 5.2E). These data suggest that the interaction between GRB10 and PP2A inhibited PP2A activity in CRPC.

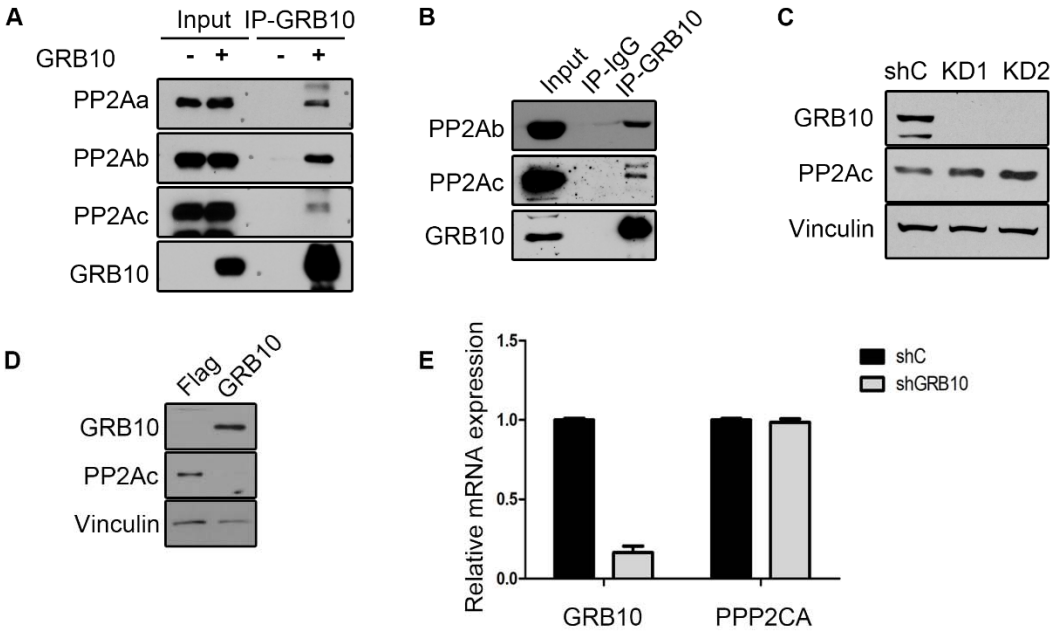

Figure 5.2. The interaction between GRB10 and PP2A inhibited PP2A activity.

(**A**) Binding of GRB10 to all three subunits of PP2A was confirmed by Co-IP. C4-2 cells expressing Flag-GRB10 or Flag-control were collected and lysed with NETN buffer. Five percent of input was collected for each sample. One mg of protein from each sample was incubated with FLAG magnetic beads. GRB10 and PP2A subunits were detected via Western Blotting. (**B**) Endogenous binding of GRB10 to PP2A was detected by Co-IP performed in C4-2 cells. Five mg of protein lysates were incubated with normal mouse IgG or anti-GRB10 antibody and then with protein A/G magnetic beads. Five percent of input was collected. GRB10 and PP2A subunits were detected via Western Blotting. (**C**) Effects of GRB10 knockdown on the protein levels of the PP2A C subunit in LNCaP were determined using stable GRB10 knockdown (KD1, KD2) and control (shC) cell lines by Western Blotting. (**D**) Effects of transient GRB10 overexpression on the protein levels of the PP2A C subunit in LNCaP were determined using Western Blotting. (**E**) Effects of GRB10 knockdown on the mRNA expression of PPP2CA (encoding PP2A C subunit) in

LNCaP were determined based on the microarray performed in Chapter 5.2.1. The mRNA expression was normalized to shControl.

5.3 Discussion

In the previous chapters, we discussed the potential role of GRB10 as a driver gene for CRPC development. To support this hypothesis, we analyzed the transcriptomic changes induced by GRB10 knockdown. We found that knockdown of GRB10 significantly downregulated the Androgen_Response gene set, suggesting knockdown of GRB10 decreased AR activity. AR, the key mediator of androgen response signaling, is still the dominant driver of CRPC progression even with continuous ADT and more potent ARPIs. In fact, the occurrence of AR genetic alterations is significantly increased from less than 2% in HNPC [67, 73] to around 60% in terminal CRPC [67, 68, 70]. This phenomenon indicates that GRB10 could support AR function during early CRPC development as it undergoes the pressure of first-line hormonal therapy. When CRPC is established, higher expression of GRB10 also assists AR in cancer progression until the PCa cells accumulate the enough genomic aberrations that finally lead to AR amplification or AR mutation.

Glycolysis is one of the other gene sets inhibited by GRB10-knockdown. Consistent with our previous findings, glycolysis is the downstream pathway regulated by both AR signaling and AKT signaling [255, 288], which were both inhibited by GRB10 knockdown. Glucose metabolism in PCa is dramatically different than that in other types

of cancer. Back in the 1920s, Dr. Otto Heinrich Warburg and his team observed that cancer cells convert glucose to lactic acid instead of preferring the more energy-efficient tricarboxylic acid (TCA) cycle and oxidative phosphorylation (OXPHOS). This occurred regardless of the presence of oxygen. It became known as aerobic glycolysis or the Warburg Effect and is a hallmark of cancer [289]. Thus, high consumption of glucose is one of the most distinctive traits of cancer cells compared to healthy tissue. It is the scientific basis upon which 2-deoxy-2-[fluorine-18] fluoro- D-glucose-positron emission tomography/ computed tomography (18F-FDG PET/CT) is used to diagnose cancer and detect its recurrence [290]. However, in PCa, and particularly in HNPC, FDG PET/CT is not clinically applicable due to limited sensitivity/ specificity [291]. The reason could arise from the unique function of the human prostate gland to produce citrate [292]. Clinical observations indicate that human semen contains 240~1,300-fold higher concentrations of citrate compared to blood plasma. This citrate is produced and secreted by healthy prostatic epithelial cells [293] and mainly functions to maintain the pH of the seminal fluid. To produce large amounts of citrate, prostate epithelial cells intake a large amount of glucose and treat citrate as an end-product rather than as an intermediate in glucose metabolism. This is distinct from other cell types, which uses citrate for energy production through the TCA cycle and OXPHOS. Therefore, healthy prostate epithelial cells have a low level of activity in the TCA cycle and OXPHOS but a relatively high intake of glucose to maintain its citrate production. In malignant prostate cells, glucose metabolism changes dramatically. PCa cells start to further catalyze citrate through the TCA cycle and OXPHOS to produce ATP and promote lipid and amino acid synthesis [292]. Eventually, as PCa progresses into mCRPC (metastatic CRPC), the TCA cycle and OXPHOS shut

down and aerobic glycolysis increases. This results in the acidification of the tumor microenvironment and the accumulation of building blocks leading to a higher proliferation rate and tumor aggressiveness [292]. In this clinical circumstance, 18F-FDG PET/CT has been shown to be an effective, non-invasive approach for the detection of PCa recurrence and metastasis [294, 295]. Here, we show that GRB10 is functionally important in glycolysis, which suggests that the upregulation of GRB10 in CRPC mediates increased aerobic glycolysis and promotes PCa progression and aggressiveness.

To further elucidate the molecular mechanism of GRB10-mediated CRPC development, we investigated the GRB10 interactome in PCa cells by using Co-IP coupled with LC/MS/MS. We found that two major groups of proteins were associated with GRB10. One group of proteins were metabolism-related proteins such as glyceraldehyde-3-phosphate dehydrogenase (*GAPDH*), pyruvate kinase (*PKM*), ADP/ATP translocase 2 (*SLC25A5*), ATP synthase subunit alpha (*ATP5F1A*), and D-3-phosphoglycerate dehydrogenase (*PHGDH*). GAPDH and PKM are major enzymes involved in the glycolysis pathway [296, 297]. PHGDH is an enzyme which catalyzes the oxidation of one of the glycolysis intermediates, 3-phopho-D-glycerate (3-PG), to 3-phosphooxypyruvate (p-Pyr), which can be used to biosynthesize L-serine and glycine [298]. The other two enzymes, ATP5F1A and SLC25A5, are located in the mitochondria and are involved in OXPHOS and energy generation [299, 300]. Overall, these proteins that we discovered to potentially interact with GRB10 are closely related to cellular metabolism and energy production. This suggests that one of the functions of GRB10 is regulating cell metabolism. Our finding could support a hypothesis that knockdown of

GRB10 downregulates overall glycolysis activity, sterol biosynthesis, and small molecule biosynthetic processes.

Another group of GRB10-interacting proteins we identified is the Hsp70 family of chaperone proteins, including heat shock protein 70 family protein 8 (*HSPA8*), heat shock protein 70 family protein 5 (*HSPA5*), and heat shock protein 70 family protein 1A (*HSPA1A*). Hsp70 family proteins are chaperone proteins which assist in the proper folding of unfolded proteins or refolding of misfolded proteins [301]. Evidence suggests that Hsp70 protects cancer cells from apoptosis induced by various cellular stresses and therapies such as reactive oxygen species, radiotherapies, and chemotherapies [301]. Thus, targeting Hsp70 has been suggested to be an effective therapeutic approach for treatment-resistant cancers including PCa [302, 303]. Based on this evidence, we suspect that the upregulation of GRB10 and the interaction of GRB10 with Hsp70 could promote the survival of treatment-resistant dormant PCa cells and eventual development of CRPC.

PP2A is a top-ranked protein complex that we identified to be associated with GRB10 in PCa cells. PP2A has long been reported to play a tumor suppressive role in cancer development and progression [280]. PP2A can dephosphorylate a variety of substrates of cyclin-dependent kinases (CDK) to inhibit cell cycle progression [304-306]. In lung and colon cancer, 15% of the primary clinical tumors harbour somatic alterations in PP2A, resulting in the instability of PP2A protein complex and leading to deregulated cell cycle control [283]. PP2A is also involved in Wnt signaling, where PP2A dephosphorylates GSK3β and decreases the expression of β-catenin to inhibit Wnt

signaling [307]. In addition, PP2A could regulate cell apoptosis. PP2A could dephosphorylate c-Jun and p53, two critical apoptosis-associated proteins, and inhibit the transcription of pro-apoptotic genes [308]. In PCa, PTEN-deletion is one of the most frequent genomic alterations in both primary and metastatic PCas. PTEN loss causes PI3K/ AKT signaling hyperactivation and promotes tumorigenesis and treatment-resistance in PCa [239, 262]. PP2A is a known inhibitor of AKT and dephosphorylates AKT at T308 [277, 309]. Therefore, activating PP2A has been suggested to be a potential therapeutic strategy in the management of PCa [310-312].

In this chapter, we provide evidence that GRB10 expression could regulate PP2A protein expression, suggesting that GRB10 could be an upstream regulator inhibiting its activity. Since PP2A is a general tumor suppressor which dephosphorylates and deactivates vital proteins involved in cell proliferation, metabolism, and apoptosis in multiple cancer types including PCa, the fact that GRB10 controls PP2A protein expression shows that GRB10 is a potential universal driver for the development and progression of CRPC.

Chapter 6 Conclusions

6.1 Summary of Findings

CRPC remains an extremely aggressive, incurable disease even though the effectiveness of ADT and recently approved Cabazitaxel, ABI, ENZ, APA, and DAR are effective. Therefore, a continued targeting of the AR pathway may not be the ultimate solution, and other factors should be taken into consideration to manage the development of CRPC. During CRPC development, particularly before the tumor progresses into the androgen-independent stage, signaling pathways other than the AR pathway should be activated to protect cancer cells and promote its proliferation. Therefore, in this doctoral study, we hypothesized that CRPC driving genes should fulfill the following criteria: (1) CRPC driving genes should be commonly expressed in CRPC; (2) CRPC driving genes should be upregulated following ADT as an early and continuous event; (3) CRPC driving genes should be upregulated after CRPC development, and lastly (4) CRPC driving genes should be functionally critical to cell growth and survival. Our hypothesis focuses more on the early time points during the CRPC development, since the genes upregulated only when CRPC is developed may be a consequence of CRPC aggressiveness but not a driver of its development.

In Chapter 2, following our hypothesis, we identified *GRB10* as a potential driving gene for the development of CRPC. Firstly, we demonstrated that HNPC PDX models are suitable tools to study the development of CRPC, especially, the lines are capable of spontaneous recurrence into to CRPC following host castration. When castration is

applied to the tumor-bearing mice, the tumor shrinks and serum PSA level decreases significantly. On the molecular level, AR signaling was markedly inhibited as indicated by the decreased expression of AR regulated genes and signatures. By analyzing the transcriptomic data acquired before, during, and after the development of CRPC, we found that *GRB10* is the top-ranked gene upregulated both during and after CRPC development. We further validated our identification of GRB10 in multiple independent studies, showing that *GRB10* expression is elevated after ADT in genetically-engineered murine PCa models. With the analysis of clinical PCa cohorts, we further confirmed that *GRB10* was significantly upregulated in clinical CRPC and its elevated expression was correlated with poor treatment outcomes. In view of these findings, we investigated the function of *GRB10* in PCa cell lines. Knockdown of *GRB10* using two independent shRNAs led to significant decreased cell proliferation. The reduction of GRB10 expression also inhibited cell cycle progression as indicated by decreased DNA synthesis and accumulation of cells at G0/1 stage. To further address the potential driver role of GRB10 in CRPC development, we overexpressed *GRB10* in LNCaP androgen-sensitive PCa cell lines and observed that the ectopic expression of *GRB10* promoted LNCaP androgen-independent proliferation. Mechanistically, given that AKT is well-reported to be one of the significant drivers of CRPC development, and given that GRB10 was reported to regulate AKT in other cell contexts, we examined the role of GRB10 in regulating AKT activity in PCa. Evidence suggest that increased expression of GRB10 during CRPC development promotes the activation of AKT, which mediates the survival and proliferation of PCa cells. Overall, the data indicate that GRB10 is a potential driver

of CRPC development and that a combination of ADT and GRB10-silencing could be a novel strategy to delay the development of PCa androgen-independent growth.

In Chapter 3, to explain the mechanism behind the upregulation of GRB10 during CRPC development, we looked into the upstream regulators of GRB10 in PCa. Since AR is a transcription factor and ADT induced the upregulation of GRB10 in PCa PDX models, we suspected that AR repressed the expression of GRB10. We first manipulated AR activity in PCa cell lines using androgen ablation, AR antagonist, ENZ, and the AR activator R1881. We found that the expression of GRB10 was associated with AR activity, where AR inhibition increased GRB10 expression while AR activation led to decreased GRB10 expression. Clinical evidence supported our findings, where *GRB10* was upregulated after neoadjuvant ADT and the expression of *GRB10* and *KLK3* (PSA) was significantly negatively correlated. Through a thorough analysis of publically available AR ChIP-seq data, we identified three potential androgen-responsive elements (AREs) located in the intron of *GRB10*. ChIP-PCR suggests all three potential AREs could interact with activated AR. Interestingly, we also found AR enrichment at the putative AREs in clinical untreated and CRPC cases but not in treatment responsive cases, suggesting that our findings were clinically relevant. Further validation of potential AREs using luciferase reporter assay confirmed that GRB10 was transcriptionally repressed by AR through an ARE located in the intron of GRB10 (chr7: 50657497-50657511).

In Chapters 4 and 5, we focused on the potential mechanisms of GRB10-mediated CRPC development. Since GRB10 is an adaptor protein that provides scaffolding for

multiple signaling pathway cascades and regulates their functions, we used multi-omics analyses to elucidate its functional partners in PCa cells. Firstly, we analyzed the transcriptomic changes induced by GRB10 knockdown. Our data suggest that reduced GRB10 expression led to a dramatic decrease in several PCa progression-related gene sets including androgen response, mTORC1 signaling, and glycolysis. Next, we performed LC/MS to investigate the interactome of GRB10 in PCa cells. Interestingly, PP2A, a well-established tumor suppressor, was found to interact with GRB10. We further provided evidence that the interaction of GRB10 and PP2A decreased PP2A expression, which suggests that partial, if not all of the function of GRB10, was achieved through the regulation of PP2A.

6.2 Limitations and Future Directions

The future directions of this study are considered closely with regards to the limitation of the current study. In terms of the findings that GRB10 is regulated by AR, assays were performed in limited PCa cell lines. Given that PCa is a heterogeneous disease, the conclusion drawn from only PCa cell lines may be biased. We could use our collections of over 40 PCa PDX models to validate our findings. One of the advantages of our PCa PDX models is that these models are transplantable. We can thus acquire enough cancer tissue samples for ChIP experiments, overcoming the common problem that patient tissue samples are of too limited quantity for satisfactory protein-based assay.

In this study, we proposed that GRB10 is a potential driver for the development of CRPC. To this end, we overexpressed GRB10 and demonstrated that the ectopic expression of GRB10 could promote LNCaP androgen-independent growth. However, the level of GRB10 overexpression we tested is much higher than that in CRPC. Since GRB10 is negatively regulated by AR, we could use the CRISPR-Cas9 technique to knockout the androgen-responsive element we discovered, which repressed the expression of GRB10. By doing so, we can monitor the function of GRB10 in a more clinically relevant manner and demonstrate its driver role in the development of CRPC.

In Chapter 4, we discovered that AR can transcriptionally regulate GRB10 expression through an ARE located in GRB10 intron. However, the precise mechanism of AR regulating GRB10 is not conclusive as only luciferase reporter assays were performed. To better prove AR represses GRB10 expression through the identified ARE, more assays need to be used. For example, as previously mentioned, we could use the CRISPR-Cas9 technique to knockout the ARE. AR can no longer regulate GRB10 expression if the repression was conducted through that regulatory elements. Furthermore, the repression function of AR is supported be co-repressor factors such as LSD1, EZH2, and Rb1 [248, 254, 313-316]. Thus, we can perform a rapid immunoprecipitation mass spectrometry of endogenous proteins (RIMS) to identify the potential co-factors of AR in this case [317].

In Chapter 5, we identified PP2A as a GRB10-interacting protein using an unbiased IP-MS in PCa cells. We then established that GRB10 downregulates PP2A

protein expression. Although we have ruled out by our findings that this is achieved through a reduction in mRNA expression, there remains multiple ways to reduce PP2A protein expression, including alternating post-translational modification, protein degradation and protein synthesis. To further elucidate the precise mechanism of GRB10-regulated PP2A expression, we will study whether the expression GRB10 would affect the protein turnover of PP2A.

6.3 Conclusion and Significance

In summary, this doctoral study led to the identification of *GRB10* as a potential driving gene of CRPC development. We have validated its significant upregulation in multiple clinical CRPC cohorts, and its elevated expression was associated with disease aggressiveness. We further confirmed its transcriptional suppression by AR, and established the effects of its knockdown on impeding CRPC cell proliferation. The overexpression of GRB10 also led to increased androgen-independent growth. Mechanistically, knockdown of GRB10 induced significant changes at the transcriptome level and downregulated multiple pathways related to androgen independence. Through unbiased immunoprecipitation-mass spectrometry (IP-MS), we demonstrated that GRB10 could directly bind to protein phosphatase 2A (PP2A), a well-established tumor suppressor. Moreover, GRB10 can suppress PP2A expression. These data suggest that GRB10 plays an important role in CRPC development and progression.

The study provides a new theory of CRPC development, where ADT, whether through androgen ablation or AR antagonists, induces the expression of *GRB10*, an AR repressed gene. Upregulation of *GRB10* increased many cancer progression-related pathways, including PI3K/AKT/mTOR, AR signaling, and glycolysis. Meanwhile, the elevated expression of GRB10 interacts with PP2A and decreases its protein expression. Taken together, these changes on the molecular level led to increased cell proliferation and survival, which eventually promotes the development of CRPC. (Fig 6.1)

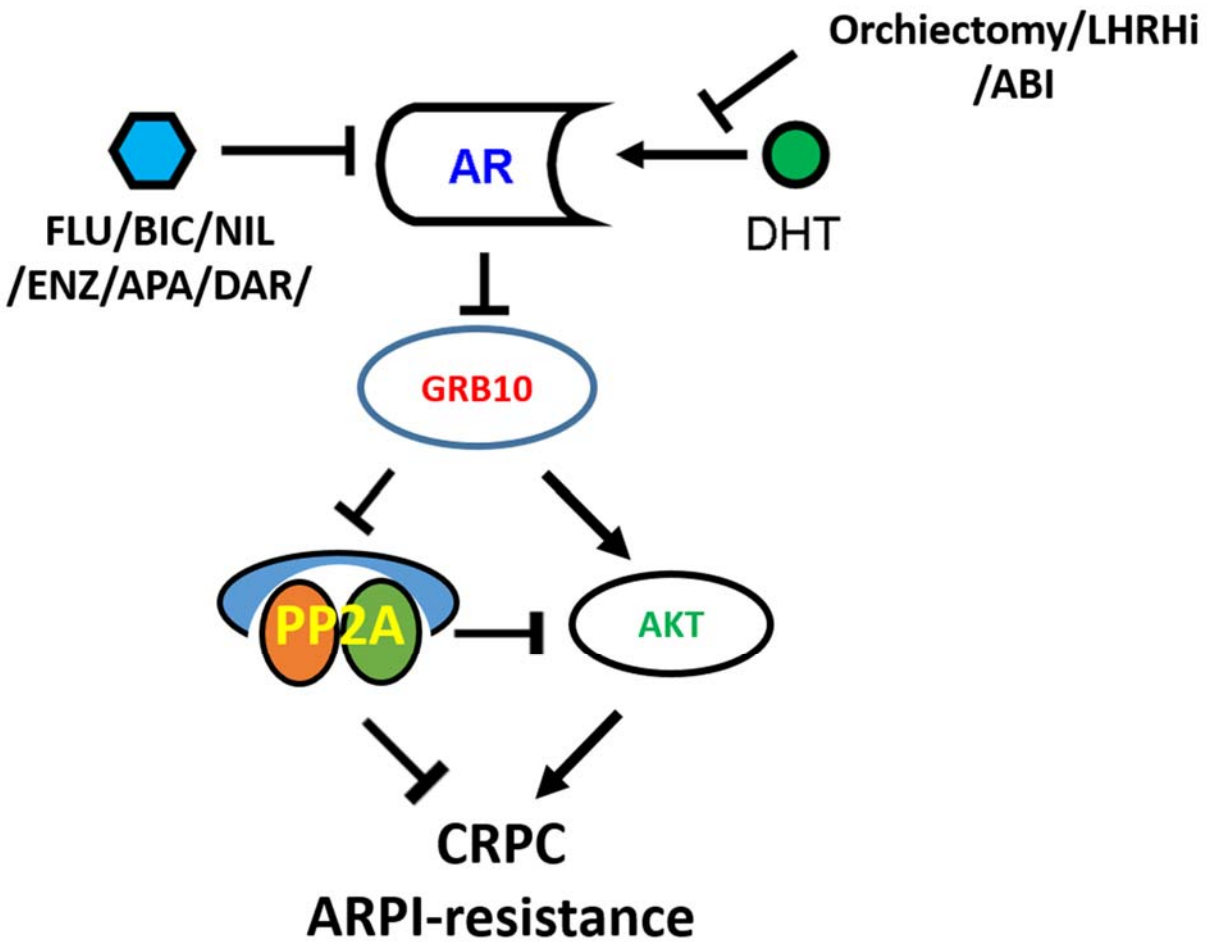

Figure 6.1. The role of GRB10 in the development of CRPC

A schematic model summarizing the mechanisms by which increased expression of GRB10 after ARPI (ADT/AR signaling inhibitor) mediates the development of CRPC and potentially ARPI resistance through enhancing AKT activity and inhibiting PP2A. FLU: Flutamide, BIC: Bicalutamide, NIL: Nilutamide, ENZ: Enzalutamide, APA: Apalutamide, DAR: Darolutamide, LHRHi: Luteinizing hormone-releasing hormone inhibition, ABI: Abiraterone.

In conclusion, this study increased our understanding of the mechanisms underlying the development of CRPC, identifying GRB10 as a potential driver for the development of CRPC and providing a novel therapeutic target to lead to improved therapy of advanced PCa.

Bibliography

[1] Cunha GR, Donjacour AA, Cooke PS, Mee S, Bigsby RM, Higgins SJ, et al. The endocrinology and developmental biology of the prostate. Endocr Rev. 1987;8:338-62.

[2] Lilja H. Structure and function of prostatic- and seminal vesicle-secreted proteins involved in the gelation and liquefaction of human semen. Scand J Clin Lab Invest Suppl. 1988;191:13-20.

[3] Hayward SW, Cunha GR. The prostate: development and physiology. Radiol Clin North Am. 2000;38:1-14.

[4] Myers RP. Structure of the adult prostate from a clinician's standpoint. Clin Anat. 2000;13:214-5.

[5] McNeal JE. Origin and development of carcinoma in the prostate. Cancer. 1969;23:24-34.

[6] McNeal JE. The zonal anatomy of the prostate. The Prostate. 1981;2:35-49.

[7] McNeal JE. Normal histology of the prostate. Am J Surg Pathol. 1988;12:619-33.

[8] Cohen RJ, Shannon BA, Phillips M, Moorin RE, Wheeler TM, Garrett KL. Central zone carcinoma of the prostate gland: a distinct tumor type with poor prognostic features. The Journal of urology. 2008;179:1762-7; discussion 7.

[9] Roehrborn CG. Benign prostatic hyperplasia: an overview. Rev Urol. 2005;7 Suppl 9:S3-S14.

[10] McNeal JE, Redwine EA, Freiha FS, Stamey TA. Zonal distribution of prostatic adenocarcinoma. Correlation with histologic pattern and direction of spread. Am J Surg Pathol. 1988;12:897-906.

[11] Abate-Shen C, Shen MM. Molecular genetics of prostate cancer. Genes & development. 2000;14:2410-34.

[12] Kwon OJ, Xin L. Prostate epithelial stem and progenitor cells. Am J Clin Exp Urol. 2014;2:209-18.

[13] Purkis PE, Steel JB, Mackenzie IC, Nathrath WB, Leigh IM, Lane EB. Antibody markers of basal cells in complex epithelia. J Cell Sci. 1990;97 (Pt 1):39-50.

[14] Wang Y, Hayward S, Cao M, Thayer K, Cunha G. Cell differentiation lineage in the prostate. Differentiation. 2001;68:270-9.

[15] Tran CP, Lin C, Yamashiro J, Reiter RE. Prostate stem cell antigen is a marker of late intermediate prostate epithelial cells. Mol Cancer Res. 2002;1:113-21.

[16] Marker PC, Donjacour AA, Dahiya R, Cunha GR. Hormonal, cellular, and molecular control of prostatic development. Dev Biol. 2003;253:165-74.

[17] Cunha GR, Shannon JM, Neubauer BL, Sawyer LM, Fujii H, Taguchi O, et al. Mesenchymal-epithelial interactions in sex differentiation. Hum Genet. 1981;58:68-77.

[18] Cunha GR, Lung B. The possible influence of temporal factors in androgenic responsiveness of urogenital tissue recombinants from wild-type and androgen-insensitive (Tfm) mice. J Exp Zool. 1978;205:181-93.

[19] Cunha GR, Lung B, Reese B. Glandular epithelial induction by embryonic mesenchyme in adult bladder epithelium of BALB/c mice. Invest Urol. 1980;17:302-4.

[20] Cunha GR, Chung LW, Shannon JM, Reese BA. Stromal-epithelial interactions in sex differentiation. Biol Reprod. 1980;22:19-42.

[21] Siegel RL, Miller KD, Jemal A. Cancer statistics, 2019. CA: a cancer journal for clinicians. 2019;69:7-34.

[22] Bray F, Ferlay J, Soerjomataram I, Siegel RL, Torre LA, Jemal A. Global cancer statistics 2018: GLOBOCAN estimates of incidence and mortality worldwide for 36 cancers in 185 countries. CA: a cancer journal for clinicians. 2018;68:394-424.

[23] Pishgar F, Ebrahimi H, Saeedi Moghaddam S, Fitzmaurice C, Amini E. Global, Regional and National Burden of Prostate Cancer, 1990 to 2015: Results from the Global Burden of Disease Study 2015. The Journal of urology. 2018;199:1224-32.

[24] Miller KD, Nogueira L, Mariotto AB, Rowland JH, Yabroff KR, Alfano CM, et al. Cancer treatment and survivorship statistics, 2019. CA: a cancer journal for clinicians. 2019.

[25] Steele CB, Li J, Huang B, Weir HK. Prostate cancer survival in the United States by race and stage (2001-2009): Findings from the CONCORD-2 study. Cancer. 2017;123 Suppl 24:5160-77.

[26] Fine SW, Reuter VE. Anatomy of the prostate revisited: implications for prostate biopsy and zonal origins of prostate cancer. Histopathology. 2012;60:142-52.

[27] Lee CH, Akin-Olugbade O, Kirschenbaum A. Overview of prostate anatomy, histology, and pathology. Endocrinol Metab Clin North Am. 2011;40:565-75, viii-ix.

[28] Bostwick DG. The pathology of early prostate cancer. CA: a cancer journal for clinicians. 1989;39:376-93.

[29] Marcus DM, Goodman M, Jani AB, Osunkoya AO, Rossi PJ. A comprehensive review of incidence and survival in patients with rare histological variants of prostate cancer in the United States from 1973 to 2008. Prostate Cancer Prostatic Dis. 2012;15:283-8.

[30] Ruijter ET, Miller GJ, van de Kaa CA, van Bokhoven A, Bussemakers MJ, Debruyne FM, et al. Molecular analysis of multifocal prostate cancer lesions. J Pathol. 1999;188:271-7.

[31] Gandhi J, Afridi A, Vatsia S, Joshi G, Joshi G, Kaplan SA, et al. The molecular biology of prostate cancer: current understanding and clinical implications. Prostate Cancer Prostatic Dis. 2018;21:22-36.

[32] Chiang YT, Wang K, Fazli L, Qi RZ, Gleave ME, Collins CC, et al. GATA2 as a potential metastasis-driving gene in prostate cancer. Oncotarget. 2014;5:451-61.

[33] Feldman BJ, Feldman D. The development of androgen-independent prostate cancer. Nat Rev Cancer. 2001;1:34-45.

[34] Karantanos T, Corn PG, Thompson TC. Prostate cancer progression after androgen deprivation therapy: mechanisms of castrate resistance and novel therapeutic approaches. Oncogene. 2013;32:5501-11.

[35] Bell N, Connor Gorber S, Shane A, Joffres M, Singh H, Dickinson J, et al. Recommendations on screening for prostate cancer with the prostate-specific antigen test. CMAJ. 2014;186:1225-34.

[36] Miller DC, Hafez KS, Stewart A, Montie JE, Wei JT. Prostate carcinoma presentation, diagnosis, and staging: an update form the National Cancer Data Base. Cancer. 2003;98:1169-78.

[37] Mottet N, Bellmunt J, Bolla M, Briers E, Cumberbatch MG, De Santis M, et al. EAU-ESTRO-SIOG Guidelines on Prostate Cancer. Part 1: Screening, Diagnosis, and Local Treatment with Curative Intent. European urology. 2017;71:618-29.

[38] Carter HB, Albertsen PC, Barry MJ, Etzioni R, Freedland SJ, Greene KL, et al. Early detection of prostate cancer: AUA Guideline. The Journal of urology. 2013;190:419-26.

[39] Chan DW, Bruzek DJ, Oesterling JE, Rock RC, Walsh PC. Prostate-specific antigen as a marker for prostatic cancer: a monoclonal and a polyclonal immunoassay compared. Clin Chem. 1987;33:1916-20.

[40] Lilja H, Ulmert D, Vickers AJ. Prostate-specific antigen and prostate cancer: prediction, detection and monitoring. Nat Rev Cancer. 2008;8:268-78.

[41] van der Kwast TH, Lopes C, Santonja C, Pihl CG, Neetens I, Martikainen P, et al. Guidelines for processing and reporting of prostatic needle biopsies. J Clin Pathol. 2003;56:336-40.

[42] Gleason DF, Mellinger GT. Prediction of prognosis for prostatic adenocarcinoma by combined histological grading and clinical staging. The Journal of urology. 1974;111:58-64.

[43] Epstein JI, Egevad L, Amin MB, Delahunt B, Srigley JR, Humphrey PA, et al. The 2014 International Society of Urological Pathology (ISUP) Consensus Conference on Gleason Grading of Prostatic Carcinoma: Definition of Grading Patterns and Proposal for a New Grading System. Am J Surg Pathol. 2016;40:244-52.

[44] Humphrey PA. Gleason grading and prognostic factors in carcinoma of the prostate. Mod Pathol. 2004;17:292-306.

[45] van Poppel H. Locally advanced and high risk prostate cancer: The best indication for initial radical prostatectomy? Asian J Urol. 2014;1:40-5.

[46] Schroder FH, Hermanek P, Denis L, Fair WR, Gospodarowicz MK, Pavone-Macaluso M. The TNM classification of prostate cancer. Prostate Suppl. 1992;4:129-38.

[47] D'Amico AV, Whittington R, Malkowicz SB, Schultz D, Blank K, Broderick GA, et al. Biochemical outcome after radical prostatectomy, external beam radiation therapy, or interstitial radiation therapy for clinically localized prostate cancer. Jama. 1998;280:969-74.

[48] Thompson I, Thrasher JB, Aus G, Burnett AL, Canby-Hagino ED, Cookson MS, et al. Guideline for the management of clinically localized prostate cancer: 2007 update. The Journal of urology. 2007;177:2106-31.

[49] Heidenreich A, Aus G, Bolla M, Joniau S, Matveev VB, Schmid HP, et al. EAU guidelines on prostate cancer. European urology. 2008;53:68-80.

[50] Klotz L, Zhang L, Lam A, Nam R, Mamedov A, Loblaw A. Clinical results of long-term follow-up of a large, active surveillance cohort with localized prostate cancer. J Clin Oncol. 2010;28:126-31.

[51] Selvadurai ED, Singhera M, Thomas K, Mohammed K, Woode-Amissah R, Horwich A, et al. Medium-term outcomes of active surveillance for localised prostate cancer. European urology. 2013;64:981-7.

[52] Lardas M, Liew M, van den Bergh RC, De Santis M, Bellmunt J, Van den Broeck T, et al. Quality of Life Outcomes after Primary Treatment for Clinically Localised Prostate Cancer: A Systematic Review. European urology. 2017;72:869-85.

[53] Meng MV, Elkin EP, Latini DM, Duchane J, Carroll PR. Treatment of patients with high risk localized prostate cancer: results from cancer of the prostate strategic urological research endeavor (CaPSURE). The Journal of urology. 2005;173:1557-61.

[54] Steuber T, Budaus L, Walz J, Zorn KC, Schlomm T, Chun F, et al. Radical prostatectomy improves progression-free and cancer-specific survival in men with lymph node positive prostate cancer in the prostate-specific antigen era: a confirmatory study. BJU Int. 2011;107:1755-61.

[55] Huggins C, Stevens RE, Hodges CV. Studies on prostate cancer II The effects of castration on advanced carcinoma of the prostate gland. Archives of surgery. 1941;43:209-23.

[56] Sharifi N, Gulley JL, Dahut WL. Androgen deprivation therapy for prostate cancer. Jama-J Am Med Assoc. 2005;294:238-44.

[57] Perlmutter MA, Lepor H. Androgen deprivation therapy in the treatment of advanced prostate cancer. Rev Urol. 2007;9 Suppl 1:S3-8.

[58] Gravis G, Fizazi K, Joly F, Oudard S, Priou F, Esterni B, et al. Androgen-deprivation therapy alone or with docetaxel in non-castrate metastatic prostate cancer (GETUG-AFU 15): a randomised, open-label, phase 3 trial. Lancet Oncol. 2013;14:149-58.

[59] Sweeney CJ, Chen YH, Carducci M, Liu G, Jarrard DF, Eisenberger M, et al. Chemohormonal Therapy in Metastatic Hormone-Sensitive Prostate Cancer. The New England journal of medicine. 2015;373:737-46.

[60] Fizazi K, Tran N, Fein L, Matsubara N, Rodriguez-Antolin A, Alekseev BY, et al. Abiraterone plus Prednisone in Metastatic, Castration-Sensitive Prostate Cancer. The New England journal of medicine. 2017;377:352-60.

[61] Hoyle AP, Ali A, James ND, Cook A, Parker CC, de Bono JS, et al. Abiraterone in "High-" and "Low-risk" Metastatic Hormone-sensitive Prostate Cancer. European urology. 2019.

[62] Davis ID, Martin AJ, Stockler MR, Begbie S, Chi KN, Chowdhury S, et al. Enzalutamide with Standard First-Line Therapy in Metastatic Prostate Cancer. The New England journal of medicine. 2019;381:121-31.

[63] Chi KN, Agarwal N, Bjartell A, Chung BH, Pereira de Santana Gomes AJ, Given R, et al. Apalutamide for Metastatic, Castration-Sensitive Prostate Cancer. The New England journal of medicine. 2019;381:13-24.

[64] Attar RM, Takimoto CH, Gottardis MM. Castration-resistant prostate cancer: locking up the molecular escape routes. Clinical cancer research : an official journal of the American Association for Cancer Research. 2009;15:3251-5.

[65] Smith MR, Kabbinavar F, Saad F, Hussain A, Gittelman MC, Bilhartz DL, et al. Natural history of rising serum prostate-specific antigen in men with castrate nonmetastatic prostate cancer. J Clin Oncol. 2005;23:2918-25.

[66] Sartor O, de Bono JS. Metastatic Prostate Cancer. The New England journal of medicine. 2018;378:1653-4.

[67] Grasso CS, Wu YM, Robinson DR, Cao X, Dhanasekaran SM, Khan AP, et al. The mutational landscape of lethal castration-resistant prostate cancer. Nature. 2012;487:239-43.

[68] Robinson D, Van Allen EM, Wu YM, Schultz N, Lonigro RJ, Mosquera JM, et al. Integrative clinical genomics of advanced prostate cancer. Cell. 2015;161:1215-28.

[69] Kumar A, Coleman I, Morrissey C, Zhang X, True LD, Gulati R, et al. Substantial interindividual and limited intraindividual genomic diversity among tumors from men with metastatic prostate cancer. Nature medicine. 2016;22:369-78.

[70] Abida W, Cyrta J, Heller G, Prandi D, Armenia J, Coleman I, et al. Genomic correlates of clinical outcome in advanced prostate cancer. Proceedings of the National Academy of Sciences of the United States of America. 2019;116:11428-36.

[71] Armenia J, Wankowicz SAM, Liu D, Gao J, Kundra R, Reznik E, et al. The long tail of oncogenic drivers in prostate cancer. Nat Genet. 2018;50:645-51.

[72] Abida W, Armenia J, Gopalan A, Brennan R, Walsh M, Barron D, et al. Prospective Genomic Profiling of Prostate Cancer Across Disease States Reveals Germline and Somatic Alterations That May Affect Clinical Decision Making. JCO Precis Oncol. 2017;2017.

[73] Cancer Genome Atlas Research N. The Molecular Taxonomy of Primary Prostate Cancer. Cell. 2015;163:1011-25.

[74] Korpal M, Korn JM, Gao X, Rakiec DP, Ruddy DA, Doshi S, et al. An F876L mutation in androgen receptor confers genetic and phenotypic resistance to MDV3100 (enzalutamide). Cancer discovery. 2013;3:1030-43.

[75] Visakorpi T, Hyytinen E, Koivisto P, Tanner M, Keinanen R, Palmberg C, et al. In vivo amplification of the androgen receptor gene and progression of human prostate cancer. Nat Genet. 1995;9:401-6.

[76] Marcelli M, Ittmann M, Mariani S, Sutherland R, Nigam R, Murthy L, et al. Androgen receptor mutations in prostate cancer. Cancer research. 2000;60:944-9.

[77] Linja MJ, Savinainen KJ, Saramaki OR, Tammela TL, Vessella RL, Visakorpi T. Amplification and overexpression of androgen receptor gene in hormone-refractory prostate cancer. Cancer research. 2001;61:3550-5.

[78] Hu R, Dunn TA, Wei S, Isharwal S, Veltri RW, Humphreys E, et al. Ligand-independent androgen receptor variants derived from splicing of cryptic exons signify hormone-refractory prostate cancer. Cancer research. 2009;69:16-22.

[79] Guo Z, Yang X, Sun F, Jiang R, Linn DE, Chen H, et al. A novel androgen receptor splice variant is up-regulated during prostate cancer progression and promotes androgen depletion-resistant growth. Cancer research. 2009;69:2305-13.

[80] Locke JA, Guns ES, Lubik AA, Adomat HH, Hendy SC, Wood CA, et al. Androgen levels increase by intratumoral de novo steroidogenesis during progression of castration-resistant prostate cancer. Cancer research. 2008;68:6407-15.

[81] Huang Y, Jiang X, Liang X, Jiang G. Molecular and cellular mechanisms of castration resistant prostate cancer. Oncol Lett. 2018;15:6063-76.

[82] Chandrasekar T, Yang JC, Gao AC, Evans CP. Mechanisms of resistance in castration-resistant prostate cancer (CRPC). Translational andrology and urology. 2015;4:365-80.

[83] Luu-The V, Belanger A, Labrie F. Androgen biosynthetic pathways in the human prostate. Best Pract Res Clin Endocrinol Metab. 2008;22:207-21.

[84] Sharifi N. Minireview: Androgen metabolism in castration-resistant prostate cancer. Molecular endocrinology. 2013;27:708-14.

[85] Tomlins SA, Rhodes DR, Perner S, Dhanasekaran SM, Mehra R, Sun XW, et al. Recurrent fusion of TMPRSS2 and ETS transcription factor genes in prostate cancer. Science. 2005;310:644-8.

[86] Knudsen KE, Penning TM. Partners in crime: deregulation of AR activity and androgen synthesis in prostate cancer. Trends Endocrinol Metab. 2010;21:315-24.

[87] Chang KH, Li R, Papari-Zareei M, Watumull L, Zhao YD, Auchus RJ, et al. Dihydrotestosterone synthesis bypasses testosterone to drive castration-resistant prostate cancer. Proceedings of the National Academy of Sciences of the United States of America. 2011;108:13728-33.

[88] Cai C, Balk SP. Intratumoral androgen biosynthesis in prostate cancer pathogenesis and response to therapy. Endocr Relat Cancer. 2011;18:R175-82.

[89] Chang KH, Li R, Kuri B, Lotan Y, Roehrborn CG, Liu J, et al. A gain-of-function mutation in DHT synthesis in castration-resistant prostate cancer. Cell. 2013;154:1074-84.

[90] Yoshino T, Shiina H, Urakami S, Kikuno N, Yoneda T, Shigeno K, et al. Bcl-2 expression as a predictive marker of hormone-refractory prostate cancer treated with taxane-based chemotherapy. Clinical cancer research : an official journal of the American Association for Cancer Research. 2006;12:6116-24.

[91] McDonnell TJ, Troncoso P, Brisbay SM, Logothetis C, Chung LW, Hsieh JT, et al. Expression of the protooncogene bcl-2 in the prostate and its association with emergence of androgen-independent prostate cancer. Cancer research. 1992;52:6940-4.

[92] Edlind MP, Hsieh AC. PI3K-AKT-mTOR signaling in prostate cancer progression and androgen deprivation therapy resistance. Asian journal of andrology. 2014;16:378-86.

[93] Crumbaker M, Khoja L, Joshua AM. AR Signaling and the PI3K Pathway in Prostate Cancer. Cancers (Basel). 2017;9.

[94] Sharifi N. Steroid receptors aplenty in prostate cancer. The New England journal of medicine. 2014;370:970-1.

[95] Claessens F, Helsen C, Prekovic S, Van den Broeck T, Spans L, Van Poppel H, et al. Emerging mechanisms of enzalutamide resistance in prostate cancer. Nature reviews Urology. 2014;11:712-6.

[96] Denayer S, Helsen C, Thorrez L, Haelens A, Claessens F. The rules of DNA recognition by the androgen receptor. Molecular endocrinology. 2010;24:898-913.

[97] Ci X, Hao J, Dong X, Choi SY, Xue H, Wu R, et al. Heterochromatin Protein 1alpha Mediates Development and Aggressiveness of Neuroendocrine Prostate Cancer. Cancer research. 2018;78:2691-704.

[98] Akamatsu S, Wyatt AW, Lin D, Lysakowski S, Zhang F, Kim S, et al. The Placental Gene PEG10 Promotes Progression of Neuroendocrine Prostate Cancer. Cell Rep. 2015;12:922-36.

[99] Tannock IF, de Wit R, Berry WR, Horti J, Pluzanska A, Chi KN, et al. Docetaxel plus prednisone or mitoxantrone plus prednisone for advanced prostate cancer. The New England journal of medicine. 2004;351:1502-12.

[100] de Bono JS, Logothetis CJ, Molina A, Fizazi K, North S, Chu L, et al. Abiraterone and increased survival in metastatic prostate cancer. The New England journal of medicine. 2011;364:1995-2005.

[101] Beer TM, Armstrong AJ, Rathkopf DE, Loriot Y, Sternberg CN, Higano CS, et al. Enzalutamide in metastatic prostate cancer before chemotherapy. The New England journal of medicine. 2014;371:424-33.

[102] Scher HI, Fizazi K, Saad F, Taplin ME, Sternberg CN, Miller K, et al. Increased survival with enzalutamide in prostate cancer after chemotherapy. The New England journal of medicine. 2012;367:1187-97.

[103] Hussain M, Fizazi K, Saad F, Rathenborg P, Shore N, Ferreira U, et al. Enzalutamide in Men with Nonmetastatic, Castration-Resistant Prostate Cancer. The New England journal of medicine. 2018;378:2465-74.

[104] Fizazi K, Shore N, Tammela TL, Ulys A, Vjaters E, Polyakov S, et al. Darolutamide in Nonmetastatic, Castration-Resistant Prostate Cancer. The New England journal of medicine. 2019;380:1235-46.

[105] Mita AC, Denis LJ, Rowinsky EK, Debono JS, Goetz AD, Ochoa L, et al. Phase I and pharmacokinetic study of XRP6258 (RPR 116258A), a novel taxane, administered as a 1-hour infusion every 3 weeks in patients with advanced solid tumors. Clinical cancer

research : an official journal of the American Association for Cancer Research. 2009;15:723-30.

[106] de Morree E, van Soest R, Aghai A, de Ridder C, de Bruijn P, Ghobadi Moghaddam-Helmantel I, et al. Understanding taxanes in prostate cancer; importance of intratumoral drug accumulation. The Prostate. 2016;76:927-36.

[107] Wyatt AW, Gleave ME. Targeting the adaptive molecular landscape of castration-resistant prostate cancer. EMBO Mol Med. 2015;7:878-94.

[108] Horoszewicz JS, Leong SS, Chu TM, Wajsman ZL, Friedman M, Papsidero L, et al. The LNCaP cell line--a new model for studies on human prostatic carcinoma. Progress in clinical and biological research. 1980;37:115-32.

[109] Veldscholte J, Ris-Stalpers C, Kuiper GG, Jenster G, Berrevoets C, Claassen E, et al. A mutation in the ligand binding domain of the androgen receptor of human LNCaP cells affects steroid binding characteristics and response to anti-androgens. Biochemical and biophysical research communications. 1990;173:534-40.

[110] Vlietstra RJ, van Alewijk DC, Hermans KG, van Steenbrugge GJ, Trapman J. Frequent inactivation of PTEN in prostate cancer cell lines and xenografts. Cancer research. 1998;58:2720-3.

[111] Thalmann GN, Anezinis PE, Chang SM, Zhau HE, Kim EE, Hopwood VL, et al. Androgen-independent cancer progression and bone metastasis in the LNCaP model of human prostate cancer. Cancer research. 1994;54:2577-81.

[112] Wu TT, Sikes RA, Cui Q, Thalmann GN, Kao C, Murphy CF, et al. Establishing human prostate cancer cell xenografts in bone: induction of osteoblastic reaction by

prostate-specific antigen-producing tumors in athymic and SCID/bg mice using LNCaP and lineage-derived metastatic sublines. Int J Cancer. 1998;77:887-94.

[113] Yamamoto Y, Loriot Y, Beraldi E, Zhang F, Wyatt AW, Al Nakouzi N, et al. Generation 2.5 antisense oligonucleotides targeting the androgen receptor and its splice variants suppress enzalutamide-resistant prostate cancer cell growth. Clinical cancer research : an official journal of the American Association for Cancer Research. 2015;21:1675-87.

[114] Matsumoto H, Yamamoto Y, Shiota M, Kuruma H, Beraldi E, Matsuyama H, et al. Cotargeting Androgen Receptor and Clusterin Delays Castrate-Resistant Prostate Cancer Progression by Inhibiting Adaptive Stress Response and AR Stability. Cancer research. 2013;73:5206-17.

[115] Sramkoski RM, Pretlow TG, 2nd, Giaconia JM, Pretlow TP, Schwartz S, Sy MS, et al. A new human prostate carcinoma cell line, 22Rv1. In Vitro Cell Dev Biol Anim. 1999;35:403-9.

[116] Nagabhushan M, Miller CM, Pretlow TP, Giaconia JM, Edgehouse NL, Schwartz S, et al. CWR22: the first human prostate cancer xenograft with strongly androgen-dependent and relapsed strains both in vivo and in soft agar. Cancer research. 1996;56:3042-6.

[117] Chlenski A, Nakashiro K, Ketels KV, Korovaitseva GI, Oyasu R. Androgen receptor expression in androgen-independent prostate cancer cell lines. The Prostate. 2001;47:66-75.

[118] Tepper CG, Boucher DL, Ryan PE, Ma AH, Xia L, Lee LF, et al. Characterization of a novel androgen receptor mutation in a relapsed CWR22 prostate cancer xenograft and cell line. Cancer research. 2002;62:6606-14.

[119] van Bokhoven A, Varella-Garcia M, Korch C, Johannes WU, Smith EE, Miller HL, et al. Molecular characterization of human prostate carcinoma cell lines. The Prostate. 2003;57:205-25.

[120] Dehm SM, Schmidt LJ, Heemers HV, Vessella RL, Tindall DJ. Splicing of a novel androgen receptor exon generates a constitutively active androgen receptor that mediates prostate cancer therapy resistance. Cancer research. 2008;68:5469-77.

[121] Korenchuk S, Lehr JE, L MC, Lee YG, Whitney S, Vessella R, et al. VCaP, a cell-based model system of human prostate cancer. In Vivo. 2001;15:163-8.

[122] Tomlins SA, Bjartell A, Chinnaiyan AM, Jenster G, Nam RK, Rubin MA, et al. ETS gene fusions in prostate cancer: from discovery to daily clinical practice. European urology. 2009;56:275-86.

[123] Kaighn ME, Narayan KS, Ohnuki Y, Lechner JF, Jones LW. Establishment and characterization of a human prostatic carcinoma cell line (PC-3). Invest Urol. 1979;17:16-23.

[124] Stone KR, Mickey DD, Wunderli H, Mickey GH, Paulson DF. Isolation of a human prostate carcinoma cell line (DU 145). Int J Cancer. 1978;21:274-81.

[125] Shappell SB, Thomas GV, Roberts RL, Herbert R, Ittmann MM, Rubin MA, et al. Prostate pathology of genetically engineered mice: definitions and classification. The

consensus report from the Bar Harbor meeting of the Mouse Models of Human Cancer Consortium Prostate Pathology Committee. Cancer research. 2004;64:2270-305.

[126] Ittmann M, Huang J, Radaelli E, Martin P, Signoretti S, Sullivan R, et al. Animal models of human prostate cancer: the consensus report of the New York meeting of the Mouse Models of Human Cancers Consortium Prostate Pathology Committee. Cancer research. 2013;73:2718-36.

[127] Greenberg NM, DeMayo F, Finegold MJ, Medina D, Tilley WD, Aspinall JO, et al. Prostate cancer in a transgenic mouse. Proceedings of the National Academy of Sciences of the United States of America. 1995;92:3439-43.

[128] Kaplan-Lefko PJ, Chen TM, Ittmann MM, Barrios RJ, Ayala GE, Huss WJ, et al. Pathobiology of autochthonous prostate cancer in a pre-clinical transgenic mouse model. The Prostate. 2003;55:219-37.

[129] Chiaverotti T, Couto SS, Donjacour A, Mao JH, Nagase H, Cardiff RD, et al. Dissociation of epithelial and neuroendocrine carcinoma lineages in the transgenic adenocarcinoma of mouse prostate model of prostate cancer. The American journal of pathology. 2008;172:236-46.

[130] Kasper S, Sheppard PC, Yan Y, Pettigrew N, Borowsky AD, Prins GS, et al. Development, progression, and androgen-dependence of prostate tumors in probasin-large T antigen transgenic mice: a model for prostate cancer. Lab Invest. 1998;78:i-xv.

[131] Klezovitch O, Chevillet J, Mirosevich J, Roberts RL, Matusik RJ, Vasioukhin V. Hepsin promotes prostate cancer progression and metastasis. Cancer cell. 2004;6:185-95.

[132] Beltran H, Prandi D, Mosquera JM, Benelli M, Puca L, Cyrta J, et al. Divergent clonal evolution of castration-resistant neuroendocrine prostate cancer. Nature medicine. 2016;22:298-305.

[133] Ku SY, Rosario S, Wang Y, Mu P, Seshadri M, Goodrich ZW, et al. Rb1 and Trp53 cooperate to suppress prostate cancer lineage plasticity, metastasis, and antiandrogen resistance. Science. 2017;355:78-83.

[134] Mu P, Zhang Z, Benelli M, Karthaus WR, Hoover E, Chen CC, et al. SOX2 promotes lineage plasticity and antiandrogen resistance in TP53- and RB1-deficient prostate cancer. Science. 2017;355:84-8.

[135] Song MS, Salmena L, Pandolfi PP. The functions and regulation of the PTEN tumour suppressor. Nat Rev Mol Cell Biol. 2012;13:283-96.

[136] Wang S, Gao J, Lei Q, Rozengurt N, Pritchard C, Jiao J, et al. Prostate-specific deletion of the murine Pten tumor suppressor gene leads to metastatic prostate cancer. Cancer cell. 2003;4:209-21.

[137] Zhang J, Thomas TZ, Kasper S, Matusik RJ. A small composite probasin promoter confers high levels of prostate-specific gene expression through regulation by androgens and glucocorticoids in vitro and in vivo. Endocrinology. 2000;141:4698-710.

[138] Chen Z, Trotman LC, Shaffer D, Lin HK, Dotan ZA, Niki M, et al. Crucial role of p53-dependent cellular senescence in suppression of Pten-deficient tumorigenesis. Nature. 2005;436:725-30.

[139] Ding Z, Wu CJ, Chu GC, Xiao Y, Ho D, Zhang J, et al. SMAD4-dependent barrier constrains prostate cancer growth and metastatic progression. Nature. 2011;470:269-73.

[140] Kim MJ, Cardiff RD, Desai N, Banach-Petrosky WA, Parsons R, Shen MM, et al. Cooperativity of Nkx3.1 and Pten loss of function in a mouse model of prostate carcinogenesis. Proceedings of the National Academy of Sciences of the United States of America. 2002;99:2884-9.

[141] Dhanasekaran SM, Barrette TR, Ghosh D, Shah R, Varambally S, Kurachi K, et al. Delineation of prognostic biomarkers in prostate cancer. Nature. 2001;412:822-6.

[142] Singh D, Febbo PG, Ross K, Jackson DG, Manola J, Ladd C, et al. Gene expression correlates of clinical prostate cancer behavior. Cancer cell. 2002;1:203-9.

[143] Jenkins RB, Qian J, Lieber MM, Bostwick DG. Detection of c-myc oncogene amplification and chromosomal anomalies in metastatic prostatic carcinoma by fluorescence in situ hybridization. Cancer research. 1997;57:524-31.

[144] Moroy T, Verbeek S, Ma A, Achacoso P, Berns A, Alt F. E mu N- and E mu L-myc cooperate with E mu pim-1 to generate lymphoid tumors at high frequency in double-transgenic mice. Oncogene. 1991;6:1941-8.

[145] Pelengaris S, Khan M, Evan GI. Suppression of Myc-induced apoptosis in beta cells exposes multiple oncogenic properties of Myc and triggers carcinogenic progression. Cell. 2002;109:321-34.

[146] Jensen NA, Pedersen KM, Lihme F, Rask L, Nielsen JV, Rasmussen TE, et al. Astroglial c-Myc overexpression predisposes mice to primary malignant gliomas. The Journal of biological chemistry. 2003;278:8300-8.

[147] Ellwood-Yen K, Graeber TG, Wongvipat J, Iruela-Arispe ML, Zhang J, Matusik R, et al. Myc-driven murine prostate cancer shares molecular features with human prostate tumors. Cancer cell. 2003;4:223-38.

[148] DeRose YS, Wang G, Lin YC, Bernard PS, Buys SS, Ebbert MT, et al. Tumor grafts derived from women with breast cancer authentically reflect tumor pathology, growth, metastasis and disease outcomes. Nature medicine. 2011;17:1514-20.

[149] Choi SY, Lin D, Gout PW, Collins CC, Xu Y, Wang Y. Lessons from patient-derived xenografts for better in vitro modeling of human cancer. Advanced drug delivery reviews. 2014;79-80:222-37.

[150] Tentler JJ, Tan AC, Weekes CD, Jimeno A, Leong S, Pitts TM, et al. Patient-derived tumour xenografts as models for oncology drug development. Nat Rev Clin Oncol. 2012;9:338-50.

[151] Lin D, Wyatt AW, Xue H, Wang Y, Dong X, Haegert A, et al. High fidelity patient-derived xenografts for accelerating prostate cancer discovery and drug development. Cancer research. 2014;74:1272-83.

[152] Wang Y, Revelo MP, Sudilovsky D, Cao M, Chen WG, Goetz L, et al. Development and characterization of efficient xenograft models for benign and malignant human prostate tissue. The Prostate. 2005;64:149-59.

[153] van Weerden WM, de Ridder CM, Verdaasdonk CL, Romijn JC, van der Kwast TH, Schroder FH, et al. Development of seven new human prostate tumor xenograft models and their histopathological characterization. The American journal of pathology. 1996;149:1055-62.

[154] Pretlow TG, Delmoro CM, Dilley GG, Spadafora CG, Pretlow TP. Transplantation of human prostatic carcinoma into nude mice in Matrigel. Cancer research. 1991;51:3814-7.

[155] Pretlow TG, Wolman SR, Micale MA, Pelley RJ, Kursh ED, Resnick MI, et al. Xenografts of primary human prostatic carcinoma. Journal of the National Cancer Institute. 1993;85:394-8.

[156] Klein KA, Reiter RE, Redula J, Moradi H, Zhu XL, Brothman AR, et al. Progression of metastatic human prostate cancer to androgen independence in immunodeficient SCID mice. Nature medicine. 1997;3:402-8.

[157] Lawrence MG, Taylor RA, Toivanen R, Pedersen J, Norden S, Pook DW, et al. A preclinical xenograft model of prostate cancer using human tumors. Nature protocols. 2013;8:836-48.

[158] Cunha GR, Chung LW, Shannon JM, Taguchi O, Fujii H. Hormone-induced morphogenesis and growth: role of mesenchymal-epithelial interactions. Recent progress in hormone research. 1983;39:559-98.

[159] Cunha GR, Lung B, Kato K. Role of the epithelial-stromal interaction during the development and expression of ovary-independent vaginal hyperplasia. Dev Biol. 1977;56:52-67.

[160] Bogden AE, Haskell PM, LePage DJ, Kelton DE, Cobb WR, Esber HJ. Growth of human tumor xenografts implanted under the renal capsule of normal immunocompetent mice. Exp Cell Biol. 1979;47:281-93.

[161] Bogden AE. The subrenal capsule assay (SRCA) and its predictive value in oncology. Ann Chir Gynaecol Suppl. 1985;199:12-27.

[162] Zhao H, Nolley R, Chen Z, Peehl DM. Tissue slice grafts: an in vivo model of human prostate androgen signaling. The American journal of pathology. 2010;177:229-39.

[163] Priolo C, Agostini M, Vena N, Ligon AH, Fiorentino M, Shin E, et al. Establishment and genomic characterization of mouse xenografts of human primary prostate tumors. The American journal of pathology. 2010;176:1901-13.

[164] Hao J, Ci X, Xue H, Wu R, Dong X, Choi SYC, et al. Patient-derived Hormone-naive Prostate Cancer Xenograft Models Reveal Growth Factor Receptor Bound Protein 10 as an Androgen Receptor-repressed Gene Driving the Development of Castration-resistant Prostate Cancer. European urology. 2018;73:949-60.

[165] Holt LJ, Siddle K. Grb10 and Grb14: enigmatic regulators of insulin action--and more? The Biochemical journal. 2005;388:393-406.

[166] Margolis B, Silvennoinen O, Comoglio F, Roonprapunt C, Skolnik E, Ullrich A, et al. High-efficiency expression/cloning of epidermal growth factor-receptor-binding proteins with Src homology 2 domains. Proceedings of the National Academy of Sciences of the United States of America. 1992;89:8894-8.

[167] Ooi J, Yajnik V, Immanuel D, Gordon M, Moskow JJ, Buchberg AM, et al. The cloning of Grb10 reveals a new family of SH2 domain proteins. Oncogene. 1995;10:1621-30.

[168] Don J, Wolgemuth DJ. Identification and characterization of the regulated pattern of expression of a novel mouse gene, meg1, during the meiotic cell cycle. Cell Growth Differ. 1992;3:495-505.

[169] Don J, Winer MA, Wolgemuth DJ. Developmentally regulated expression during gametogenesis of the murine gene meg1 suggests a role in meiosis. Mol Reprod Dev. 1994;38:16-23.

[170] Daly RJ, Sanderson GM, Janes PW, Sutherland RL. Cloning and characterization of GRB14, a novel member of the GRB7 gene family. The Journal of biological chemistry. 1996;271:12502-10.

[171] Hynes NE, Lane HA. ERBB receptors and cancer: the complexity of targeted inhibitors. Nat Rev Cancer. 2005;5:341-54.

[172] Gschwind A, Fischer OM, Ullrich A. The discovery of receptor tyrosine kinases: targets for cancer therapy. Nat Rev Cancer. 2004;4:361-70.

[173] Slamon DJ, Godolphin W, Jones LA, Holt JA, Wong SG, Keith DE, et al. Studies of the HER-2/neu proto-oncogene in human breast and ovarian cancer. Science. 1989;244:707-12.

[174] Joensuu H, Roberts PJ, Sarlomo-Rikala M, Andersson LC, Tervahartiala P, Tuveson D, et al. Effect of the tyrosine kinase inhibitor STI571 in a patient with a metastatic gastrointestinal stromal tumor. The New England journal of medicine. 2001;344:1052-6.

[175] Stein D, Wu J, Fuqua SA, Roonprapunt C, Yajnik V, D'Eustachio P, et al. The SH2 domain protein GRB-7 is co-amplified, overexpressed and in a tight complex with HER2 in breast cancer. The EMBO journal. 1994;13:1331-40.

[176] Tanaka S, Mori M, Akiyoshi T, Tanaka Y, Mafune K, Wands JR, et al. Coexpression of Grb7 with epidermal growth factor receptor or Her2/erbB2 in human advanced esophageal carcinoma. Cancer research. 1997;57:28-31.

[177] Chu PY, Li TK, Ding ST, Lai IR, Shen TL. EGF-induced Grb7 recruits and promotes Ras activity essential for the tumorigenicity of Sk-Br3 breast cancer cells. The Journal of biological chemistry. 2010;285:29279-85.

[178] Pradip D, Bouzyk M, Dey N, Leyland-Jones B. Dissecting GRB7-mediated signals for proliferation and migration in HER2 overexpressing breast tumor cells: GTP-ase rules. Am J Cancer Res. 2013;3:173-95.

[179] Chan DW, Hui WW, Cai PC, Liu MX, Yung MM, Mak CS, et al. Targeting GRB7/ERK/FOXM1 signaling pathway impairs aggressiveness of ovarian cancer cells. PLoS One. 2012;7:e52578.

[180] Chu PY, Huang LY, Hsu CH, Liang CC, Guan JL, Hung TH, et al. Tyrosine phosphorylation of growth factor receptor-bound protein-7 by focal adhesion kinase in the regulation of cell migration, proliferation, and tumorigenesis. The Journal of biological chemistry. 2009;284:20215-26.

[181] Cariou B, Bereziat V, Moncoq K, Kasus-Jacobi A, Perdereau D, Le Marcis V, et al. Regulation and functional roles of Grb14. Frontiers in bioscience : a journal and virtual library. 2004;9:1626-36.

[182] Reilly JF, Mickey G, Maher PA. Association of fibroblast growth factor receptor 1 with the adaptor protein Grb14. Characterization of a new receptor binding partner. The Journal of biological chemistry. 2000;275:7771-8.

[183] Bereziat V, Kasus-Jacobi A, Perdereau D, Cariou B, Girard J, Burnol AF. Inhibition of insulin receptor catalytic activity by the molecular adapter Grb14. The Journal of biological chemistry. 2002;277:4845-52.

[184] Balogh K, Asa SL, Zheng L, Cassol C, Cheng S, Ezzat S. The insulin resistance Grb14 adaptor protein promotes thyroid cancer ret signaling and progression. Oncogene. 2012;31:4012-21.

[185] Kairouz R, Parmar J, Lyons RJ, Swarbrick A, Musgrove EA, Daly RJ. Hormonal regulation of the Grb14 signal modulator and its role in cell cycle progression of MCF-7 human breast cancer cells. J Cell Physiol. 2005;203:85-93.

[186] Yang P, Wei J, Li W, He F, Zeng S, Zhang T, et al. High expression of growth factor receptor-bound protein 14 predicts poor prognosis for colorectal cancer patients. Biotechnol Lett. 2016;38:1043-7.

[187] Huang O, Jiang M, Zhang X, Xie Z, Chen X, Wu J, et al. Grb14 as an independent good prognosis factor for breast cancer patients treated with neoadjuvant chemotherapy. Jpn J Clin Oncol. 2013;43:1064-72.

[188] Liu F, Roth RA. Grb-IR: a SH2-domain-containing protein that binds to the insulin receptor and inhibits its function. Proceedings of the National Academy of Sciences of the United States of America. 1995;92:10287-91.

[189] Wang J, Dai H, Yousaf N, Moussaif M, Deng Y, Boufelliga A, et al. Grb10, a positive, stimulatory signaling adapter in platelet-derived growth factor BB-, insulin-like growth factor I-, and insulin-mediated mitogenesis. Molecular and cellular biology. 1999;19:6217-28.

[190] O'Neill TJ, Rose DW, Pillay TS, Hotta K, Olefsky JM, Gustafson TA. Interaction of a GRB-IR splice variant (a human GRB10 homolog) with the insulin and insulin-like growth factor I receptors. Evidence for a role in mitogenic signaling. The Journal of biological chemistry. 1996;271:22506-13.

[191] He W, Rose DW, Olefsky JM, Gustafson TA. Grb10 interacts differentially with the insulin receptor, insulin-like growth factor I receptor, and epidermal growth factor receptor via the Grb10 Src homology 2 (SH2) domain and a second novel domain located between the pleckstrin homology and SH2 domains. The Journal of biological chemistry. 1998;273:6860-7.

[192] Deng Y, Bhattacharya S, Swamy OR, Tandon R, Wang Y, Janda R, et al. Growth factor receptor-binding protein 10 (Grb10) as a partner of phosphatidylinositol 3-kinase in metabolic insulin action. The Journal of biological chemistry. 2003;278:39311-22.

[193] Stein EG, Gustafson TA, Hubbard SR. The BPS domain of Grb10 inhibits the catalytic activity of the insulin and IGF1 receptors. FEBS Lett. 2001;493:106-11.

[194] Wick KR, Werner ED, Langlais P, Ramos FJ, Dong LQ, Shoelson SE, et al. Grb10 inhibits insulin-stimulated insulin receptor substrate (IRS)-phosphatidylinositol 3-kinase/Akt signaling pathway by disrupting the association of IRS-1/IRS-2 with the insulin receptor. The Journal of biological chemistry. 2003;278:8460-7.

[195] Mounier C, Lavoie L, Dumas V, Mohammad-Ali K, Wu J, Nantel A, et al. Specific inhibition by hGRB10zeta of insulin-induced glycogen synthase activation: evidence for a novel signaling pathway. Mol Cell Endocrinol. 2001;173:15-27.

[196] Frantz JD, Giorgetti-Peraldi S, Ottinger EA, Shoelson SE. Human GRB-IRbeta/GRB10. Splice variants of an insulin and growth factor receptor-binding protein with PH and SH2 domains. The Journal of biological chemistry. 1997;272:2659-67.

[197] Murdaca J, Treins C, Monthouel-Kartmann MN, Pontier-Bres R, Kumar S, Van Obberghen E, et al. Grb10 prevents Nedd4-mediated vascular endothelial growth factor receptor-2 degradation. The Journal of biological chemistry. 2004;279:26754-61.

[198] Giorgetti-Peraldi S, Murdaca J, Mas JC, Van Obberghen E. The adapter protein, Grb10, is a positive regulator of vascular endothelial growth factor signaling. Oncogene. 2001;20:3959-68.

[199] Pandey A, Duan H, Di Fiore PP, Dixit VM. The Ret receptor protein tyrosine kinase associates with the SH2-containing adapter protein Grb10. The Journal of biological chemistry. 1995;270:21461-3.

[200] Stein E, Cerretti DP, Daniel TO. Ligand activation of ELK receptor tyrosine kinase promotes its association with Grb10 and Grb2 in vascular endothelial cells. The Journal of biological chemistry. 1996;271:23588-93.

[201] Readinger JA, Mueller KL, Venegas AM, Horai R, Schwartzberg PL. Tec kinases regulate T-lymphocyte development and function: new insights into the roles of Itk and Rlk/Txk. Immunol Rev. 2009;228:93-114.

[202] Mano H, Ohya K, Miyazato A, Yamashita Y, Ogawa W, Inazawa J, et al. Grb10/GrbIR as an in vivo substrate of Tec tyrosine kinase. Genes to cells : devoted to molecular & cellular mechanisms. 1998;3:431-41.

[203] Nantel A, Mohammad-Ali K, Sherk J, Posner BI, Thomas DY. Interaction of the Grb10 adapter protein with the Raf1 and MEK1 kinases. The Journal of biological chemistry. 1998;273:10475-84.

[204] Depetris RS, Wu J, Hubbard SR. Structural and functional studies of the Ras-associating and pleckstrin-homology domains of Grb10 and Grb14. Nat Struct Mol Biol. 2009;16:833-9.

[205] Kebache S, Ash J, Annis MG, Hagan J, Huber M, Hassard J, et al. Grb10 and active Raf-1 kinase promote Bad-dependent cell survival. The Journal of biological chemistry. 2007;282:21873-83.

[206] Chang L, Karin M. Mammalian MAP kinase signalling cascades. Nature. 2001;410:37-40.

[207] Cantley LC. The phosphoinositide 3-kinase pathway. Science. 2002;296:1655-7.

[208] Jahn T, Seipel P, Urschel S, Peschel C, Duyster J. Role for the adaptor protein Grb10 in the activation of Akt. Molecular and cellular biology. 2002;22:979-91.

[209] Urschel S, Bassermann F, Bai RY, Munch S, Peschel C, Duyster J. Phosphorylation of grb10 regulates its interaction with 14-3-3. The Journal of biological chemistry. 2005;280:16987-93.

[210] Kazi JU, Ronnstrand L. FLT3 signals via the adapter protein Grb10 and overexpression of Grb10 leads to aberrant cell proliferation in acute myeloid leukemia. Molecular oncology. 2013;7:402-18.

[211] Hsu PP, Kang SA, Rameseder J, Zhang Y, Ottina KA, Lim D, et al. The mTOR-regulated phosphoproteome reveals a mechanism of mTORC1-mediated inhibition of growth factor signaling. Science. 2011;332:1317-22.

[212] Yu Y, Yoon SO, Poulogiannis G, Yang Q, Ma XM, Villen J, et al. Phosphoproteomic analysis identifies Grb10 as an mTORC1 substrate that negatively regulates insulin signaling. Science. 2011;332:1322-6.

[213] Casas S, Ollila J, Aventin A, Vihinen M, Sierra J, Knuutila S. Changes in apoptosis-related pathways in acute myelocytic leukemia. Cancer genetics and cytogenetics. 2003;146:89-101.

[214] Roszak J, Smok-Pieniazek A, Nocun M, Stepnik M. Characterization of arsenic trioxide resistant clones derived from Jurkat leukemia T cell line: focus on PI3K/Akt signaling pathway. Chemico-biological interactions. 2013;205:198-211.

[215] Bai RY, Jahn T, Schrem S, Munzert G, Weidner KM, Wang JY, et al. The SH2-containing adapter protein GRB10 interacts with BCR-ABL. Oncogene. 1998;17:941-8.

[216] Illert AL, Albers C, Kreutmair S, Leischner H, Peschel C, Miething C, et al. Grb10 is involved in BCR-ABL-positive leukemia in mice. Leukemia. 2015;29:858-68.

[217] Gilliland DG, Griffin JD. The roles of FLT3 in hematopoiesis and leukemia. Blood. 2002;100:1532-42.

[218] Qi L, Ding Y. Screening and regulatory network analysis of survival-related genes of patients with colorectal cancer. Sci China Life Sci. 2014;57:526-31.

[219] Zhang T, Ma Y, Fang J, Liu C, Chen L. A Deregulated PI3K-AKT Signaling Pathway in Patients with Colorectal Cancer. J Gastrointest Cancer. 2019;50:35-41.

[220] Khan MI, Al Johani A, Hamid A, Ateeq B, Manzar N, Adhami VM, et al. Proproliferative function of adaptor protein GRB10 in prostate carcinoma. FASEB journal : official publication of the Federation of American Societies for Experimental Biology. 2019;33:3198-211.

[221] Boot A, Oosting J, de Miranda NF, Zhang Y, Corver WE, van de Water B, et al. Imprinted survival genes preclude loss of heterozygosity of chromosome 7 in cancer cells. J Pathol. 2016;240:72-83.

[222] Cheng W, Huang PC, Chao HM, Jeng YM, Hsu HC, Pan HW, et al. Glypican-3 induces oncogenicity by preventing IGF-1R degradation, a process that can be blocked by Grb10. Oncotarget. 2017;8:80429-42.

[223] Doroszko M, Chrusciel M, Stelmaszewska J, Slezak T, Anisimowicz S, Plockinger U, et al. GnRH antagonist treatment of malignant adrenocortical tumors. Endocr Relat Cancer. 2019;26:103-17.

[224] Subramanian A, Tamayo P, Mootha VK, Mukherjee S, Ebert BL, Gillette MA, et al. Gene set enrichment analysis: a knowledge-based approach for interpreting genome-wide expression profiles. Proceedings of the National Academy of Sciences of the United States of America. 2005;102:15545-50.

[225] Lee MS, Jeong MH, Lee HW, Han HJ, Ko A, Hewitt SM, et al. PI3K/AKT activation induces PTEN ubiquitination and destabilization accelerating tumourigenesis. Nature communications. 2015;6:7769.

[226] Varambally S, Dhanasekaran SM, Zhou M, Barrette TR, Kumar-Sinha C, Sanda MG, et al. The polycomb group protein EZH2 is involved in progression of prostate cancer. Nature. 2002;419:624-9.

[227] Ross-Adams H, Lamb AD, Dunning MJ, Halim S, Lindberg J, Massie CM, et al. Integration of copy number and transcriptomics provides risk stratification in prostate cancer: A discovery and validation cohort study. EBioMedicine. 2015;2:1133-44.

[228] Cerami E, Gao J, Dogrusoz U, Gross BE, Sumer SO, Aksoy BA, et al. The cBio cancer genomics portal: an open platform for exploring multidimensional cancer genomics data. Cancer discovery. 2012;2:401-4.

[229] Gao J, Aksoy BA, Dogrusoz U, Dresdner G, Gross B, Sumer SO, et al. Integrative analysis of complex cancer genomics and clinical profiles using the cBioPortal. Science signaling. 2013;6:pl1.

[230] Taylor BS, Schultz N, Hieronymus H, Gopalan A, Xiao Y, Carver BS, et al. Integrative genomic profiling of human prostate cancer. Cancer cell. 2010;18:11-22.

[231] Dunning MJ, Vowler SL, Lalonde E, Ross-Adams H, Boutros P, Mills IG, et al. Mining Human Prostate Cancer Datasets: The "camcAPP" Shiny App. EBioMedicine. 2017;17:5-6.

[232] Cleutjens KB, van der Korput HA, Ehren-van Eekelen CC, Sikes RA, Fasciana C, Chung LW, et al. A 6-kb promoter fragment mimics in transgenic mice the prostate-

specific and androgen-regulated expression of the endogenous prostate-specific antigen gene in humans. Molecular endocrinology. 1997;11:1256-65.

[233] Shevchenko A, Wilm M, Vorm O, Mann M. Mass spectrometric sequencing of proteins silver-stained polyacrylamide gels. Anal Chem. 1996;68:850-8.

[234] Rappsilber J, Mann M, Ishihama Y. Protocol for micro-purification, enrichment, pre-fractionation and storage of peptides for proteomics using StageTips. Nature protocols. 2007;2:1896-906.

[235] Boersema PJ, Aye TT, van Veen TA, Heck AJ, Mohammed S. Triplex protein quantification based on stable isotope labeling by peptide dimethylation applied to cell and tissue lysates. Proteomics. 2008;8:4624-32.

[236] Cox J, Mann M. MaxQuant enables high peptide identification rates, individualized p.p.b.-range mass accuracies and proteome-wide protein quantification. Nat Biotechnol. 2008;26:1367-72.

[237] Yuan X, Cai C, Chen S, Chen S, Yu Z, Balk SP. Androgen receptor functions in castration-resistant prostate cancer and mechanisms of resistance to new agents targeting the androgen axis. Oncogene. 2014;33:2815-25.

[238] Riedel H. Grb10 exceeding the boundaries of a common signaling adapter. Frontiers in bioscience : a journal and virtual library. 2004;9:603-18.

[239] Bitting RL, Armstrong AJ. Targeting the PI3K/Akt/mTOR pathway in castration-resistant prostate cancer. Endocr Relat Cancer. 2013;20:R83-99.

[240] Gao D, Vela I, Sboner A, Iaquinta PJ, Karthaus WR, Gopalan A, et al. Organoid cultures derived from patients with advanced prostate cancer. Cell. 2014;159:176-87.

[241] Jarrard DF, Kinoshita H, Shi Y, Sandefur C, Hoff D, Meisner LF, et al. Methylation of the androgen receptor promoter CpG island is associated with loss of androgen receptor expression in prostate cancer cells. Cancer research. 1998;58:5310-4.

[242] Bluemn EG, Coleman IM, Lucas JM, Coleman RT, Hernandez-Lopez S, Tharakan R, et al. Androgen Receptor Pathway-Independent Prostate Cancer Is Sustained through FGF Signaling. Cancer cell. 2017;32:474-89 e6.

[243] Su W, Han HH, Wang Y, Zhang B, Zhou B, Cheng Y, et al. The Polycomb Repressor Complex 1 Drives Double-Negative Prostate Cancer Metastasis by Coordinating Stemness and Immune Suppression. Cancer cell. 2019;36:139-55 e10.

[244] Chee KG, Longmate J, Quinn DI, Chatta G, Pinski J, Twardowski P, et al. The AKT inhibitor perifosine in biochemically recurrent prostate cancer: a phase II California/Pittsburgh cancer consortium trial. Clinical genitourinary cancer. 2007;5:433-7.

[245] Posadas EM, Gulley J, Arlen PM, Trout A, Parnes HL, Wright J, et al. A phase II study of perifosine in androgen independent prostate cancer. Cancer biology & therapy. 2005;4:1133-7.

[246] Jenster G. The role of the androgen receptor in the development and progression of prostate cancer. Seminars in oncology. 1999;26:407-21.

[247] van Royen ME, van Cappellen WA, de Vos C, Houtsmuller AB, Trapman J. Stepwise androgen receptor dimerization. J Cell Sci. 2012;125:1970-9.

[248] Gritsina G, Gao WQ, Yu J. Transcriptional repression by androgen receptor: roles in castration-resistant prostate cancer. Asian journal of andrology. 2019;21:215-23.

[249] Brawer MK. Prostate-specific antigen: current status. CA: a cancer journal for clinicians. 1999;49:264-81.

[250] Kanno Y, Zhao S, Yamashita N, Yanai K, Nemoto K, Inouye Y. Androgen receptor functions as a negative transcriptional regulator of DEPTOR, mTOR inhibitor. J Toxicol Sci. 2015;40:753-8.

[251] Liu YN, Liu Y, Lee HJ, Hsu YH, Chen JH. Activated androgen receptor downregulates E-cadherin gene expression and promotes tumor metastasis. Molecular and cellular biology. 2008;28:7096-108.

[252] Verras M, Lee J, Xue H, Li TH, Wang Y, Sun Z. The androgen receptor negatively regulates the expression of c-Met: implications for a novel mechanism of prostate cancer progression. Cancer research. 2007;67:967-75.

[253] Bishop JL, Thaper D, Vahid S, Davies A, Ketola K, Kuruma H, et al. The Master Neural Transcription Factor BRN2 Is an Androgen Receptor-Suppressed Driver of Neuroendocrine Differentiation in Prostate Cancer. Cancer discovery. 2017;7:54-71.

[254] Cai C, He HH, Chen S, Coleman I, Wang H, Fang Z, et al. Androgen receptor gene expression in prostate cancer is directly suppressed by the androgen receptor through recruitment of lysine-specific demethylase 1. Cancer cell. 2011;20:457-71.

[255] Massie CE, Lynch A, Ramos-Montoya A, Boren J, Stark R, Fazli L, et al. The androgen receptor fuels prostate cancer by regulating central metabolism and biosynthesis. The EMBO journal. 2011;30:2719-33.

[256] Wang Q, Li W, Liu XS, Carroll JS, Janne OA, Keeton EK, et al. A hierarchical network of transcription factors governs androgen receptor-dependent prostate cancer growth. Molecular cell. 2007;27:380-92.

[257] Chen Y, Chi P, Rockowitz S, Iaquinta PJ, Shamu T, Shukla S, et al. ETS factors reprogram the androgen receptor cistrome and prime prostate tumorigenesis in response to PTEN loss. Nature medicine. 2013;19:1023-9.

[258] Shaw GL, Whitaker H, Corcoran M, Dunning MJ, Luxton H, Kay J, et al. The Early Effects of Rapid Androgen Deprivation on Human Prostate Cancer. European urology. 2016;70:214-8.

[259] Jin HJ, Zhao JC, Wu L, Kim J, Yu J. Cooperativity and equilibrium with FOXA1 define the androgen receptor transcriptional program. Nature communications. 2014;5:3972.

[260] Sharma NL, Massie CE, Ramos-Montoya A, Zecchini V, Scott HE, Lamb AD, et al. The androgen receptor induces a distinct transcriptional program in castration-resistant prostate cancer in man. Cancer cell. 2013;23:35-47.

[261] Tombal B, van Soest RJ. Prostate cancer: STAMPEDE, LATITUDE and Fernand Labrie's legacy. Nature reviews Urology. 2017;14:588-90.

[262] Carver BS, Chapinski C, Wongvipat J, Hieronymus H, Chen Y, Chandarlapaty S, et al. Reciprocal feedback regulation of PI3K and androgen receptor signaling in PTEN-deficient prostate cancer. Cancer cell. 2011;19:575-86.

[263] Yamamoto Y, Ishino F, Kaneko-Ishino T, Shiura H, Uchio-Yamada K, Matsuda J, et al. Type 2 diabetes mellitus in a non-obese mouse model induced by Meg1/Grb10 overexpression. Experimental animals. 2008;57:385-95.

[264] Shiura H, Miyoshi N, Konishi A, Wakisaka-Saito N, Suzuki R, Muguruma K, et al. Meg1/Grb10 overexpression causes postnatal growth retardation and insulin resistance via negative modulation of the IGF1R and IR cascades. Biochemical and biophysical research communications. 2005;329:909-16.

[265] Cao XR, Lill NL, Boase N, Shi PP, Croucher DR, Shan H, et al. Nedd4 controls animal growth by regulating IGF-1 signaling. Science signaling. 2008;1:ra5.

[266] Wang H, Sun X, Zhao L, Chen X, Zhao J. Androgen deprivation therapy is associated with diabetes: Evidence from meta-analysis. Journal of diabetes investigation. 2016;7:629-36.

[267] Smith MR. Androgen deprivation therapy and risk for diabetes and cardiovascular disease in prostate cancer survivors. Current urology reports. 2008;9:197-202.

[268] Keating NL, Liu PH, O'Malley AJ, Freedland SJ, Smith MR. Androgen-deprivation therapy and diabetes control among diabetic men with prostate cancer. European urology. 2014;65:816-24.

[269] Alibhai SM, Duong-Hua M, Sutradhar R, Fleshner NE, Warde P, Cheung AM, et al. Impact of androgen deprivation therapy on cardiovascular disease and diabetes. J Clin Oncol. 2009;27:3452-8.

[270] Teo MY, Rathkopf DE, Kantoff P. Treatment of Advanced Prostate Cancer. Annual review of medicine. 2019;70:479-99.

[271] Lim MA, Riedel H, Liu F. Grb10: more than a simple adaptor protein. Frontiers in bioscience : a journal and virtual library. 2004;9:387-403.

[272] Holt LJ, Turner N, Mokbel N, Trefely S, Kanzleiter T, Kaplan W, et al. Grb10 regulates the development of fiber number in skeletal muscle. FASEB journal : official publication of the Federation of American Societies for Experimental Biology. 2012;26:3658-69.

[273] Janssens V, Goris J. Protein phosphatase 2A: a highly regulated family of serine/threonine phosphatases implicated in cell growth and signalling. The Biochemical journal. 2001;353:417-39.

[274] DeGrande ST, Little SC, Nixon DJ, Wright P, Snyder J, Dun W, et al. Molecular mechanisms underlying cardiac protein phosphatase 2A regulation in heart. The Journal of biological chemistry. 2013;288:1032-46.

[275] Yang CS, Xin HW, Kelley JB, Spencer A, Brautigan DL, Paschal BM. Ligand binding to the androgen receptor induces conformational changes that regulate phosphatase interactions. Molecular and cellular biology. 2007;27:3390-404.

[276] Wlodarchak N, Xing Y. PP2A as a master regulator of the cell cycle. Crit Rev Biochem Mol Biol. 2016;51:162-84.

[277] Kuo YC, Huang KY, Yang CH, Yang YS, Lee WY, Chiang CW. Regulation of phosphorylation of Thr-308 of Akt, cell proliferation, and survival by the B55alpha regulatory subunit targeting of the protein phosphatase 2A holoenzyme to Akt. The Journal of biological chemistry. 2008;283:1882-92.

[278] Letourneux C, Rocher G, Porteu F. B56-containing PP2A dephosphorylate ERK and their activity is controlled by the early gene IEX-1 and ERK. The EMBO journal. 2006;25:727-38.

[279] Eichhorn PJ, Creyghton MP, Wilhelmsen K, van Dam H, Bernards R. A RNA interference screen identifies the protein phosphatase 2A subunit PR55gamma as a stress-sensitive inhibitor of c-SRC. PLoS Genet. 2007;3:e218.

[280] Perrotti D, Neviani P. Protein phosphatase 2A: a target for anticancer therapy. Lancet Oncol. 2013;14:e229-38.

[281] Curtis C, Shah SP, Chin SF, Turashvili G, Rueda OM, Dunning MJ, et al. The genomic and transcriptomic architecture of 2,000 breast tumours reveals novel subgroups. Nature. 2012;486:346-52.

[282] Ruediger R, Ruiz J, Walter G. Human cancer-associated mutations in the Aalpha subunit of protein phosphatase 2A increase lung cancer incidence in Aalpha knock-in and knockout mice. Molecular and cellular biology. 2011;31:3832-44.

[283] Ruediger R, Pham HT, Walter G. Alterations in protein phosphatase 2A subunit interaction in human carcinomas of the lung and colon with mutations in the A beta subunit gene. Oncogene. 2001;20:1892-9.

[284] Chou HC, Chen CH, Lee HS, Lee CZ, Huang GT, Yang PM, et al. Alterations of tumour suppressor gene PPP2R1B in hepatocellular carcinoma. Cancer letters. 2007;253:138-43.

[285] Shih Ie M, Panuganti PK, Kuo KT, Mao TL, Kuhn E, Jones S, et al. Somatic mutations of PPP2R1A in ovarian and uterine carcinomas. The American journal of pathology. 2011;178:1442-7.

[286] Kalla C, Scheuermann MO, Kube I, Schlotter M, Mertens D, Dohner H, et al. Analysis of 11q22-q23 deletion target genes in B-cell chronic lymphocytic leukaemia: evidence for a pathogenic role of NPAT, CUL5, and PPP2R1B. Eur J Cancer. 2007;43:1328-35.

[287] Baysal BE, Willett-Brozick JE, Taschner PE, Dauwerse JG, Devilee P, Devlin B. A high-resolution integrated map spanning the SDHD gene at 11q23: a 1.1-Mb BAC contig, a partial transcript map and 15 new repeat polymorphisms in a tumour-suppressor region. Eur J Hum Genet. 2001;9:121-9.

[288] Elstrom RL, Bauer DE, Buzzai M, Karnauskas R, Harris MH, Plas DR, et al. Akt stimulates aerobic glycolysis in cancer cells. Cancer research. 2004;64:3892-9.

[289] Warburg O. On respiratory impairment in cancer cells. Science. 1956;124:269-70.

[290] Kostakoglu L, Agress H, Jr., Goldsmith SJ. Clinical role of FDG PET in evaluation of cancer patients. Radiographics. 2003;23:315-40; quiz 533.

[291] Schoder H, Larson SM. Positron emission tomography for prostate, bladder, and renal cancer. Semin Nucl Med. 2004;34:274-92.

[292] Cutruzzola F, Giardina G, Marani M, Macone A, Paiardini A, Rinaldo S, et al. Glucose Metabolism in the Progression of Prostate Cancer. Front Physiol. 2017;8:97.

[293] Costello LC, Franklin RB. Concepts of citrate production and secretion by prostate. 1. Metabolic relationships. The Prostate. 1991;18:25-46.

[294] Jadvar H, Desai B, Ji L, Conti PS, Dorff TB, Groshen SG, et al. Baseline 18F-FDG PET/CT parameters as imaging biomarkers of overall survival in castrate-resistant metastatic prostate cancer. J Nucl Med. 2013;54:1195-201.

[295] Jadvar H. PET of Glucose Metabolism and Cellular Proliferation in Prostate Cancer. J Nucl Med. 2016;57:25S-9S.

[296] Ercolani L, Florence B, Denaro M, Alexander M. Isolation and complete sequence of a functional human glyceraldehyde-3-phosphate dehydrogenase gene. The Journal of biological chemistry. 1988;263:15335-41.

[297] Ashizawa K, McPhie P, Lin KH, Cheng SY. An in vitro novel mechanism of regulating the activity of pyruvate kinase M2 by thyroid hormone and fructose 1, 6-bisphosphate. Biochemistry. 1991;30:7105-11.

[298] Pind S, Slominski E, Mauthe J, Pearlman K, Swoboda KJ, Wilkins JA, et al. V490M, a common mutation in 3-phosphoglycerate dehydrogenase deficiency, causes enzyme deficiency by decreasing the yield of mature enzyme. The Journal of biological chemistry. 2002;277:7136-43.

[299] Qi B, Han M. Microbial Siderophore Enterobactin Promotes Mitochondrial Iron Uptake and Development of the Host via Interaction with ATP Synthase. Cell. 2018;175:571-82 e11.

[300] Ito S, Tan LJ, Andoh D, Narita T, Seki M, Hirano Y, et al. MMXD, a TFIIH-independent XPD-MMS19 protein complex involved in chromosome segregation. Molecular cell. 2010;39:632-40.

[301] Radons J. The human HSP70 family of chaperones: where do we stand? Cell Stress Chaperones. 2016;21:379-404.

[302] Kumar S, Stokes J, 3rd, Singh UP, Scissum Gunn K, Acharya A, Manne U, et al. Targeting Hsp70: A possible therapy for cancer. Cancer letters. 2016;374:156-66.

[303] Murphy ME. The HSP70 family and cancer. Carcinogenesis. 2013;34:1181-8.

[304] Mochida S, Maslen SL, Skehel M, Hunt T. Greatwall phosphorylates an inhibitor of protein phosphatase 2A that is essential for mitosis. Science. 2010;330:1670-3.

[305] Grallert A, Boke E, Hagting A, Hodgson B, Connolly Y, Griffiths JR, et al. A PP1-PP2A phosphatase relay controls mitotic progression. Nature. 2015;517:94-8.

[306] Queralt E, Lehane C, Novak B, Uhlmann F. Downregulation of PP2A(Cdc55) phosphatase by separase initiates mitotic exit in budding yeast. Cell. 2006;125:719-32.

[307] Seeling JM, Miller JR, Gil R, Moon RT, White R, Virshup DM. Regulation of beta-catenin signaling by the B56 subunit of protein phosphatase 2A. Science. 1999;283:2089-91.

[308] Kong M, Fox CJ, Mu J, Solt L, Xu A, Cinalli RM, et al. The PP2A-associated protein alpha4 is an essential inhibitor of apoptosis. Science. 2004;306:695-8.

[309] Andjelkovic M, Jakubowicz T, Cron P, Ming XF, Han JW, Hemmings BA. Activation and phosphorylation of a pleckstrin homology domain containing protein kinase (RAC-PK/PKB) promoted by serum and protein phosphatase inhibitors. Proceedings of the National Academy of Sciences of the United States of America. 1996;93:5699-704.

[310] McClinch K, Avelar RA, Callejas D, Izadmehr S, Wiredja D, Perl A, et al. Small-Molecule Activators of Protein Phosphatase 2A for the Treatment of Castration-Resistant Prostate Cancer. Cancer research. 2018;78:2065-80.

[311] Mukhopadhyay A, Tabanor K, Chaguturu R, Aldrich JV. Targeting inhibitor 2 of protein phosphatase 2A as a therapeutic strategy for prostate cancer treatment. Cancer biology & therapy. 2013;14:962-72.

[312] Bhardwaj A, Singh S, Srivastava SK, Honkanen RE, Reed E, Singh AP. Modulation of protein phosphatase 2A activity alters androgen-independent growth of prostate cancer cells: therapeutic implications. Mol Cancer Ther. 2011;10:720-31.

[313] Yu J, Yu J, Mani RS, Cao Q, Brenner CJ, Cao X, et al. An integrated network of androgen receptor, polycomb, and TMPRSS2-ERG gene fusions in prostate cancer progression. Cancer cell. 2010;17:443-54.

[314] Zhao JC, Yu J, Runkle C, Wu L, Hu M, Wu D, et al. Cooperation between Polycomb and androgen receptor during oncogenic transformation. Genome Res. 2012;22:322-31.

[315] Fong KW, Zhao JC, Kim J, Li S, Yang YA, Song B, et al. Polycomb-Mediated Disruption of an Androgen Receptor Feedback Loop Drives Castration-Resistant Prostate Cancer. Cancer research. 2017;77:412-22.

[316] Gao S, Gao Y, He HH, Han D, Han W, Avery A, et al. Androgen Receptor Tumor Suppressor Function Is Mediated by Recruitment of Retinoblastoma Protein. Cell Rep. 2016;17:966-76.

[317] Mohammed H, Taylor C, Brown GD, Papachristou EK, Carroll JS, D'Santos CS. Rapid immunoprecipitation mass spectrometry of endogenous proteins (RIME) for analysis of chromatin complexes. Nature protocols. 2016;11:316-26.

Appendices

Appendix A: Primers used in the study (5'→3')

qRT-PCR primers	
GRB10_F	CAGACACCTCGCAGTCAACA
GRB10_R	TATCGTTCACCAGGGCTTCC
PSA_F	CACCTGCTCGGGTGATTCTG
PSA_R	CCACTTCCGGTAATGCACCA
GAPDH_F	CACCAGGGCTGCTTTTAACTC
GAPDH_R	GACAAGCTTCCCGTTCTCAG
FGFR2_F	AACAGTTTCGGCTGAGTCCA
FGFR2_R	CCCAAAGCAACCTTCTCCCA
FILIP1_F	TGCACCGAGATGCCATTCTT
FILIP1_R	GGTGCGCCTATGACACTTCT
NPC2_F	GCGGTTCTGTGGATGGAGTT
NPC2_R	CGGCCTTGCTGCTTTTAGAC
ChIP-PCR primers	
PSA_ChIP_F	GCCTGGATCTGAGAGAGATATCAT
PSA_ChIP_R	ACACCTTTTTTTTTCTGGATTGTTG
ARE1_ChIP_F	GGCCATCTAAAAGTCAATACTGG
ARE1_ChIP_R	TGGACATGTTCGCACGTGTG
ARE2_ChIP_F	AGACCAGGGACTGTGTGA
ARE2_ChIP_R	TATGAGGAAATCCCCGAAAAG
ARE3_ChIP_F	AGGAAGCTGAGCATGGAAGAG
ARE3_ChIP_R	AGAAGCTGGGGACATGCTG
NC_ChIP_F	TAGGCGCTCACTGTTCTCTC
NC_ChIP_R	CGTTGACTCCGACCTTCAC
Plasmid construction primers	
ARE1_Nhe1F	CTAGCTAGCTGACAGGGAATAGCTGCTTAATTG
ARE1_Mlu1R	CGACGCGTCGGAATGATCTGGTTGACTGACAGAAG
ARE2_Mlu1F	CGACGCGTCGTTCCCGCGGCTCCTGGCATGGC
ARE2_Sac1R	CGAGCTCGCTCTTAACTGGCTGAAGGACAAG
ARE3_Xho1F	CGACGCGTCGGAATGATCTGGTTGACTGACAGAAG
ARE3_Nhe1R	CTAGCTAGCTAGAAACCTCACAGAAAACAGAACTGA
ARE2mut_F	GAGAGGAATGTGCGCCGTTGGGTGGGGGTCCCATTTAAATCTTTTC
ARE2mut_R	GAAAAGATTTAAATGGGACCCCCACCCAACGGCGCACATTCCTCTC
ARE2del_F	GAGAGGAATGTGCGCCGGTTCCCATTTAAATCTTTTC
ARE2del_R	GAAAAGATTTAACGCCGGTTCCCATCACATTCCTCTC

GRB10_Hind3_F	CCCAAGCTTATGGACTACAAGGATGACGATGACA
GRB10_Cla1_R	CCATCGATTCATAAGGCCACTCGGATGCAG

Appendix B: Significantly upregulated genes identified in PCa PDX models

	CRPC vs HNPC		Cx 12wk vs Pre Cx	
GeneSymbol	Fold change (log2)	p value	Fold change (log2)	p value
BASP1P1	0.974234	0.001241	0.25094063	0.474518696
BTBD9	0.767076	0.002725	0.73120973	0.032053459
CBX7	0.836602	0.003684	1.07930445	0.004057882
BAALC-AS1	0.984251	0.003897	0.41719876	0.312893912
BASP1	1.444986	0.004285	0.62175365	0.354049428
PTPRB	1.131169	0.004567	1.13152512	0.017908128
MED12	0.32725	0.00485	0.28956356	0.303586835
GRB10	1.054059	0.006795	1.74549185	0.00043506
POMGNT1	0.498621	0.006895	0.3962618	0.019258141
HOXA-AS3	2.386454	0.007151	1.19388985	0.111174706
PLD1	1.890935	0.007947	1.60342177	0.070812192
CDK10	0.634572	0.00821	-0.26044984	0.451509505
PRDM2	0.323889	0.008721	1.92351539	0.001393164
LOC101927479	1.15497	0.009638	0.45951144	0.242875852
DNAH8	2.143747	0.009989	-0.6489366	0.367007726
MED15	0.331679	0.010651	-0.29861478	0.168187976
LINC00663	0.501226	0.010932	0.10501498	0.678097869
VAMP2	0.566094	0.012016	0.39472445	0.088336064
ZRSR2	0.400643	0.0133	0.41544505	0.046497415
FNDC3B	0.899199	0.013684	0.6489845	0.025500728
TOM1	0.499679	0.013775	0.4706437	0.047637542
MKNK1	0.542426	0.014099	0.2214761	0.310666601
NENF	0.761291	0.014474	0.69035545	0.008220115
OTUD5	0.332642	0.016133	-0.55583017	0.053283534
LINC00643	1.678318	0.016207	0.56770056	0.378151363
LIMK2	0.376589	0.017562	0.2978218	0.302594742
ESPN	2.01749	0.018427	-0.33650754	0.495860204
C5orf63	0.516815	0.018568	0.3471672	0.000647732
FGFR2	1.289497	0.019653	1.41575859	0.026530083
SEPT1	1.214467	0.020271	0.51650596	0.443993228
BRE	0.42859	0.021026	0.24240835	0.266698833
CDHR1	1.52512	0.021632	1.14731598	0.118427825
SSBP3	0.69001	0.021879	0.814047	0.049316794

DUOXA1	1.762907	0.022037	0.53212992	0.269646057
GJD3	0.490907	0.022881	-1.11086832	0.135730577
LOC152225	2.350453	0.023087	0.73519615	0.250534699
SP4	0.511433	0.023184	0.43473935	0.099438657
EBF4	0.876654	0.023229	0.71372057	0.11525054
EMC10	0.412999	0.023584	0.45085502	0.161904268
RHBDD2	0.442733	0.02405	0.11177525	0.701237243
PBXIP1	0.705326	0.02433	0.70903787	0.075512198
LOC101929106	1.21292	0.025912	0.24246477	0.545058196
CAB39	0.655879	0.02623	0.73165455	0.045293911
NSF	0.493317	0.026453	0.1582931	0.535081
UPK3A	1.739387	0.027497	1.09910185	0.080759931
SIDT2	0.717035	0.028195	0.4574249	0.127045893
DDX3X	0.407582	0.02824	0.5273518	0.053450508
SPINT2	0.444534	0.028771	0.34422085	0.117363594
MBNL3	1.074781	0.029928	0.84307561	0.109739636
COPS7A	0.398459	0.030489	0.3398831	0.071632345
MSX1	0.579057	0.030644	-0.31265983	0.606518481
NPC2	1.331313	0.032504	1.4892755	0.011806133
PCDHGA8	0.770709	0.036243	0.96374625	0.017656256
CYP21A2	0.726514	0.036745	0.46004437	0.038546997
LOC100131756	0.979815	0.03685	0.98513414	0.072224675
TMEM200A	2.739402	0.036902	-0.56397554	0.709329625
RASAL2	0.543557	0.036979	0.52933918	0.151569838
SNX21	0.515421	0.037095	0.36645297	0.124625199
ELK4	0.442271	0.038015	-0.2765354	0.337032689
NDFIP1	0.551982	0.038466	0.24093392	0.340507978
CLCA3P	1.069014	0.038706	0.17389814	0.55148463
EDN1	1.35617	0.039794	-0.28907882	0.536295379
NTRK1	0.959147	0.041172	0.66419466	0.052857788
NPC1L1	0.900588	0.041319	0.35648643	0.286005508
TTTY6	1.964533	0.041414	-0.67347316	0.0856616
ETV3	0.386611	0.042505	-0.08717923	0.584383632
KPTN	0.575059	0.042638	-0.20138991	0.541106697
NUDT18	0.85235	0.042967	-0.22454569	0.608975976
RREB1	1.007622	0.04352	-0.15603478	0.618328712
ZFAND2B	0.509727	0.043571	0.3005792	0.139246811
FNDC4	1.525577	0.0446	0.43648605	0.286584628
DBNL	0.388396	0.044847	0.17144461	0.355126515
FUNDC1	0.530143	0.044854	-0.1277144	0.609052158

FAM153B	1.110716	0.045019	-0.34404239	0.699252668
TTTY11	0.859317	0.046391	-0.37903546	0.434020099
FILIP1	1.6701	0.047046	1.68412107	0.003904824
TPRG1	0.730384	0.048326	0.34986219	0.084512059
NFATC2	0.799431	0.048657	0.63716362	0.065832651
IDS	0.51157	0.048863	0.31647899	0.485725614
MAN2B2	0.497536	0.049269	-0.19639271	0.557799515

Appendix C: Gene Ontology gene sets significantly enriched by GRB10 knockdown

NAME	SIZE	NES	NOM p	FDR q
GO_STEROL_BIOSYNTHETIC_PROCESS	39	2.449	0.000	0.000
GO_ANTIGEN_PROCESSING_AND_PRESENTATION_OF_PEPTIDE_ANTIGEN_VIA_MHC_CLASS_I	85	2.345	0.000	0.000
GO_SMALL_MOLECULE_BIOSYNTHETIC_PROCESS	385	2.165	0.000	0.004
GO_ALCOHOL_BIOSYNTHETIC_PROCESS	99	2.162	0.000	0.004
GO_ANTIGEN_PROCESSING_AND_PRESENTATION_OF_EXOGENOUS_PEPTIDE_ANTIGEN_VIA_MHC_CLASS_I	62	2.160	0.000	0.003
GO_REGULATION_OF_CELLULAR_AMINE_METABOLIC_PROCESS	77	2.142	0.000	0.003
GO_FATTY_ACID_BIOSYNTHETIC_PROCESS	97	2.141	0.000	0.003
GO_GLUTATHIONE_DERIVATIVE_METABOLIC_PROCESS	21	2.123	0.000	0.003
GO_REGULATION_OF_FATTY_ACID_BIOSYNTHETIC_PROCESS	28	2.107	0.000	0.004
GO_ERAD_PATHWAY	71	2.097	0.000	0.004
GO_LIPOPROTEIN_BIOSYNTHETIC_PROCESS	80	2.067	0.000	0.007
GO_NUCLEOSIDE_BISPHOSPHATE_BIOSYNTHETIC_PROCESS	16	2.057	0.000	0.008
GO_THIOESTER_BIOSYNTHETIC_PROCESS	47	2.032	0.000	0.012
GO_ER_ASSOCIATED_UBIQUITIN_DEPENDENT_PROTEIN_CATABOLIC_PROCESS	59	2.030	0.000	0.011
GO_THIOESTER_METABOLIC_PROCESS	70	2.002	0.000	0.016
GO_LIPID_BIOSYNTHETIC_PROCESS	466	2.000	0.000	0.016
GO_LIPOPROTEIN_METABOLIC_PROCESS	112	1.996	0.000	0.016
GO_FATTY_ACYL_COA_METABOLIC_PROCESS	46	1.985	0.000	0.018
GO_STEROL_METABOLIC_PROCESS	106	1.980	0.000	0.018
GO_ANTIGEN_PROCESSING_AND_PRESENTATION	188	1.971	0.000	0.019
GO_CARBOHYDRATE_BIOSYNTHETIC_PROCESS	104	1.968	0.000	0.019
GO_COFACTOR_BIOSYNTHETIC_PROCESS	152	1.966	0.000	0.019
GO_STEROID_BIOSYNTHETIC_PROCESS	94	1.956	0.000	0.022
GO_COENZYME_BIOSYNTHETIC_PROCESS	114	1.954	0.000	0.022
GO_ANTIGEN_PROCESSING_AND_PRESENTATION_OF_PEPTIDE_ANTIGEN	161	1.952	0.000	0.021
GO_MONOSACCHARIDE_BIOSYNTHETIC_PROCESS	48	1.933	0.000	0.027
GO_FATTY_ACID_TRANSPORT	47	1.918	0.000	0.033
GO_MEMBRANE_LIPID_BIOSYNTHETIC_PROCESS	107	1.904	0.000	0.039
GO_NUCLEOSIDE_BISPHOSPHATE_METABOLIC_PROCESS	32	1.903	0.000	0.038
GO_ORGANIC_HYDROXY_COMPOUND_BIOSYNTHETIC_PROCESS	143	1.902	0.000	0.037
GO_PHOSPHATIDYLSERINE_METABOLIC_PROCESS	25	1.894	0.000	0.040
GO_REGULATION_OF_CELLULAR_RESPIRATION	20	1.894	0.002	0.039
GO_ALDITOL_PHOSPHATE_METABOLIC_PROCESS	31	1.882	0.002	0.045
GO_ANTIGEN_PROCESSING_AND_PRESENTATION_OF_ENDOGENOUS_ANTIGEN	14	1.873	0.002	0.050
GO_CHROMATIN_SILENCING_AT_RDNA	34	-2.160	0.000	0.013
GO_REGULATION_OF_HEMATOPOIETIC_PROGENITOR_CELL_DIFFERENTIATION	38	-2.079	0.000	0.047
GO_TELOMERE_CAPPING	28	-2.054	0.000	0.047

NES: normalized enrichment score; NOM p: nominal p-value; FDR q: false discovery rate q-value.